Investigation of Phthalazine, Quinazoline and Pyrimidine Derivatives as ABCG2 Inhibitors

Dissertation

zur

Erlangung des Doktorgrades (Dr. rer. nat.)

der Mathematisch-Naturwissenschaftlichen Fakultät

der

Rheinischen Friedrich-Wilhelms-Universität Bonn

vorgelegt von

Jiyang Li

aus Chuzhou, China

Bonn 2018

Angefertigt mit Genehmigung der Mathematisch-Naturwissenschaftlichen Fakultät
der Rheinischen Friedrich-Wilhelms-Universität Bonn

1. Referent: Prof. Dr. Michael Wiese

2. Referent: Prof. Dr. Gerd Bendas

Tag der Promotion: 08.05.2018

Erscheinungsjahr: 2018

Dedicated to my family

The important thing is not to stop questioning.
—— Albert Einstein

Abstract

Globally, cancer is the second leading cause of death. Chemotherapy is commonly used in the treatment of cancer. However, in clinic, a wide variety of cancers display resistance to chemotherapy leading to the failure of cancer therapy. This phenomenon is called multidrug resistance (MDR). MDR could occur via various mechanisms. An important mechanism is related to overexpression of drug efflux transporters, especially ATP-binding cassette (ABC) transporters. In the whole ABC transporter family, P-glycoprotein (ABCB1/P-gp), multidrug resistance associated protein 1 (ABCC1/MRP1) and breast cancer resistance protein (ABCG2/BCRP) are mostly reported to confer MDR. They efflux diverse structurally unrelated anticancer drugs outside of cells and reduce cytotoxic effects. To overcome multidrug resistance, a possible strategy is to develop potent inhibitors which target efflux transporters and inhibit the transportation process.

In this study, we adopted the essential features which were depicted before and synthesized various phthalazine, quinazoline and pyrimidine derivatives as ABCG2 inhibitors. Hoechst 33342 and pheophorbide A assays were carried out by my colleague to investigate their inhibitory potency. In project 1 and 2, several compounds with phthalazine or quinazoline scaffold displayed moderate inhibitory activities against ABCG2. But, generally, they were less potent than corresponding 4-anilino-2-phenylquinazoline derivatives. In project 3 and 4, 2-phenylpyrimidine derivatives were synthesized and biologically evaluated. In comparison to Ko143 which is a very potent ABCG2 inhibitor, compound **61**, **62**, **71**, **72**, **81** and **82** showed comparable or even higher inhibitory efficacy. The structure activity relationship was discussed in the following chapters. Owing to the excellent potency of these substances, further *in vitro* and *in vivo* studies such as intrinsic cytotoxicity are on the way.

Contents

1. Introduction

1.1 Multidrug resistance (MDR) and chemotherapy

One of the leading causes of mortality in the world is cancer. Except surgery, chemotherapy is commonly used in treatment of a variety of cancers. Drug sensitive malignant cells are killed, but some cells are tolerant and resistant to anticancer drugs. After a period of time, tumor begins to grow again resulting in failure of chemotherapy. This phenomenon is called multidrug resistance (MDR).[1]

MDR in cancer could occur via various mechanisms including activation of detoxifying systems, blocked drug uptake, drug efflux, activation of DNA repair mechanisms etc.[2] An important mechanism is related to drug efflux transporters, especially ATP-binding cassette (ABC) transporters which are able to efflux many structurally diverse anticancer drugs.[3] P-glycoprotein (P-gp, ABCB1), breast cancer resistance protein (BCRP, ABCG2) and multidrug resistance-associated protein 1 (MRP1, ABCC1) are the extensively studied members associated with MDR in the ABC transporter family.[4]

1.2 ATP-binding cassette transport proteins

1.2.1 Introduction of ABC transporter family

ATP-binding cassette (ABC) proteins play various roles in biological processes, such as importing nutrients into the cell,[5] detoxification[6] and secretion of substrates.[7] Most of them are members of complexes which mediate transportation of compounds across membranes. Based on the direction of transportation, ABC transporters are separated into importers and exporters. Both importers and exporters typically contain two transmembrane domains (TMDs) and two nucleotide-binding domains (NBDs).[8] TMDs

of different ABC members are phylogenetically diverse to facilitate transportation of various structurally unrelated substrates.[9] NBD is the engine and provides the power of transport via hydrolysis of ATP. The sequences of NBDs are highly conserved to facilitate ATP binding process.[10] One TMD and one NBD are fused as half transporter which is not functional. To be biologically active, these half transporters have to dimerize to full transporters.[11] The examples of ABC half transporters are ABCG2, Sav1866 from *Staphylococcus aureus* and MsbA from *Escherichia coli*.[12]

48 ABC genes exist in human genome and they were divided into seven subfamilies: ABCA to ABCG.[13] The members of this diverse family exert different effects in various biological processes.

The ABCA subfamily contains 12 full transporters and is related to some genetic diseases. For example, mutation of ABCA1 protein results in recessive Tangier's disease. Stargardt disease, retinitis pigmentosa and age-related macular degeneration are related with ABCA4 mutation.[14]

The ABCB subfamily contains 4 full transporters and 7 half-transporters. Mutations of ABCB genes are associated with different diseases, such as diabetes type 2 and lethal neonatal syndrome. The member ABCB1 is also called P-glycoprotein (P-gp) or multidrug resistance protein 1 (MDR1) which is the most extensively studied protein involved in multi-drug resistance.[14, 15]

The ABCC subfamily contains 13 genes. ABCC7 is also called cystic fibrosis transmembrane conductance regulator (CFTR). Mutations of the CFTR gene result in cystic fibrosis which means dysregulation of epithelial fluid transport in the lung, pancreas and other organs derived from chloride ion channel dysfunction. Sulfonylurea receptor (SUR) coded by ABCC8 gene is a protein involved in insulin secretion, neuronal function and muscle function. Mutations in SUR may lead to neonatal diabetes mellitus. ABCC1, which is also called multidrug resistance-associated protein 1 (MRP1), is another well-studied protein involved in multi-drug resistance.[16]

ABCD subfamily contains 4 genes coding half-transporters. Mutation of ABCD1 gene

is known to cause Adrenoleukodystrophy (ALD) which is characterized by neurodegeneration and adrenal deficiency. The functions of other members are not clear now.[17]

The ABCE subfamily has only one member ABCE1 which is an organic anion-binding protein. It has only ATP-binding domain and lacks TMD precluding its function as a transporter. But, it was found to promote interferon activity in the processes of certain virus infections.[14, 18]

Similar to ABCE1, the ABCF subfamily has 3 members which only have NBD but no TMD. Therefore, they are not able to transport compounds inside or outside of cells, but are believed to play a role in inflammation processes.[14]

The ABCG subfamily contains 5 genes which code six "reversed" half transporters. Opposite to the orientation of all other ABC genes, NBD of these six transporters is on the N terminus and TMD at the C terminus. Mutations of ABCG genes are associated with sterol accumulation disorders and atherosclerosis. ABCG1 plays a role in cholesterol efflux in macrophages. ABCG3 might be involved in the transport of hydrophobic compounds or specific peptides from lymphocytes. ABCG5 and ABCG8 seem to block intestinal absorption and increase biliary excretion of sterols. Most notably, ABCG2 whose normal function is not clear can export diverse anticancer drugs outside of cells leading to multidrug resistance.[19] Detailed information about it is provided in section 1.2.5.

1.2.2 Structure and mechanism of ABC transporters

Since the first discovery of an ABC transporter in mid-1970, many researchers have devoted much effort to obtain the crystal structures of ABC transporters and elucidate the molecular mechanism of their transport activities.[20] Before 2006, studies of structural biology of ABC proteins were focused on NBDs. NBD structures of TAP1/2,[21] CFTR,[22] MRP1[23] and the hemolysin transporter HlyB[24] were studied and

published. The knowledge derived from analyzing these structures is very essential to understand how the "engine" works. As a result, the ATP switch model was proposed.[25] The model revealed that NBD has two critical conformations: closed dimer when two ATPs binding and open dimer after ATP hydrolysis. Transforming NBD conformation from open to closed dimer leads to conformational changes in TMD and final release of substrate. Later, two complete structures of MsbA (lipd A flippase) were reported. But the interpretations were wrong in the beginning and have been rectified now.[26] In 2006, Sav1866 from *Staphylococcus aureus* — the first full-length high-resolution structure of ABC exporters — was published.[27] It was the first time to reveal the structural organization of TMDs. NBDs and TMDs are connected via coupling helices which are responsible for mechanically transmitting the movement of NBD fueled by ATP hydrolysis to TMDs. In 2009, the mouse P-gp structure was solved.[28] It was the first time to reveal the structure of a full transporter from eukaryotic origin with four domains sharing one polypeptide chain. But the structure was not accurate and major correction was applied later.[29] In 2013, the structure of ABCB10 was solved, extending the structural interpretation to an ABC protein of human origin.[30] Recently, the structure of ABCG2 was also reported.[31]

Although the development of structural studies on ABC transporters is obvious, the detailed molecular mechanism of transportation is still not fully understood.

In Figure 1, a generally accepted mechanistic proposal of exportation is described — the alternating access model.[32] State 1 is the resting state of ABC transporter. TMDs are in an inward-facing orientation, while NBDs are in an open conformation with low binding affinity for ATP. Substrates could bind at binding pocket of TMD from not only cytoplasm but also lipid bilayer. Especially some hydrophobic compounds are able to be recruited directly from membrane. Some studies suggested that the binding site on the same transporter which is accessed by diverse substrates might be not unique, there might exist multiple sites. The initiate point of transport cycle is the interaction of substrate and high-affinity binding site on TMD. It induces a conformational change of

NBDs enhancing the affinity for ATP. The interaction of NBDs and ATP converts transporter to a closed conformation (state 2). Such a state has been observed in some crystal structures. Closing NBDs leads to conformational changes of TMDs, so TMD is converted to an outward-facing conformation reducing the affinity of substrates to TMD, and the substrates are finally released toward periplasm (state 3). From state 1 to state 3, the surface of cavity surrounding substrates must change. When ATP is hydrolyzed, the produced energy drives NBDs apart. The movement of NBDs is transmitted to TMDs via coupling helices, so the conformation of TMD is converted from outward-facing to inward-facing and the transporter is restored to state 1. It is still unclear whether two ATPs are hydrolyzed simultaneously or consecutively and which step in the cycle provides power stroke, or how many ATPs are consumed in one cycle? Many questions still remain to be answered.[33]

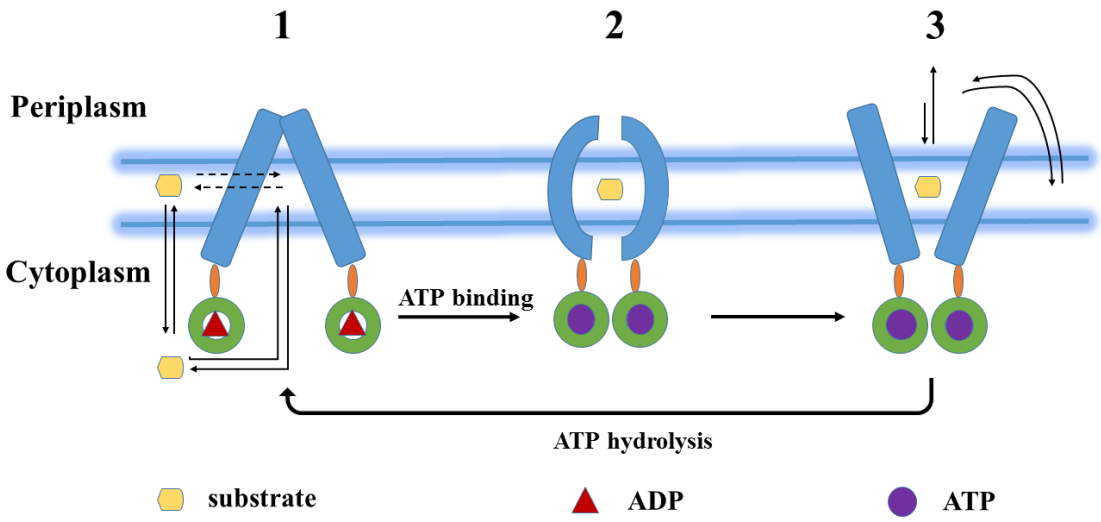

Figure 1: The generally accepted alternating access mechanism of exportation for ABC transporters.[34] Glowed blue double line: boundary of membrane bilayer; blue rectangle: TMD; orange oval: coupling helices; green concentric circle: NBD; yellow hexagon: substrate; purple circle: ATP; red triangle: ADP; number denotes state.

Except the alternating access model, other models or mechanisms such as outward-only mechanism[35] and Constant-Contact-Model[36] were also proposed. Due to the diversity

and complexity of ABC transporter members and substrates, one single conserved mechanism is probably not able to explain the movements of every exporter in ABC transporter family. The same transporter might also use different mechanisms for transporting different substrates.[34]

1.2.3 ABCB1 / P-glycoprotein (P-gp)

In 1976, Juliano and Ling discovered that the sensitivity to some cytotoxic anticancer drugs was reduced in rodent cells.[37] The "culprit" was called as "permeability glycoprotein", named P-glycoprotein. P-gp (ABCB1/MDR1) is the first discovered and most widely investigated transporter of the ABC protein family. Several thousand compounds have been reported to bind to it and to be excluded out of cells.[38] It is widely expressed and distributed on the Golgi membrane, intracellular canaliculi and plasma membrane of different tissues, including colon, intestine, liver, adrenal gland, kidney, lung, muscle, pancreas, stomach, placenta and endothelial cells at blood-testis barrier, blood-brain, blood-placenta barriers.[39, 40] The ways it disposes xenobiotics (such as anticancer drugs) and metabolites include biliary excretion in liver, urinary excretion in kidney and absorption barrier of oral bioavailability.[41] As consequence, the accumulation of anticancer drugs in various tissue cells is limited leading to multidrug resistance.

1.2.3.1 Structure and mechanism

P-gp is a 170 kDa glycosylated membrane protein. Like many other members of the ABC transporter family, the P-gp protein is composed of two halves. Each contains a transmembrane domain (TMD) which consists of six hydrophobic transmembrane helics and a nucleotide binding domain (NBD) which is located on the inner part of membrane and binds ATP to facilitate transport (Figure 2).[42]

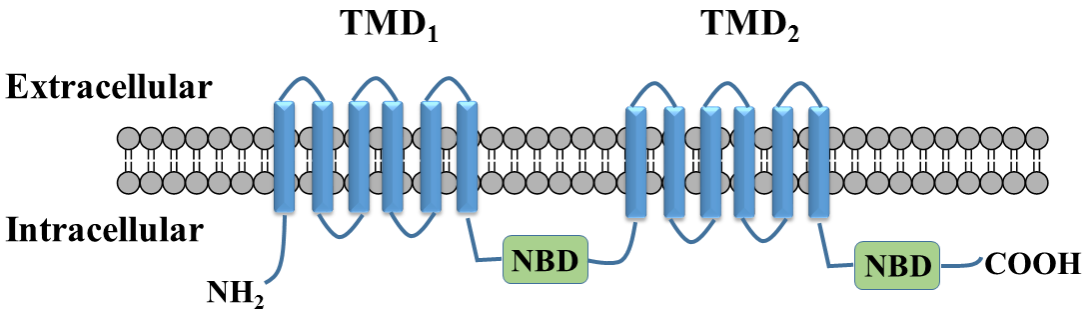

Figure 2: Topology model of ABCB1 (P-gp)

Since the discovery of the ABCB1 gene, many mutations and polymorphisms have been detected, but only a few variants were found to be crucial for protein expression and function of transportation. Genetic variations of ABCB1 gene in the form of single nucleotide polymorphisms (SNP) have shown impact on disease susceptibility and drug response. For example, mutation in the Walker B domain resulted in blockage of efflux.[43] Mutation in TMD led to altered affinity for substrate.[44] The 3435 C>T polymorphism is perhaps one of the best-studied silent mutations. But the correlation of this polymorphism with decreased/increased expression of P-gp and drug response is still under debate.[45]

Before the structure of P-gp was obtained, many different biochemical and biophysical strategies including mutagenesis, photo-affinity labelling and fluorescence measurements were employed to reveal the mechanism of translocation process. The collective data led to generation of a hypothesis called "substrate-induced fit" model.[46] According to the model, drugs bind at a common large domain in the cavity of P-gp. But distinct types of drugs may bind with different residues. There is evidence to support two different drugs occupying distinct regions in the binding pocket.[47] Both halves of polypeptide participate in drug binding. However, in order to elucidate drug binding process in more detail, structural data are needed. The first structure of P-gp purified from CHB30 cells was obtained in 1997 using electron microscopy-single-particle analysis (EM-SPA).[48] However, EM-SPA technique was not able to give a high

resolution for this size protein (resolution: 25 Å). Therefore, except for the general dimensions of protein, not much valuable information was displayed. Over the next years, the same group spent much efforts on improving the resolution with electron microscopy. 2D structural data was updated three times and the resolution was improved to 8 Å.[49-51] In these reports, multiple conformations were presented and it was provided that the major conformational movements were driven by NBDs and the central pore existed. These were essential evidence for elucidating the translocation mechanism. In 2009, the first X-ray crystal structure of mouse P-gp was obtained with resolution of 3.8-4.4 Å.[28] But, in 2014, this structure had been corrected.[29] An interesting feature reported in the paper was that the physical separation of NBDs reached 30 Å. It is under debate whether this configuration belongs to real empty P-gp or is just an artefact of crystallization. Another paper has also reported three crystal structures of mouse P-gp.[42] The different separation distances of NBDs in three structures proved the flexibility of conformation of P-gp. Although all of these structural data have provided us with a wealthy of information to understand the function of this transporter, the detailed understanding of how P-gp is able to bind such a large variety of compounds remains unsolved.

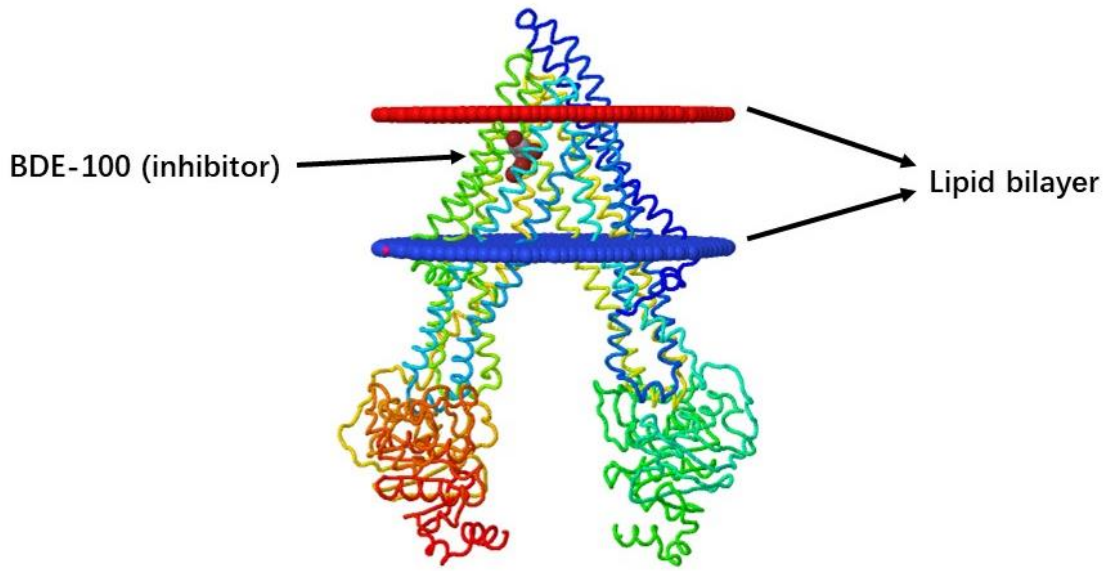

Figure 3: P-glycoprotein co-crystallized with BDE-100 (PDB ID: 4XWK)[52]

There are two models (Figure 4) that were postulated to explain the action of P-gp: Hydrophobic vacuum cleaner model and Flippase model.[53] As the substrates of P-gp are relatively hydrophobic, these models both accept that the substrates partition into the lipid bilayer at first.[50] Afterwards, hydrophobic vacuum cleaner model assumes that substrates are extracted by protein. They pass through the lateral gate composed by TM domains 4/6 and 10/12 and interact with ~6000 angstroms cubed binding cavity[28] of P-gp. Finally, substrates are expelled directly by P-gp into extracellular medium. The flippase model assumes that substrates approach binding sites from inner bilayer of membrane. Afterwards, they are translocated by protein to outer layer of lipid bilayer and released to extracellular environment via passive diffusion. Both models have supported evidence,[54, 55] but it is difficult to distinguish them experimentally.[56]

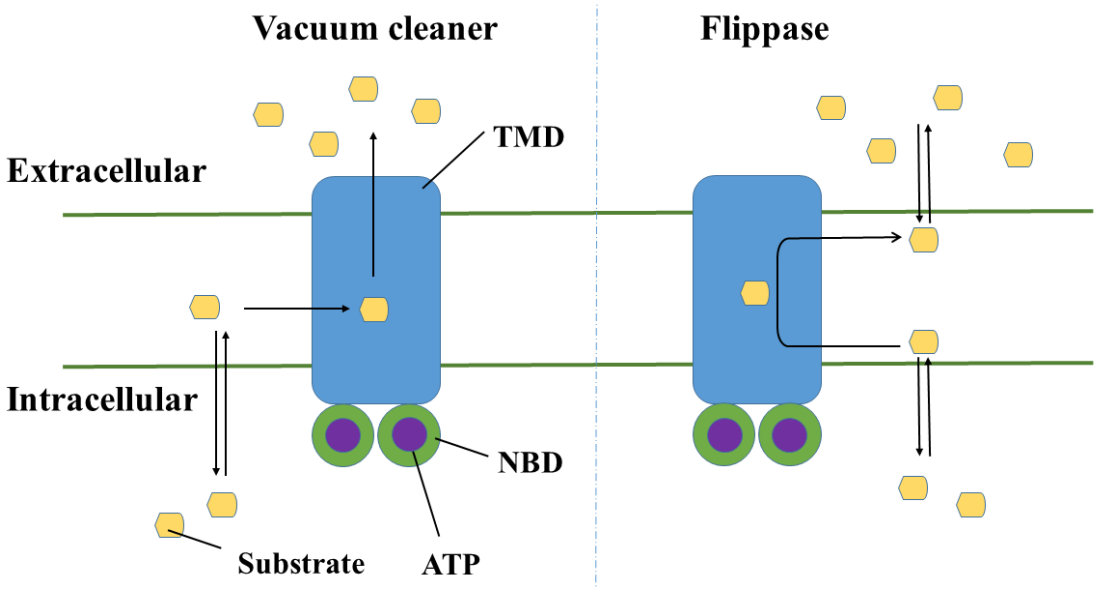

Figure 4: Hydrophobic vacuum cleaner and flippase model for P-gp transport mechanism (modified from Sharom).[57]

1.2.3.2 Substrates and inhibitors

Since its discovery, P-gp is well-known for its capability to interact with and to export a broad spectrum of structurally diverse compounds which have different pharmacological functions. In table 1 selected substrates of P-gp are listed, including

anticancer agents, HIV protease inhibitors, immunosuppressive drugs, steroids, fluorescent dyes and antibiotics.[58] The details about interaction of P-gp with these compounds are not fully understood. But some physico-chemical properties including lipid solubility, molar refractivity, hydrogen bonding potential, cationic charge, presence of amine and aromatic ring were addressed as essential determinants for substrate binding and functionality.[59, 60]

Table 1: Selected substrates of P-gp

Anti-cancer drugs	Topotecan
	Paclitaxel
	Docetaxel
	Vinblastine
	Vincristine
	Doxorubicin
	Daunorubicin,
Steroids	Aldosterone
	Corticosterone
	Dexamethasone
Antibiotics	Erythromycin
HIV protease inhibitors	Nelfinavir
	Ritonavir
	Saquinavir
Immunosuppressive drugs	Cyclosporine A
	Tacrolimus
Fluorescent dyes	Rhodamine 123
	Hoechst 33342
	Calcein
	Acetoxymethylester

There are also some compounds that are able to block the efflux of P-gp and reverse MDR effect. These compounds are named P-gp inhibitors or modulators. From a historic perspective, they are classified into three generations. The first generation inhibitors are some existing drugs which were primarily developed for other purposes. For example, verapamil is an antihypertensive calcium channel blocker, and

cyclosporine A is an immunosuppressant. Selectivity and toxicity were always the weakness of these compounds which limited the further exploration.[61] To overcome the disadvantage of first generation inhibitors, the second generation inhibitors were developed. For instance, dexverapamil (the R-isomer of verapamil) has less cardiac activity. PSC833 (a cyclosporine A analogue) lacks immunosuppressive property. These modifications achieved improved selectivity for P-gp and reduced toxicity in comparison to the parent compounds. However, they faced another challenge. They were found to cause pharmacokinetic alterations of co-administrated anticancer drugs leading to unexpected low clearance of drugs and increased toxicity.[62] The third generation inhibitors including GF120918 and LY335979 were developed by quantitative structure-activity relationship (QSAR) technique, high throughput screening (HTS) or combinational chemistry. They did not possess the deficiencies of first and second generation inhibitors. Due to the promising potency and low toxicity, XR 9576 (tariquidar) was even applied in phase III clinical trial.[63]

Table 2: Selected modulators/inhibitors of P-gp

First generation	Verapamil
	Cyclosporine A
	Tamoxifen
Second generation	Dexverapamil
	Valspodar (PSC-833)
Third generation	Zosuquidar (LY335979)
	Tariquidar (XR9576)
	Elacridar (GF120918)

At last, it is worth to note that the discrimination between substrates and inhibitors is not unambiguous. For example, 5-hydroxypropafenone was able to inhibit P-gp-mediated digoxin accumulation. But, it could also be translocated by P-gp across membrane.[64] Therefore, it could not only be assigned as substrate but also competitive inhibitor of P-gp. Some selected P-gp inhibitors are given in Table 2.

1.2.4 ABCC1 / Multidrug Resistance associated Protein 1 (MRP1)

1.2.4.1 Structure and function

Multidrug Resistance associated Protein 1 (MRP1 or ABCC1) is a transporter widely expressed in different tissues including testis, lung, liver, cardiac and skeletal muscles, macrophages, intestine, choroid plexus cells and blood-brain barrier (BBB) where protecting brain from xenobiotics together with P-gp and ABCG2.[16, 65] Unlike most other members of ABC transporter family, it is a 190 kDa protein containing three transmembrane domains (TMDs) composed by 17 transmembrane helices and two NBDs. In addition to the ABCB1-like central core which consists of TMD1, TMD2 and two NBDs, it has an extra N-terminal transmembrane domain (TMD0) which contains 5 α-helices.[66] The central core is the functional part which effluxes substrates out of cells. TMD0 does not participate in transportation but plays a role in maintaining protein in cell membrane.[67] The topological structure is displayed in Figure 5.

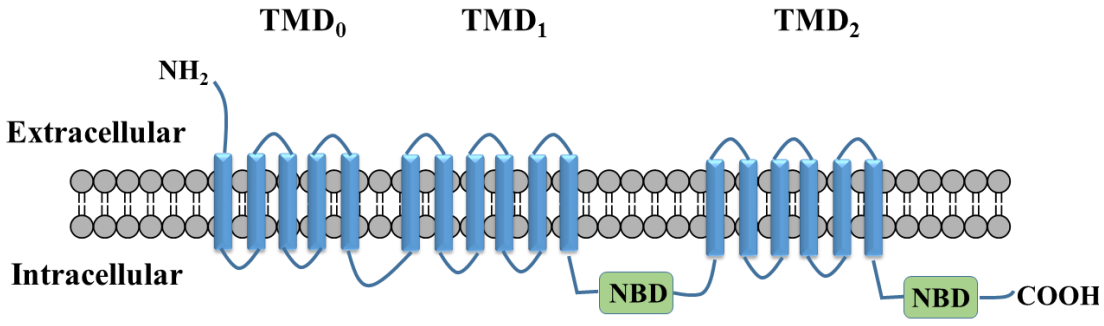

Figure 5: Topology model of ABCC1 (MRP1)

1.2.4.2 Substrates and inhibitors

Similar to P-gp, MRP1 is also able to mediate multidrug resistance. Overexpression of MRP1 was detected in various tumors. For example, Nooter et al. observed a very high

level of MRP1 mRNA expression in chronic lymphocytic leukemia.[68] A few years later, overexpression of MRP1 and P-gp was also observed in renal cell carcinoma.[69] There are also some studies to support MRP1 playing a role in drug resistance of non-small-cell lung cancer, some kinds of breast cancer and prostate cancer.[70]

A variety of structurally different compounds including anticancer drugs, organic conjugates, peptides, HIV protease inhibitors and fluorescent dyes are recognized and effluxed by MRP1.[71] Most interestingly, several drugs and conjugated organic anions are only able to be transported in the presence of glutathione (GSH) which broadens the substrate spectrum of MRP1. But the reason why some substrates are translocated in a GSH-dependent way is still not well understood.[72]

Table 3: Selected substrates of MRP1[71]

Anticancer drugs	Daunorubicin
	Doxorubicin
	Vinblastine
	Vincristine
	SN-38
	Methotrexate
GSH conjugates	Chlorambucil-SG
	Melphalan-SG
	Leukotriene C4
	Leukotriene D4
	Hydroxynonenal-SG
Sulfate conjugates	Estrone 3-sulfate
Peptides	GSH
	GSSG
Fluorescent dyes	Calcein-AM
	Calcein

Until now, there are not many potent and efficient MRP1-specific inhibitors and no MRP1-inhibitor has been tested in clinical trials. In early time, some nonspecific inhibitors for organic anion transporter including probenecid, benzbromarone and indomethacin were used as modulators of MRP1. However, these compounds also

demonstrated inhibitory effects on importers of solute carrier (SLC) family which hindered their further application.[73] Later, several cysteinyl leukotriene receptor 1 (CysLTR1) antagonists including MK-571,[74] ONO-1078[75] and LY171883[76] were identified as more specific inhibitors of MRP1. Whereas, these compounds are primarily designed to treat asthma and could not distinguish between other MRP homologs. Therefore, they are also not ideal modulators. In 2005, Norman et al. discovered several tricyclic isoxazoles with cyclohexyl-linker exhibiting excellent selectivity and inhibitory potency against MRP1. In the presence of GSH, the EC_{50} values of few compounds showing no cytotoxicity were lower than 100 nM.[77] Nevertheless, to find more specific and potent inhibitors with unwanted side effects and toxicities, there are still much work to do.

1.2.5 ABCG2 / Breast Cancer Resistance Protein (BCRP)

In 1998, Ross's group successfully cloned ABCG2 from a drug-resistant human breast cancer subline — MCF-7/AdrVp. They named the expressed protein as breast cancer resistance protein (BCRP) which conferred resistance to various anticancer drugs including mitoxantrone, doxorubicin and daunorubicin.[78] Simultaneously, Allikmets et al. characterized ABCG2 gene which was abundantly expressed in placenta on chromosome 4q22[79] and Miyake et al. successfully cloned cDNAs of ABCG2 from mitoxantrone-resistant S1-M1-80 human colon carcinoma cells without overexpression of P-glycoprotein and MRP1.[80] Nowadays, ABCG2 has been well accepted as an important member which confers innate and acquired multidrug-resistance.

1.2.5.1 Distribution and physiological roles

Maliepaard et al. used specific monoclonal antibodies BXP-34 and BXP-21 to characterize the distribution and localization of ABCG2 protein. High expression of

ABCG2 was observed in placental syncytiotrophoblasts, epithelium of the small intestine and colon, liver canalicular membrane, ducts and lobules of breast. The presence of ABCG2 in epithelium of the veinous and capillary endothelium was also noticed, but not in arterial endothelium. These distributions indicated ABCG2 may play a role in transporting them back to gut lumen, regulating uptake of substrates such as topotecan or irinotecan and protecting fetus from xenobiotics.[81] Huls et al. used immunohistochemical analysis to localize ABCG2 and found its expression in proximal tubule brush border membrane of kidney which indicated its importance in renal drug exceretion.[82] Cooray et al. found the presence of ABCG2 at the blood-brain barrier, especially at the luminal surface of microvessel endothelium. It may suggest, besides P-gp and MRP1, ABCG2 is also important for hindering drugs accessing the brain.[83] Similarly, its expression was also shown in Sertoli cells indicating it may play a protective role at the blood-testis barrier.[84] Asashima et al. identified its expression on the mouse luminal membrane of retinal capillary endothelial cells. This indicates its importance in restricting the accumulation of phototoxins and xenobiotics such as pheophorbide A and protoporphyrin IX in retinal tissue.[85] In short, the wild distribution of ABCG2 in these studies implies that it can exert essential effects on limiting absorption (small intestine), mediating distribution (blood-brain, blood-testis, blood-placental barriers) and facilitating elimination (liver, kidney and colon) of xenobiotics including anticancer drugs. And these physiological functions were also proven in some studies by using ABCG2-knockout mice.[86]

Although ABCG2 has demonstrated protective roles in various normal tissues, it was found over-expressed in various drug-resistant cell lines including ovarian tumor cell line T8, mitoxantrone-selected human gastric carcinoma cell line EPG85-257RNOV, colon cancer cell lines S1-M1-80 and HT29, gefitinib-resistant non-small cell lung cancer (NSCLC) cells, human small cell lung cancer cells PC- 6/SN2-5, epirubicin-resistant human hepatocyte carcinoma cells HLE-EP and topotecan and doxorubicin-selected human multiple myeloma cells.[87] This high expression is thought to be

associated with MDR in hematopoietic malignancies and solid tumors. Besides, Jablonski et al. observed increased P-gp and ABCG2 expression at the blood-spinal cord barrier in Amyotrophic lateral sclerosis (ALS). It implicated these two transporters may also be the obstacle inducing MDR in ALS.[88]

1.2.5.2 Structure of ABCG2

The six members of G subfamily including ABCG2 are all half transporters which contain only one TMD and one NBD. Membrane topology determined by epitope insertion and immunofluorescence demonstrated that ABCG2 contains 6 transmembrane α-helices (Figure 6) and the arrangement of TMD-NBD is reversed in comparison to P-gp and MRP1.[89]

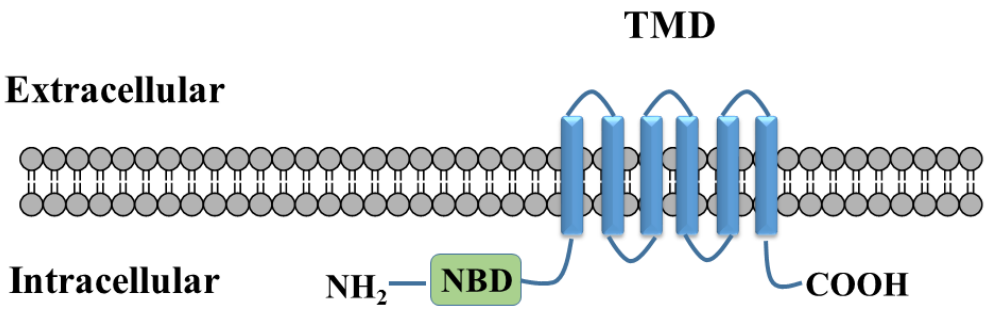

Figure 6: Topology model of ABCG2 (BCRP)

Due to its nature of half transporter, dimerization or oligomerization which has been supported by evidence from various studies is required to function as a transporter.[90, 91] The first structure of ABCG2 was determined by McDevitt et al. They used cryonegative stain electron microscopy to construct 3D structural data of purified ABCG2(R482G) at a resolution of approximately 18 Å and a tetrameric complex with an aqueous center was revealed by single-particle analysis.[91] Later, Rosenberg et al. subjected ABCG2 to 2D crystallization and revealed a symmetry. The projected structures which were determined at 5 Å resolution indicated the existence of an

oligomeric complex and illustrated that ABCG2 had a more symmetric and closed conformation in the presence of mitoxantrone than without mitoxantrone.[92] Recently, the first high-resolution 3D crystal structure of human ABCG2 in complex with two antigen-binding fragments of antibody 5D3 was determined by cryo-electron microscopy.[31] The local resolution of TMD and fragments of 5D3 approached 3 Å, but NBDs were resolved at lower resolution. Therefore, the NBD homology model based on ABCG5/G8 heterodimer was docked into the EM density map. Albeit, these structural data still revealed much valuable information.

NBD and TMD are linked by a highly charged linker which is flexible and the distance between NBD and membrane was shorter than other members of B-subfamily. Notably, NBDs are still in contact even though nucleotide is not bound to NBD. The previous postulations that GXXXG motif at TMD and C2 motif at NBD involved in dimerization and ATP binding respectively[93, 94] were not supported (Figure 7A). The longest extracellular loop EL3 which connects TM5 and TM6 contains three cysteines (C592, C603, C608) and an N-glycosylation site — N596, to which two GlcNAc residues are attached (Figure 7B). C592 and C608 form one intramolecular disulfide bond which is essential for ABCG2 activity, but the intermolecular disulfide bond formed by C603s seems not crucial for transportation. This observation is consistent with previous studies.[90, 95] N-glycosylation at N596 does not affect the binding of antibody fragments. But this site is critical for ABCG2 maturation.[96] Most critically, a deep slit-like cavity which is suitable to accommodate hydrophobic and flat compounds was revealed. The residues in this cavity which contact with two cholesterols are L539, I543, V546, M549, F432 and F439. All of them are hydrophobic residues (Figure 7C). Besides, another smaller cavity below EL3 was also observed. These two cavities are separated by two leucine residues which form a plug between them. Previous biochemical studies have supported the existence of multiple binding sites.[86] Due to less hydrophobic surface and unfavorable substrate-binding conformation of cavity 2, cavity 1 might be the place where binding sites locate.

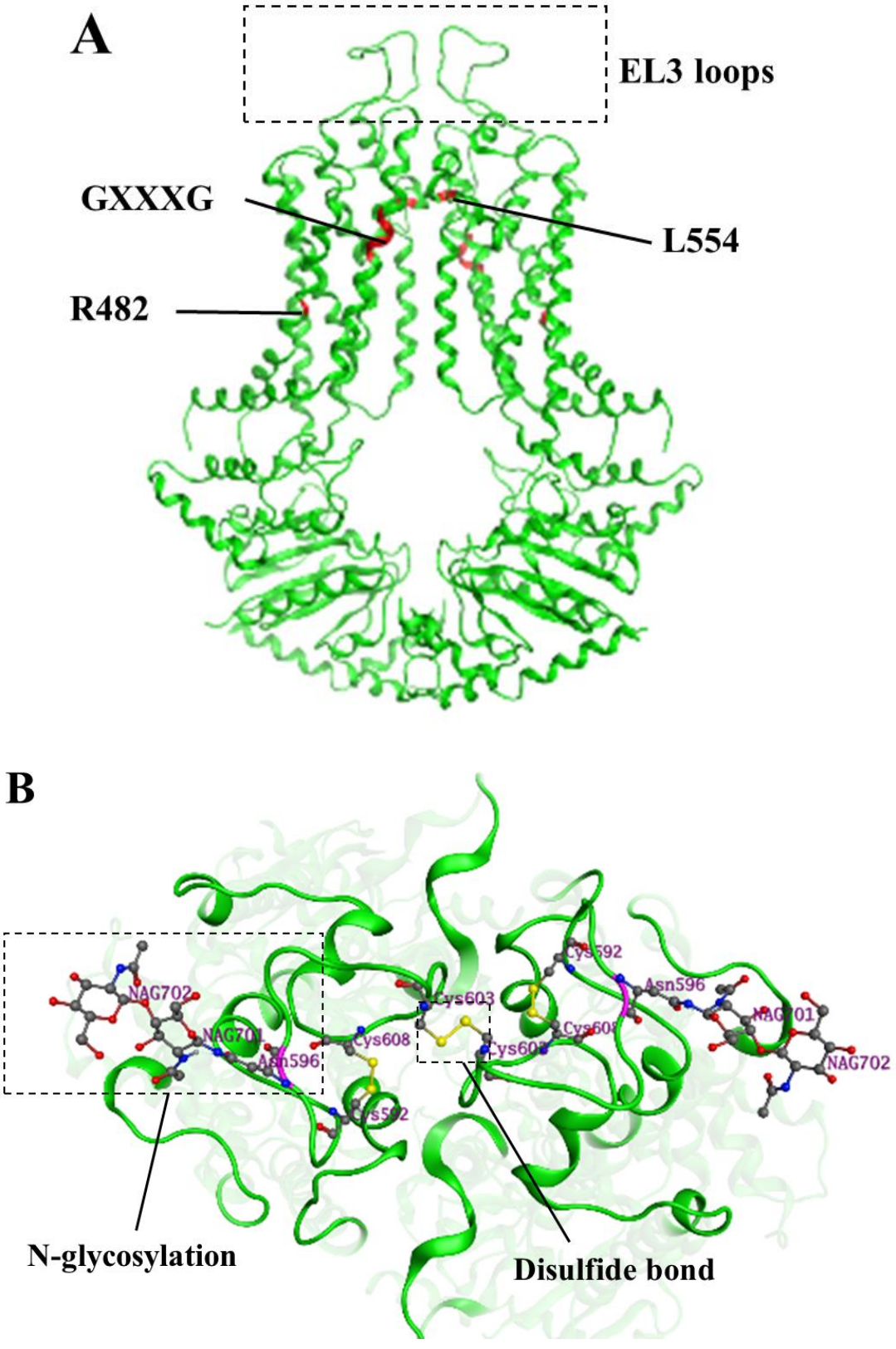
A
EL3 loops
GXXXG
L554
R482
B
NAG702
NAG701
Asn596
Cys608
Cys603
Cys592
Asn596
NAG701
NAG702
N-glycosylation
Disulfide bond

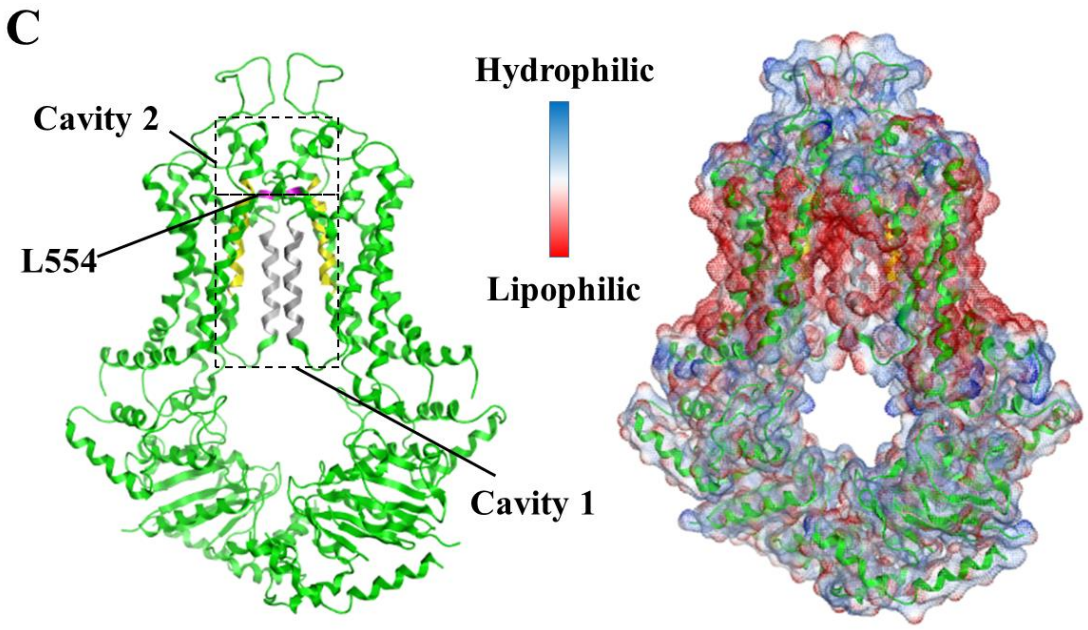

Figure 7: Structure of ABCG2 (PDB ID: 5NJ3).[31] *A: Ribbon diagram of ABCG2 dimers. B: Top view of EL3 loops. C: The left picture demonstrates two cavities on TMD, silver helix (part of TM5) and yellow helix (part of TM2) are the area cholesterols bound. The right picture displays calculated molecular surface of ABCG2 dimers by MOE 2015.*

1.2.5.3 Substrates and inhibitors

A wide spectrum of compounds is reported to be substrates of ABCG2. Among them are some anticancer drugs including mitoxantrone, flavopiridol, camptothecin derivatives and several tyrosine kinase inhibitors (imatinib, gefitinib and nilotinib). Several other drugs including prazosin, cimetidine, rosuvastatin, glyburide, sulfasalazine and several nucleotide analogs such as lamivudine and AZT could be effluxed by ABCG2.[97] But ABCG2 is not able to export vinblastine, cisplatin and paclitaxel out of cells.[98] Some chemical toxicants including protoporphyrin IX, some fluorescence probes including Hoechst 33342, BODIPY-prazosin and pheophorbide A, some organic conjugates of xenobiotics and conjugated organic anions including dehydroepiandrosterone and estrone-3-sulfate are also ABCG2 substrates.[97] Some of them are overlapping with substrates of P-gp or MRP1. Selected substrates of ABCG2 are listed in Table 4.

Table 4: Selected substrates of ABCG2[87]

Topoisomerase inhibitors	Daunorubicin
	Doxobucincin
	Mitoxantrone
	Etoposide
	Becatecarin
Tyrosine kinase inhibitors	Gefitinib
	Erlotinib
	Nilotinib
Conjugates of xenobiotics	Estrone 3-sulfate
	SN-38-glucuronide
	Troglitazone sulfate
Fluorescent dyes	Hoechst 33342
	pheophorbide A
	BODIPY-prazosin
	Lysotracker green
Others	Diclofenac
	Rosuvastatin
	Nicardipine

To overcome MDR mediated by ABCG2, a few array of inhibitors with various structures have been identified and developed. Some selected ABCG2 inhibitors are presented in Table 5. Gupta et al. reported some HIV protease inhibitors including ritonavir, saquinavir and nelfinavir to be effective ABCG2 inhibitors, but not substrates.[99] Zhang et al. discovered that dipyridamole and several calcium channel blockers including nicardipine, nitrendipine and nimodipine could effectively inhibit ABCG2-mediated mitoxantrone efflux.[100] A typical selective ABCG2 inhibitor is fumitremorgin C (FTC) obtained from the fungi *Aspergillus fumigatus*. It did not show inhibition of P-gp and MRP1,[101] but its neurotoxicity hindered its further application *in vivo*. Therefore, several analogues of FTC including Ko132, Ko134 and Ko143 were developed and showed lower neurotoxicity, higher inhibitory potency and selectivity for ABCG2.[102] Except the abovementioned compounds, many derivatives of various scaffolds including tariquidar,[103] chalcone,[104] chromone[105] and flavone[106] were also

synthesized and tested as potent and selective ABCG2 inhibitors.

Table 5: Selected ABCG2 inhibitors[86]

HIV protease inhibitors	Saquinavir
	Nelfinavir
	Lopinavir
Calcium channel blockers	Nicardipine
	Nimodipine
	Nitrendipine
Tyrosine kinase inhibitors	Gefitinib
	Imatinib
	Erlotinib
	Nilotinib
	Lapatinib
Other drugs	Novobiocin
	Fumitremorgin C

An interesting family of compounds in Table 5 are tyrosine kinase inhibitors (TKIs). TKIs were initially designed as specific and selective anticancer agents for inhibiting targets like epidermal growth factor receptor or vascular endothelial growth factor receptor to stop transducing signal in cell proliferation. But later some of them were also reported with obviously inhibitory activity on ABCG2.

Nakamura et al. reported that topotecan, SN-38 and mitoxantrone resistance were effectively reversed by ten micromoles of gefitinib in three multidrug-resistant cancer cell lines overexpressing ABCG2.[107] Imatinib mesylate was reported to be able to reverse resistance towards topotecan and SN-38 in ABCG2 overexpression cells.[108] Both of them are also substrates of ABCG2. Dai et al. observed increasing accumulation of doxorubicin or mitoxantrone in ABCB1- or ABCG2-overexpressing cells in treatment with lapatinib and the transport of methotrexate was also inhibited.[109] Mi et al. reported apatinib to significantly increase the intracellular accumulation of rhodamine 123 and doxorubicin in three different cell lines overexpressing ABCG2. And it reversed resistance of ABCB1 and ABCG2 mediated by directly inhibiting them

but not by blocking AKT or ERK1/2 pathways or downregulating expression of ABCB1 and ABCG2.[110] Lapatinib (GW572016), GW583340, GW2974, canertinib and erlotinib were found to be able to circumvent MDR by inhibiting the activity of P-gp and ABCG2.[109, 111, 112] Canertinib (CI1033) was found to enhance cytotoxicity of 7-ethyl-10-hydroxycamptothecin and topotecan in cancer cells by inhibiting ABCG2-mediated drug efflux.[113] Many other TKIs which are able to interact with ABCG2 are reviewed elsewhere.[114, 115] The structures of selected TKIs which have also been reported as ABCG2 modulators are displayed in Figure 8.

The mechanism of inhibition is not fully understood. Some ABCG2 inhibitors are called "general" inhibitors that inhibit ATPase activity of the transporter such as FTC and Ko143. Some others are "substrate-dependent" inhibitors that are also ABCG2 substrates. The latter series of modulators may interact with ABCG2 (i) at the same binding site of one class of substrates, (ii) or at allosteric sites to induce conformational changes in the large binding pocket that subsequently affect transportation of certain substrates.[86] Due to the complex mechanism of inhibition, predicting and screening novel ABCG2 modulators is still a challenge. Further studies are required for developing more potent compounds which are able to be applied in the clinic.

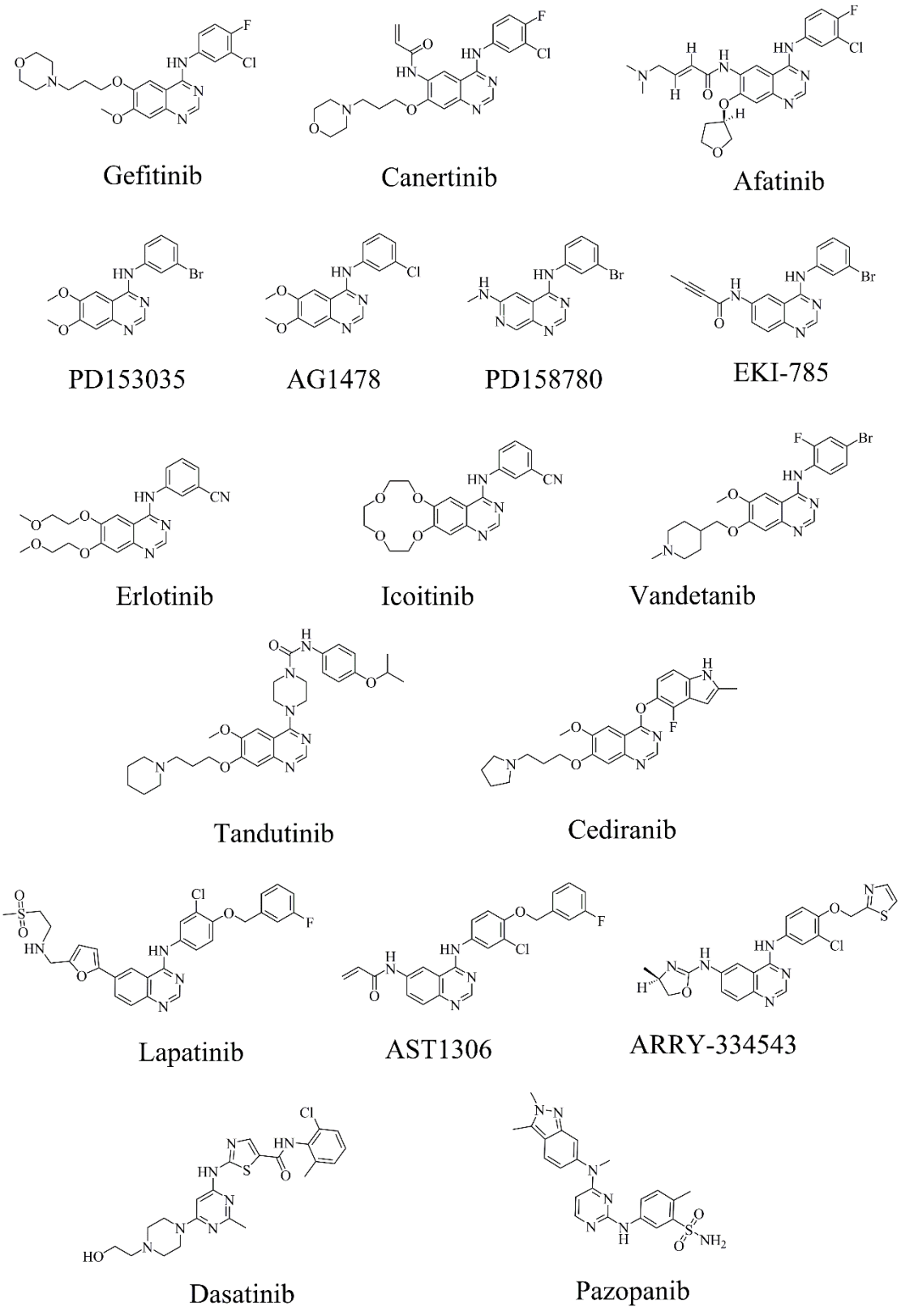

Figure 8: Structures of selected TKIs which are reported to be ABCG2 inhibitors[116]

1.3 Biochemical evaluation of ABCG2 inhibitors

In the following chapters, different types of compounds were synthesized as ABCG2 inhibitors. To compare and evaluate the inhibitory effects of different inhibitors, Hoechst 33342 and pheophorbide A accumulation assays were carried out.

Hoechst 33342 is a bis-benzimidazole fluorescent dye which binds to cell membrane and the minor groove of double-stranded DNA in live or fixed cells. It can be efficiently excited by ultraviolet light (361nm when bound to double-stranded DNA) and emits blue fluorescence at 460-490 nm wavelength. Although it can bind with any nucleic acids in DNA strands, binding with AT (adenine-thymine) regions enhances fluorescence obviously. The exact emission spectra are dependent on the ratios of dyes to base pairs. Pheophorbide A is a photosensitizer for photodynamic therapy and its fluorescence emission does not require to bind to DNA. The absorption maximum of pheophorbide A is at 395 nm and the emission maximum at 670 nm.

In table 4, we introduced both of them as substrates of ABCG2. They will be effluxed by ABCG2 leading to weaker intracellular fluorescence in ABCG2-overexpressing cells than in normal cells. Inhibition of ABCG2 will increase the intensity of fluorescence owing to higher intracellular concentration of Hoechst 33342 or pheophorbide A (Figure 9). Therefore, quantitatively evaluating inhibitory effects of different inhibitors is possible by detecting intensity of intracellular fluorescence. A representative concentration-response curve of Ko143 is displayed in Figure 10. Alongside the increase of concentration of Ko143, the intracellular fluorescence is intensified until it reaches a plateau.

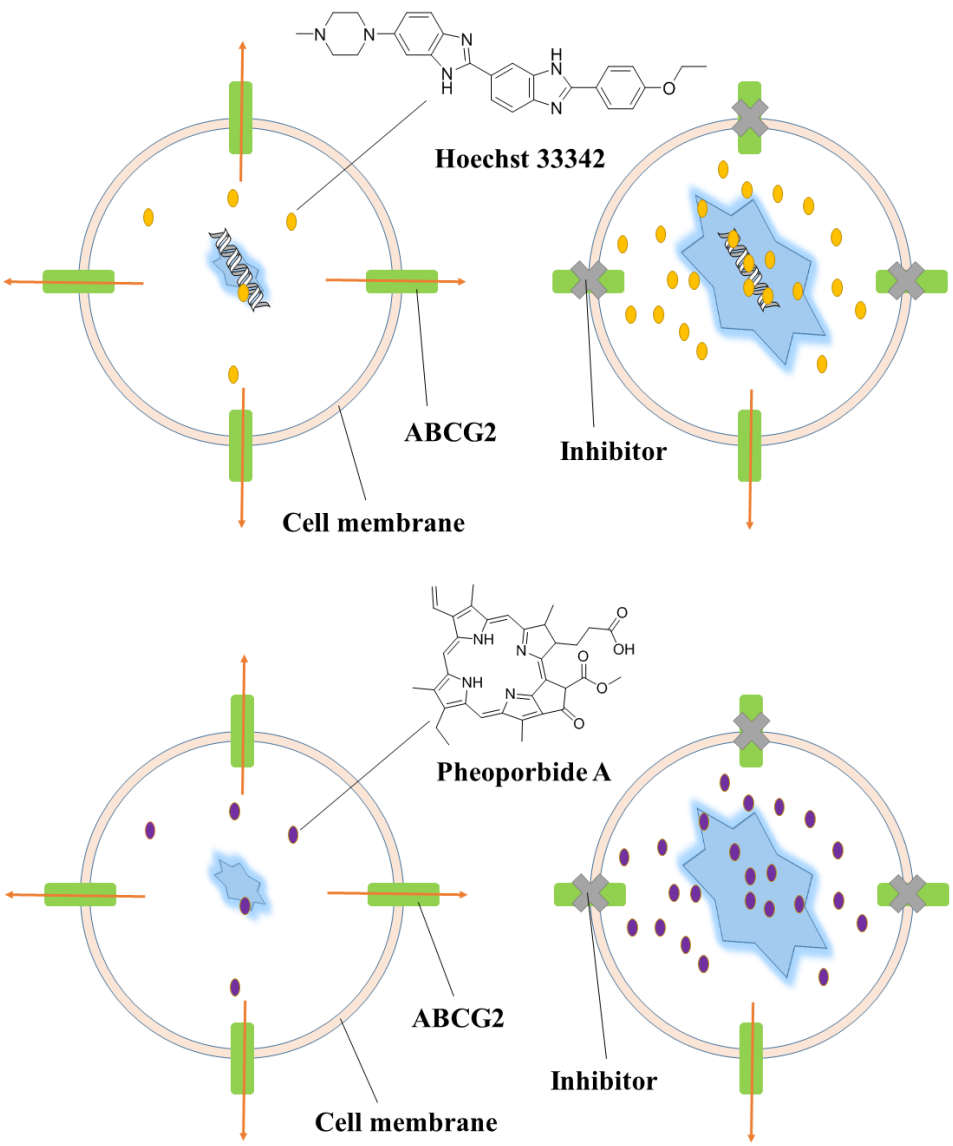

Figure 9: Accumulation of Hoechst 33342 and pheophorbide A.

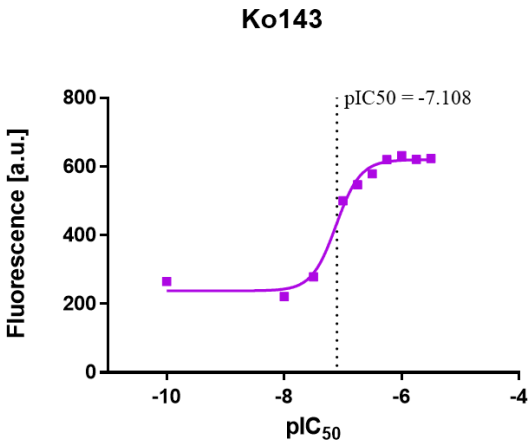

Figure 10: Concentration-response curve of Ko143 in pheophorbide A assay

The curve can give two important parameters which are useful for evaluating inhibitory activities of various inhibitors. One parameter is IC_{50} value which is the inflection point of curve and shown in Figure 10. The other is plateau value of maximal inhibition which demonstrates the maximal inhibitory effect of a compound. After comparing the maximal fluorescence values of tested inhibitor and reference compound, I_{max} value can be calculated via equation:

$$I_{max}(\%) = \frac{F_{max}(inhibitor) - F_{min}(inhibitor)}{F_{max}(reference) - F_{min}(reference)} \times 100\%$$

For example, Figure 11 shows two concentration-response curves. Purple line belongs to Ko143 and green line belongs to compound LJY-114. We set Ko143 as reference compound which means its I_{max} was set as 100% and its span (F_{max}-F_{min}) is 447. But the span of LJY-114 is only 187. According to the equation, I_{max} of LJY-114 is 42%. It is only a partial inhibitor. Although the pIC_{50} value of LJY-114 is -7.32 which is lower than -7.108 of Ko143, LJY-114 is still obviously less potent than Ko143.

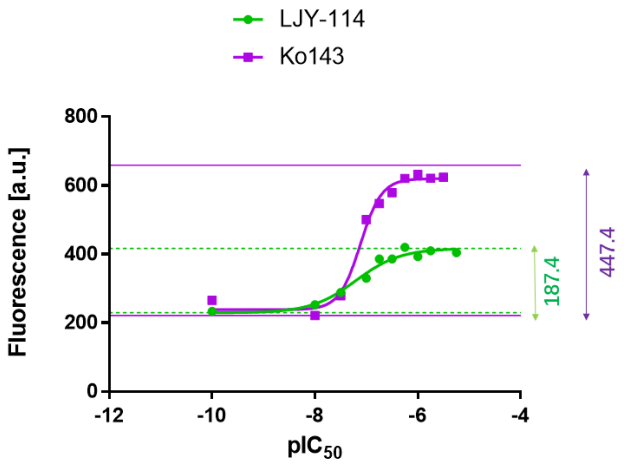

Figure 11: Concentration-response curve of LJY-114 and Ko143 in pheophrobid A assay

The compound with both higher I_{max} and lower IC_{50} value is regarded as more potent ABCG2 inhibitor.

In comparison to Hoechst 33342 assay, pheophorbide A assay has three advantages. (1) The range of Hoechst 33342 emitting wavelength is at 460-490 nm which is overlapped with some compounds which also have fluorescence properties. But pheophorbide A emits at 670 nm which is never reached by all tested compounds in this thesis. (2) Hoechst 33342 is not only transported by ABCG2, but also by P-gp. But pheophorbide A is a specific ABCG2 substrate. Therefore, the source of error derived from P-gp exportation is excluded. (3) The measurement of fluorescence is applied only in healthy cells which are detected on a FACSCalibur flow cytometer. All of these factors lead to higher accuracy of biochemical results. But the measurement process of pheophorbide A assay is also time-consuming, Hoechst 33342 assay is faster. Therefore, we applied an evaluating strategy for all synthesized compounds. The compounds were tested in Hoechst 33342 assay at first. After analysis, some interesting modulators were selected to be tested in pheophorbide A assay. The detailed biochemical data of every modulator are provided in following chapters.

All biological work presented in this thesis was done by Katja Silberman.

2 Aim of the work

In introduction chapter, we have presented some tyrosine kinase inhibitors that also demonstrated ABCG2 inhibition (Figure 8). After comparing structures of these selected TKIs, it is noticed that most of them shared the same scaffold — 4-anilinoquinazoline. Inspired by this observation, much work has been done in our group to investigate potent ABCG2 inhibitors.

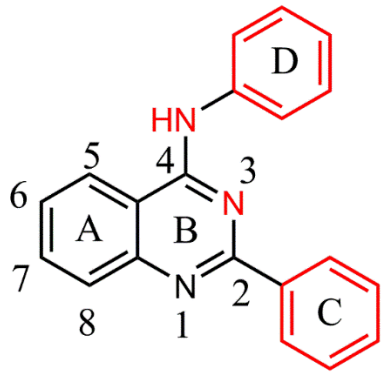

Figure 12: The essential features (red) of 4-anlinoquinazolin derivatives for ABCG2 inhibition.

Pick et al. determined the potency of seven different TKIs (gefitinib, erlotinib, AG1478, PD158780, PD153035, nilotinib and imatinib) for overcoming resistance of ABCG2, ABCB1 and ABCC1.[117] As a result, these compounds obviously displayed higher affinity towards ABCG2 than ABCB1 and ABCC1. In both Hoechst 33342 and pheophorbide A assays, all of them yielded IC_{50} values which were less than 10 µM and PD158780 even reached nanomolar level. Subsequently, Juvale et al. adopted 4-anilinoquinazoline as scaffold and investigated dozens of derivatives as novel ABCG2 inhibitors.[118, 119] Several variations at positions 2, 4, 6 and 7 of quinazoline ring were carried out. When both position 6 and 7 were substituted by methoxy, the inhibitory activities decreased in comparison to unsubstituted compounds. When position 2 was substituted by phenyl, 3,4-dimethoxyphenyl or substituted aniline, the potency was significantly improved. However, some weakness including cytotoxicity and potential

solubility problem limited the further exploration. At position 4, different substituents on aniline moiety were applied. In general, *meta*-substituted aniline produced higher activity than corresponding *ortho*- or *para*-substituted aniline. NO_2, CN, CF_3 were found to be optimum substituents. Afterwards, Spindler et al. further investigated position 3 and 4.[120] Replacing quinazoline scaffold as quinoline apparently decreased potency against ABCG2 as well as replacing N of aniline moiety at position 4 by O or S. Besides, Krapf et al. has done more variations in the scaffold.[121-123] At position 4, phenyl of aniline moiety was replaced by cyclohexane ring and a drastic decrease of activity was observed. Meanwhile, the replacement of the hydrogen atom of NH linker at position 4 by methyl group drastically decreased the inhibitory efficiency. Therefore, hydrogen atom, nitrogen atom and phenyl of aniline moiety were all proven crucial for interaction with ABCG2. Furthermore, the influence of different substitutions was also explored. Substitution in *meta* and *para* positions led to higher potencies than *ortho*. It might be attributed to reduced planarity derived from *ortho* substitution which resulted in more twisted conformation. Planarity is regarded as an important feature of potent ABCG2 inhibitors. Whereas, the electronic effect of the substituents did not exert obvious effect on activity as well as steric requirement. No apparent correlation between IC_{50} value and bulkiness of substituents was demonstrated. Cyano, nitro (electron-withdrawing group) and hydroxyl (electron-donating group) were all potent substituents no matter at *meta* or *para* position. But when both aromatic rings at position 2 and 4 were substituted, the combination of substituents with opposite electronic effects was favorable. For example, the combination of 3,4-dimethoxy and nitro group led to highly potent ABCG2 inhibitors with IC_{50} values below 100 nM. Besides, phenyl at position 2 was replaced by *o*-, *m*- and *p*- pyridyl, thienyl and pyrrolyl. Although they led to higher solubility and lower cytotoxicity, the potency on ABCG2 inhibition was not improved. Correlation between log P and IC_{50} values of many substances was studied. Although membrane permeability would prefer more lipophilic compounds, no clear correlation was observed. Several compounds which had similar log P values

showed different inhibitory activities and *vice versa*. Besides, swapping substituents at at position 2 and 4 did not lead to distinct activity. This might indicate the interchangeability of substituents at corresponding aromatic systems. Replacing carbon at position 8 by nitrogen did not show negative effect on potency. When position 6 was substituted by nitro group but not amine or amide, the activity was improved. Replacement of the left benzene ring of quinazoline scaffold by a methyl group had no negative effect on the inhibitory efficiency.

In summary, the essential features of 4-anlinoquonazolin derivatives for ABCG2 inhibition are depicted in Figure 12. Phenyl ring at position 2, N at position 3, NH linker and phenyl ring of aniline at position 4 are indispensable parts. Removal of any of them would lead to apparent decrease of activity. *Ortho* substitution at position 2 and position 4 should be avoided as well as methoxy substituents at position 6 and 7.

In this thesis, we adopted the results described above and did other modifications which are briefly illustrated below.

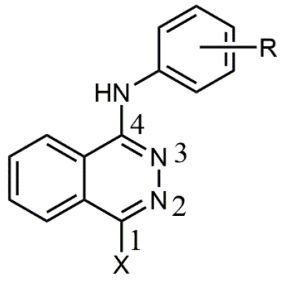

Project 1

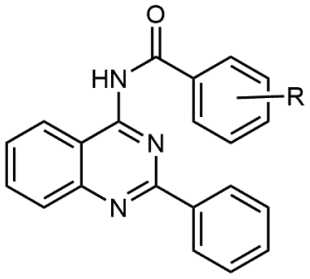

Project 2

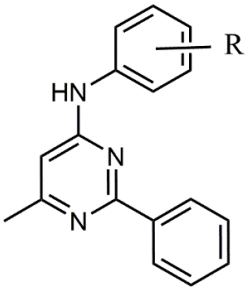

Project 3

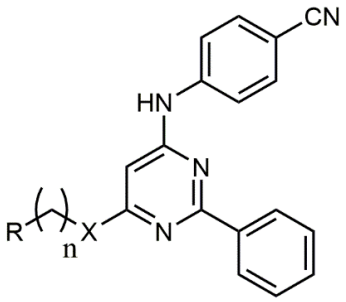

Project 4

Figure 13: Overview of all projects.

1. In project 1, the importance of a nitrogen atom at position 1 of the quinazoline scaffold was investigated. We exchanged carbon at position 2 and nitrogen at position 1 in quinazoline scaffold and synthesized dozens of mono- or bis-substituted phthalazine derivatives to investigate the potency of these compounds as ABCG2 inhibitors. Due to the unfavorable effect of *ortho* substitution on quinazoline derivatives, we only carried out substitution at *meta* and *para* position for phthalazine derivatives. The results are discussed in detail in phthalazine chapter.
2. In project 2, the influence of replacing linker at position 4 was investigated. As mentioned before, NH and phenyl of aniline moiety are all crucial features. Planarity was also an important characteristic of potent ABCG2 inhibitors. We applied a strategy which not only preserved the essential features but also improved the planarity of molecular conformation — replacement of NH linker between aromatic ring B and D by amide and urea linker. The results are discussed in detail in quinazoline chapter.
3. In project 3, we continued the work of our colleague on pyrimidine derivatives. In comparison to corresponding quinazoline derivatives, several pyrimidine derivatives with a methyl group at position 6 improved solubility and demonstrated similar inhibitory effects on ABCG2. Inspired by this preliminary study, we introduced a broader spectrum of substituents on aniline moiety and investigated the activities of derivatives. The results are discussed in detail in pyrimidine I chapter.
4. In project 4, potential modifications at position 6 of pyrimidine scaffold were investigated. As mentioned before, replacement of carbon of quinazoline ring as nitrogen did not exhibit any negative effect on ABCG2 inhibition. Therefore, methyl group at position 6 of pyrimidine ring was altered while other critical

features were preserved. The results are discussed in detail in pyrimidine II chapter.

3 Project I: Phthalazine derivatives as ABCG2 inhibitors

3.1 Overview

The previous studies revealed the influence of variation at position 2, 3, 4, 6, 7 and 8 of quinazoline scaffold on ABCG2 inhibtion, but the effect of variation at position 1 was not clear. Therefore, in this chapter, we introduced anilinophthalazine as novel scaffold of ABCG2 inhibitors. It preserves N at position 3 and aniline moiety at position 4 which were proven crucial for ABCG2 inhibition.

Phthalazine derivatives were reported to possess different biological activities. Some of them have been used in the clinic. Hydralazine, patented in 1949, was used to treat high blood pressure and heart failure. Budralazine was an antihypertensive drug due to its vasodilator property. Zopolrestat showed potential use in prevention of diabetes by inhibiting aldose reductase. Azelastine was an antihistaminic drug and often used for treatment of allergic rhinitis. These successful samples suggest phthalazine is a potent drug-like scaffold. The synthesis and biological investigation of its derivatives are discussed below.

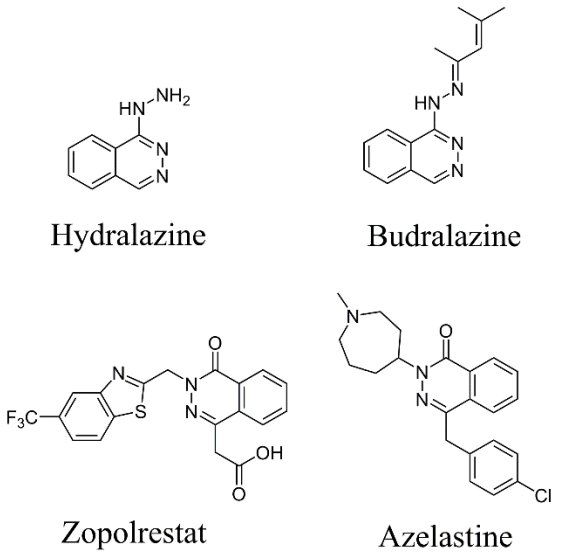

Figure 14: Selected drugs with phthalazine scaffold

3.2 Synthesis

The modification was divided into two parts. On one hand, amination was only carried out at position 4. Position 1 of phthalazine scaffold was unsubstituted or substituted by Ph or Cl. On the other hand, both position 1 and 4 were substituted with anilines. The aniline moiety at position 1 might compensate for the loss of phenyl ring at position 2 of 4-anilinoquinazoline scaffold which was also proven essential for inhibiting ABCG2. The general synthesis scheme is described in Scheme 1 and the reaction mechanism in Scheme 2.

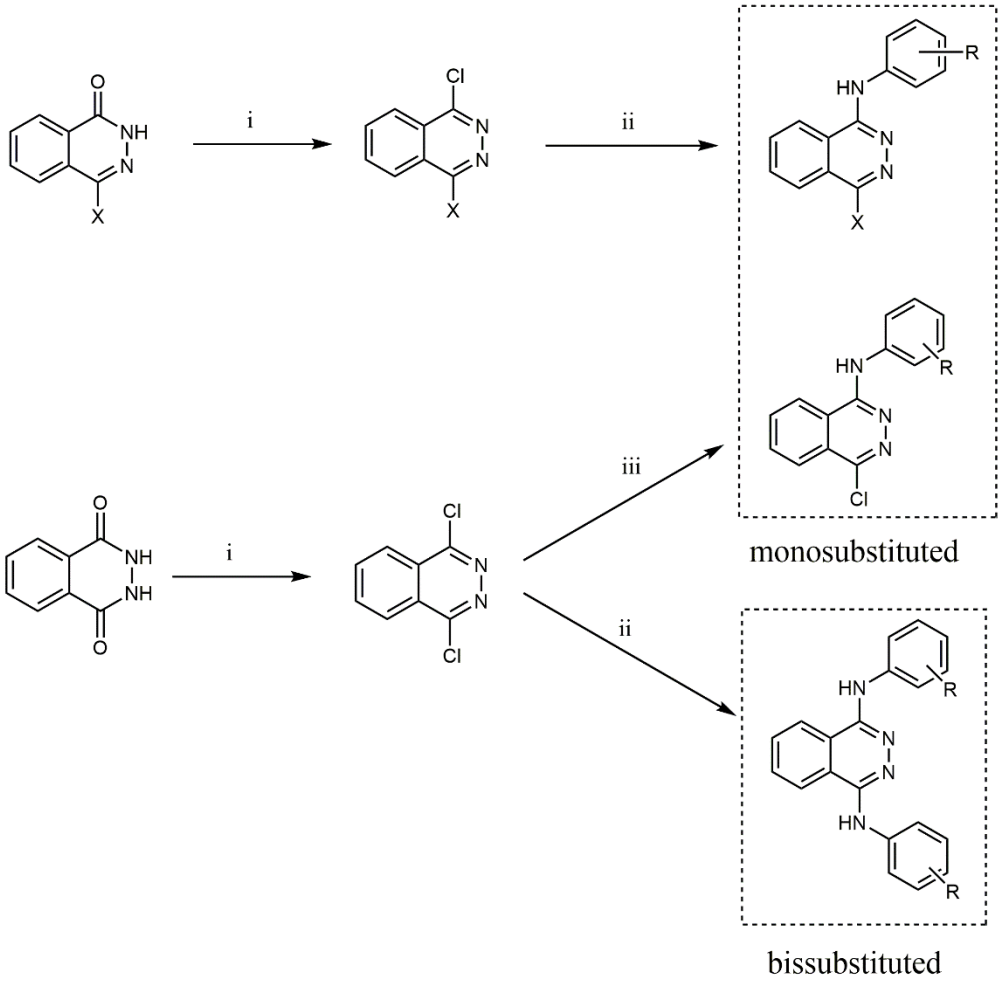

Scheme 1: General synthesis scheme of anilinophthalazine derivatives[*]

[*]: Reagents and conditions for synthesis of phthalazine derivatives (X = Ph or H): (i) POCl3, reflux, 8-9 h (ii) i-PrOH, microwave, 70 - 110 °C, 30 min. (iii) i-PrOH, reflux, overnight.

Phthalazones (commercially available) were chlorinated using phosphorus oxychloride to afford corresponding chlorophthalazines. Subsequently, nucleophilic heteroaromatic substitution was performed on the obtained chlorinated phthalazine to produce various substituted anilinophthalazines. Substituents were selected according to potency of corresponding quinazoline derivatives and were only introduced at *meta*- or *para*-position of aniline moiety. In case of 1,4-dichlorophthalazine, ratio of 1,4-dichlorophthalazine to aniline determined products with mono- or bis-substitution. The mechanism is described below.

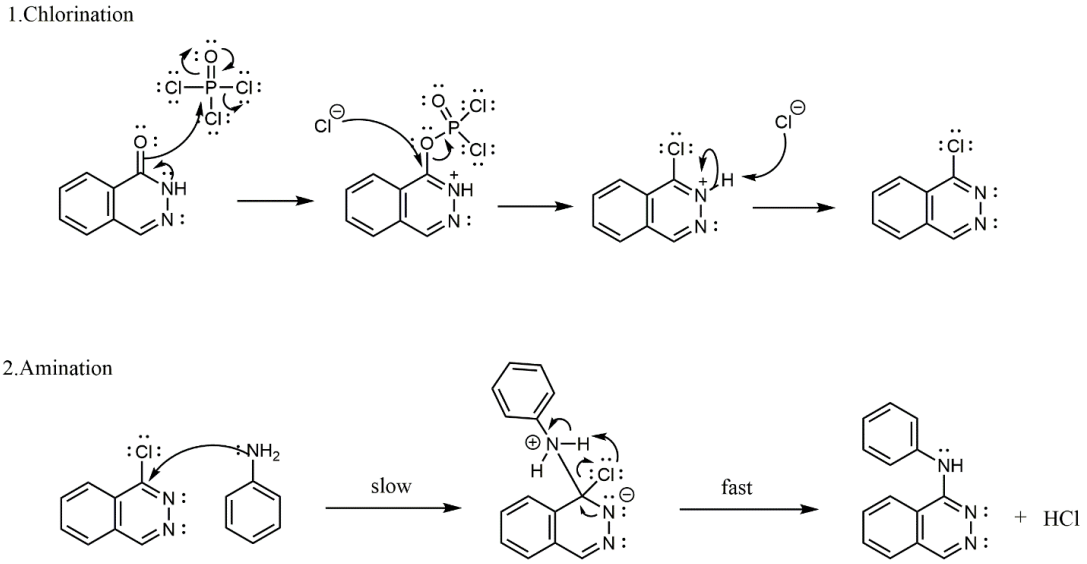

Scheme 2: Proposed mechanism for synthesis of anilinophthalazine derivatives.

Chlorination of phthalazone is achieved by treatment with phosphorus oxychloride which is widely used in activating Cl formation. Amide of phthalazone reacts with phosphorus oxychloride to produce an electrophilic iminium cation at first. Subsequently, this imninium cation is attacked by chloride to give imidoyl chlorides cation which is deprotonated to afford chlorophthalazine.

Amination of chlorinated phthalazine is generally assumed to proceed via S_NAr_2 mechanism.[124-126] This mechanism is supported by spectroscopic, synthetic, and kinetic studies.[127] Due to the electrophile property of carbon of imidoyl chloride, it is attacked

by nitrogen of aniline to produce an unstable cyclohexadienide intermediate. This step is postulated as rate determining. Afterwards, chloride is quickly eliminated to give final compounds.

In 1971, Hill et al. published a study about the kinetics of the methoxydechlorination of a series of 1-chloro-4-substituted phthalazines and related compounds.[124] They found the reaction was quite sensitive to the nature of X at position 4 of phthalazine ring. Decreased electron density on the ring facilitated reaction. This is also probably applicable to our reaction. The details about synthesis and potential pitfalls are described in experimental section.

3.3 Results and Discussion

The inhibitory potency of synthesized phthalazine derivatives was investigated in Hoechst 33342 accumulation assay. ABCG2 overexpressing MDCK II BCRP and parental cell line were used in biological test. More information about Hoechst 33342 accumulation assay is described in introduction chapter. WK-X-24 (XR9577) was used as a standard inhibitor due to its easy availability and lower cost than Ko143. The activity data of monosubstituted and bis-substituted phthalazine derivatives are shown in Tables 6 and 7. The potency of compounds was evaluated not only by IC_{50} value, but also by maximal inhibition which is discussed in introduction chapter. When the maximal plateau of a partial inhibitor is low enough, it is not worth to report IC_{50}. Therefore, to simplify discussion, all compounds with I_{max} less than 50% are regarded as inactive.

3.3.1 Biological investigation of monosubstituted phthalazine derivatives

Firstly, position 1 of phthalazine scaffold was unsubstituted and we only modified position 4 with different substituted anilines. The study of quinazoline derivatives

Table 6: Inhibitory potency of synthesized monosubstituted phthalazine derivatives against ABCG2 in the Hoechst 33342 accumulation assay.

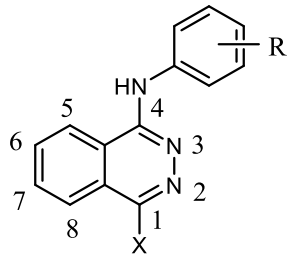

No.	X	R	$IC_{50} \pm SD^{*}$ [µM]	$I_{max} \pm SD^{\#}$ [%]
2	H	3,4-OCH_3	n.a.	16 ± 2
3	H	3-Br	n.a.	16 ± 2
4	H	3-CN	n.a.	14 ± 1
5	H	4-F	n.a.	11 ± 2
6	H	4-NO_2	n.a.	15 ± 3
7	Ph	3,4-OCH_3	4.18 ± 0.64	62 ± 4
8	Ph	3-OH	6.26 ± 1.44	-[a]
10	Cl	3,4-OCH_3	1.26 ± 0.18	74 ± 10
11	Cl	3-OCH_3	n.a.	34 ± 5
12	Cl	3-Br	n.a.	46 ± 4
13	Cl	4-F	n.a.	29 ± 7
14	Cl	3-CN	n.a.	24 ± 6
15	Cl	4-NO_2	n.a.	40 ± 7
16	Cl	3-NO_2	n.a.	46 ± 9
17	Cl	3-OH	n.a.	42 ± 5
18	Cl	4-CN	n.a.	26 ± 6
WK-X-24	-	-	0.704 ± 0.147	100

[*]: Data are expressed as mean ± SD (n = 3)

[#]: Percentage of inhibition with regard to WK-X-24

[a]: plateau of curve was fixed to top of Ko143.

n.a. = not active

showed when R is on *meta* or *para* position of aniline moiety, compounds are generally more active than *ortho* positon substituted compounds. Thus, 3,4-dimethoxy, 4-fluoro, 4-nitro, 3-bromo and 3-cyano were initially introduced as substituents. However, their negligible maximal responses revealed all of them had no inhibitory effects on ABCG2. It suggested, except substituted aniline at position 4 and N at position 3, some other indispensable parts were missing.

Next, position 1 was also included in the modification. As described before, when a phenyl ring is introduced at position 2 of quinazoline scaffold, the inhibitory activity against ABCG2 is significantly improved. Therefore, we also took Ph as priority for modifying position 1 of phthalazine scaffold. Besides, chlorine was introduced as the other choice. 3,4-dimethoxy and 3-methoxy were firstly chosen as substituents at the aniline ring, because methoxy in different series of compounds was reported to play a role in ABCG2 inhibition.[128-130] Interestingly, substantial difference of inhibition was observed. Compound **7** and **10** (both bearing 3,4- dimethoxy group) displayed 62% and 74% maximal inhibition respectively. Whereas, compound **11** (bearing 3-methoxy group) could only achieve 34%. Both compound **7** and **10** demonstrated significantly promoted maximal inhibition than compound **2**. All compounds with substitution at position 1 (**7** to **11**) displayed improved inhibitory effects compared to unsubstituted compounds (**2** to **6**). Therefore, it is reasonable to assume that X at position 1 of phthalazine scaffold is also a necessary part for ABCG2 inhibition. Nevertheless, phenyl ring did not improve activity as much as chlorine did. Compound **10** containing Cl at position 1 was more active than **7** containing Ph at position 1. An explanation is attributed to planarity which is thought as an important property for designing ABCG2 inhibitors.[131] Due to the steric hindrance, Ph does not prefer to share same plane with phthalazine scaffold and steric strain in compound **7** and **8** were regarded as an unfavorable feature for ABCG2 inhibition.

Afterwards, the moderate inhibitory effect of compound **10** motivated us to further explore the influence of aniline ring while keeping the substituent at position 1 as

chlorine. Seven more structurally similar compounds (**12** to **18**) were synthesized. Although the positive role of Cl is evident in compound **12** to **15** by comparison to compounds **3** to **6**, they are still partial inhibitors. All of their I_{max} data were lower than 50%. Hence, substituting position 1 with Cl is still not a very effective strategy.

Instead of replacing Cl as new element, we decided to elongate the substituent at position 1 of phthalazine scaffold. Bis-substituted derivatives were synthesized. The aniline moiety at position 1 might also be a substitute for the crucial Ph at position 2 of quinazoline scaffold. The biological data are shown below.

3.3.2 Biological investigation of bis-substituted derivatives

As mentioned before, 3,4-OMe and 3-OMe bis-substituted compounds were explored initially. Unlike monosubstitution, 3,4-OMe didn't show distinct advantage over 3-OMe. Bis-substituted compound **19** (3,4-OMe) showed lower IC_{50} value than **20** (3-OMe), but its maximal plateau was not as high as the latter one. Comparing both monosubstituted and bis-substituted compounds led to an interesting observation. Comparing compound **10** versus **19** (3,4-OMe), bis-substituted compound **19** demonstrated only slightly improved activity than monosubstituted compound **10**. Whereas, in compound **11** versus **20** (3-OMe), the activity of compound **20** was considerably increased and its maximal inhibition was comparable to WK-X-24. It might indicate the number of methoxy groups might be a factor that influences the activity. Inspired by potency of compound **20**, eight more bis-substituted compounds were synthesized subsequently.

As shown in table 7, compound **21** (4-F) displayed low inhibitory activity towards ABCG2. The I_{max} data of compounds **22**, **23** and **24** were negligible. It might be owing to their poor solubility or lipophilicity. However, 3-CF_3 and 3-Br bis-substituted derivatives (**25** and **26**) displayed complete inhibition and high potency. The latter one was even more potent than the standard inhibitor. Although, 3-CF_3, 3-Br and 3-OMe

have different electrostatic effect on aniline ring, compounds **20**, **25** and **26** exhibit comparable ABCG2 inhibition results. Therefore, it is reasonable to assume that electrostatic properties (electron-withdrawing or electron donating) of substituents in aniline moiety are not essential for ABCG2 inhibition.

Table 7: Inhibitory potency of synthesized bis-substituted phthalazine derivatives against ABCG2 in the Hoechst 33342 accumulation assay.

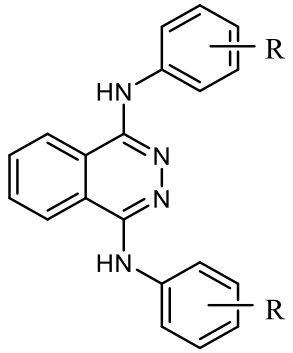

No.	R	IC_{50} ± SD* [μM]	I_{max} ± SD# [%]
19	3,4-OCH_3	1.01 ± 0.07	76 ± 17
20	3-OCH_3	3.13 ± 0.33	93 ± 5
21	4-F	n.a.	20 ± 4
22	3-NO_2	n.a.	0
23	4-NO_2	n.a.	0
24	3-OH	n.a.	0
25	3-CF_3	1.70 ± 0.18	94 ± 8
26	3-Br	0.652 ± 0.099	96 ± 30
27	3-CN	n.a.	25 ± 4
28	4-CN	1.01 ± 0.17	61 ± 18
WK-X-24	-	0.704 ± 0.147	100

**: Data are expressed as mean ± SD (n = 3)*

#: Percentage of inhibition with regard to WK-X-24

n.a. = not active

At last, compounds **27** (3-CN) and **28** (4-CN) were synthesized. While compound **28** is a moderate ABCG2 inhibitor, compound **27** is apparently inactive. Due to the similar lipophilicity and electrostatic property of them, the substantial difference in inhibitory potency might be attributed to steric effect.

Table 8: Comparative study of selected phthalazine and quinazoline derivatives against ABCG2 in the Hoechst 33342 accumulation assay.

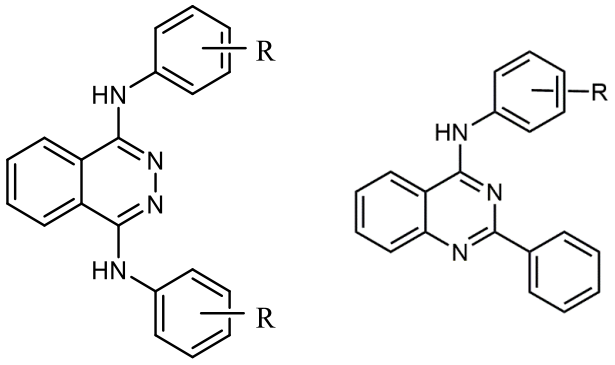

R	IC_{50} ± SD (μM)	IC_{50} ± SD[#] (μM)
3,4-OCH_3	1.01 ± 0.07	0.19 ± 0.01
3-OCH_3	3.13 ± 0.33	1.32 ± 0.10
3-CF_3	1.70 ± 0.18	0.25 ± 0.10
3-Br	0.652 ± 0.099	0.57 ± 0.04
3-CN	n.a.	0.14 ± 0.04

#: IC_{50} value taken from reference.[118]

n.a. = not active

In summary, some phthalazine derivatives were synthesized and evaluated as ABCG2 inhibitors. Several factors that might exert effects on the activity are discussed below: (i) variation of substituents at position 1 of phthalazine scaffold showed apparent influence on ABCG2 inhibition. (ii) Bis-substituted phthalazine derivatives demonstrated higher affinity towards ABCG2 than monosubstituted derivatives. (iii) As substituents on aniline moiety, 3,4-dimethoxy was more favorable than 3-methoxy in the monosubstituted series. But in bis-substituted series, they did not show

substantial difference. (iv) Lipophilicity and steric effect, but not electrostatic property, might be important determinants in these series of compounds for ABCG2 inhibition.

Although several compounds (**10**, **19**, **20**, **25** and **26**) in this series displayed apparent inhibitory effects against ABCG2 and compound **26** was even more potent than WK-X-24, the comparative study revealed that phthalazine did not show an advantage in comparison to quinazoline scaffold. In table 8, it is obviously seen that all of the selected potent phthalazine derivatives were less potent than the corresponding quinazoline derivatives. Therefore, swapping N and C of quinazoline scaffold at position 1 and 2 might not be an effective strategy. Nitrogen at position 1 might also be an essential component for ABCG2 inhibition. In the next chapter, we further explored quinazoline derivatives.

4 Project II: Quinazoline derivatives as ABCG2 inhibitors

4.1 Overview

In view of high-affinity of 4-anilino-2-phenylquinazoline derivatives towards ABCG2, we stopped phthalazine exploration and continued to investigate quinazonlines. Quinazoline, a heterocyclic compound, is an important skeleton in medicinal chemistry. Its derivatives have displayed a broad spectrum of therapeutic and pharmacological properties such as antihypertensive,[132] anticonvulsant,[133] antimalarial,[134] antibacterial and anti-inflammatory.[135] A variety of quinazoline derivatives were also developed as potent anticancer drugs.

Some of these anticancer drugs based on the quinazoline scaffold were reported as modulators of ABC transporters. In previous chapters, it was described that many TKIs with quinazoline scaffold were potent ABCG2 inhibitors. From the structure-activity-relationship presented, planarity was thought to be an important descriptor for designing potent ABCG2 inhibitors. In some series of compounds, more planarity correlated with improved ABCG2 affinity. Thus, we decided to keep all of the crucial components described before and increase planarity of quinazoline derivatives.

2-phenyl-4-anilinoquinazoline derivatives were shown to possess excellent potency as ABCG2 inhibitors. Since the hybridization type of nitrogen in aniline is between sp^2 and sp^3, quinazoline scaffold does not share the same plane with aniline ring at position 4. To increase planarity, we introduced amide and urea linkers at position 4. Thus, a planer conformation would be preferred. The synthesis scheme and biological activities are discussed below.

4.2 Synthesis

Novel quinazoline derivatives were synthesized in two steps (Scheme 3). In step 1, anthranilonitrile and benzonitrile reacted with strong base at high temperature to produce 4-amino-2-phenylquinazoline. In step 2, 4-amino-2-phenylquinazoline either condensed with substituted benzoic acid or substituted phenyl isocyanate under mild conditions to afford final products. Substituents were selected from the potent 4-anilino-2-phenylquinazoline derivatives and were only introduced at *meta*- or *para*-position of aniline moiety. The mechanism of each step is described below.

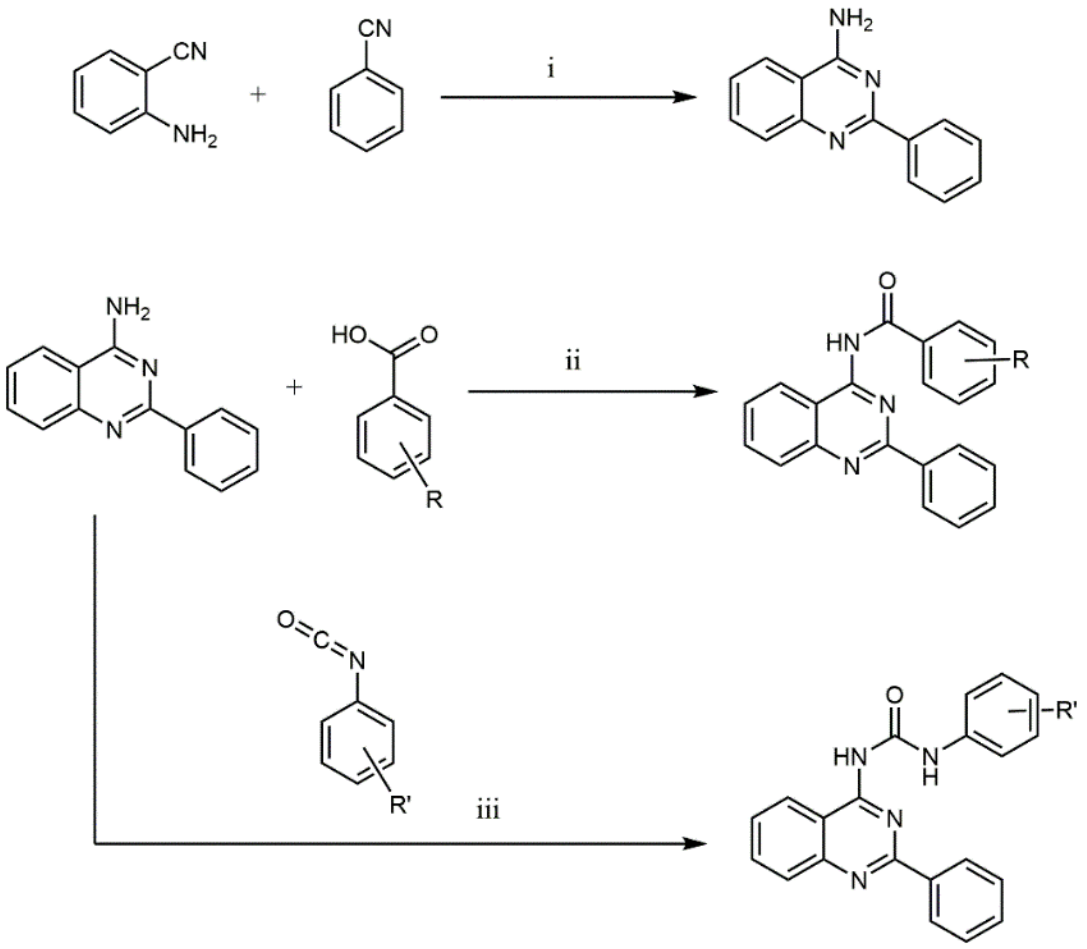

Scheme 3: Synthesis of 2-phenylquinazoline derivatives.[*]

[*]*: Reagents and conditions for synthesis of 2-phenylquinazoline derivatives: (i) t-BuOK, 150 watt microwave irradiation, 170 °C, 5 mins. (ii) TBTU, DIPEA, DMF, 85°C, overnight (iii) anhydrous THF, RT, overnight.*

4.2.1 Synthesis of 4-amino-2-phenylquinazoline

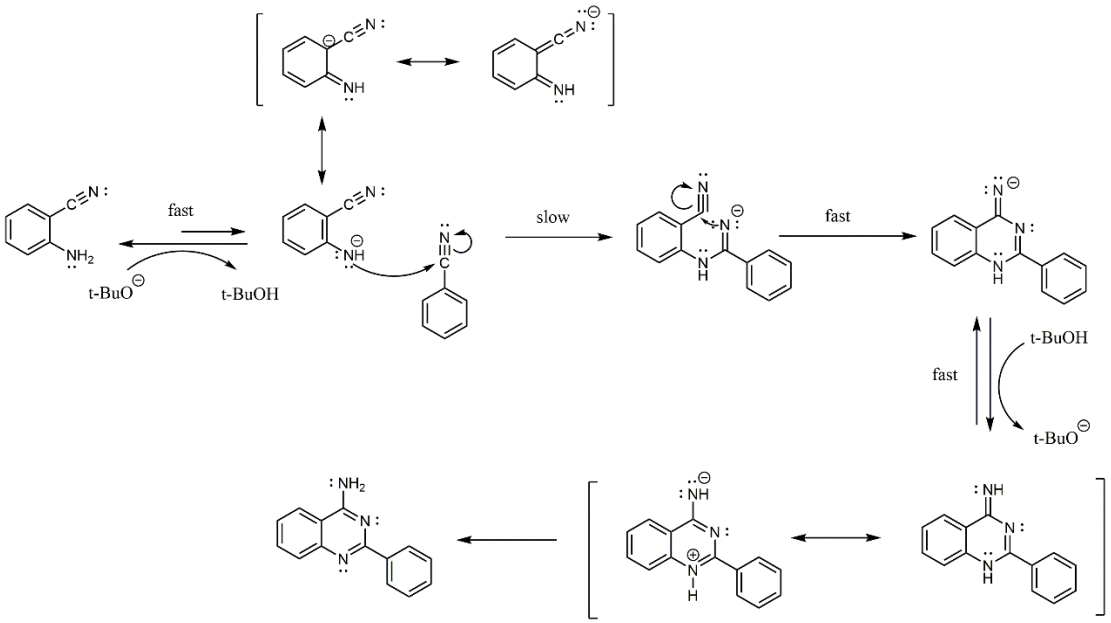

Scheme 4: Proposed synthesis mechanism of 4-amino-2-phenylquinazoline adapted from Ogata et al. [136-138]

The preparation of 4-amino-2-phenylquinazoline was performed following the base-catalyzed synthetic strategy described by Seijas et al.[139] They simplified the synthesis by carrying out reaction under microwave condition. Anthranilonitrile, benzonitrile and potassium tert-butoxide reacted at high temperature until no starting materials were observed. After protonation and purification, final 4-amino-2-phenylquinazoline was obtained. The details about experiment procedures and potential pitfalls are described in experiment section.

The synthesis mechanism of 4-amino-2-phenylquinazoline is depicted in Scheme 4. It was adapted from the work of Ogata et al. who had done much kinetic studies about formation of different aromatic amines from dicyandiamide and nitriles.[136-138] Firstly, treatment of 2-aminobenzonitrile with strong base potassium tert-butoxide results in an equilibrium between 2-aminobenzonitrile and its deprotonated anion. Due to mesomeric effect, the anion is relatively stable. Afterwards, the intermediate anion (nucleophile reagent) attacks nitrile leading to an intermediate amidine. This intermolecular amine-nitrile condensation is the rate-determining step. Subsequently, a

six-membered ring closure occurs due to the second, intramolecular, amine-nitrile condensation reaction. At last, final product is obtained after protonation by alcohol. Although the equilibrium between starting material and amine anion is undoubtedly favorable to starting material, the intermediate amidine is removed from equilibrium by conversion into the aromatic and stable 4-aminoquinazoline system.

4.2.2 Formation of amide linker

The second step is to build the amide linker at position 4 of quinazoline scaffold. Many papers about amide bond formation have been published.[140, 141] It usually starts by activating carboxylic acid which means converting OH of the acid into a good leaving group. In our reaction, TBTU was used as activating reagent. Afterwards, condensation is achieved by treatment with desired amines. The details about experiment procedures and potential pitfalls are described in experimental section.

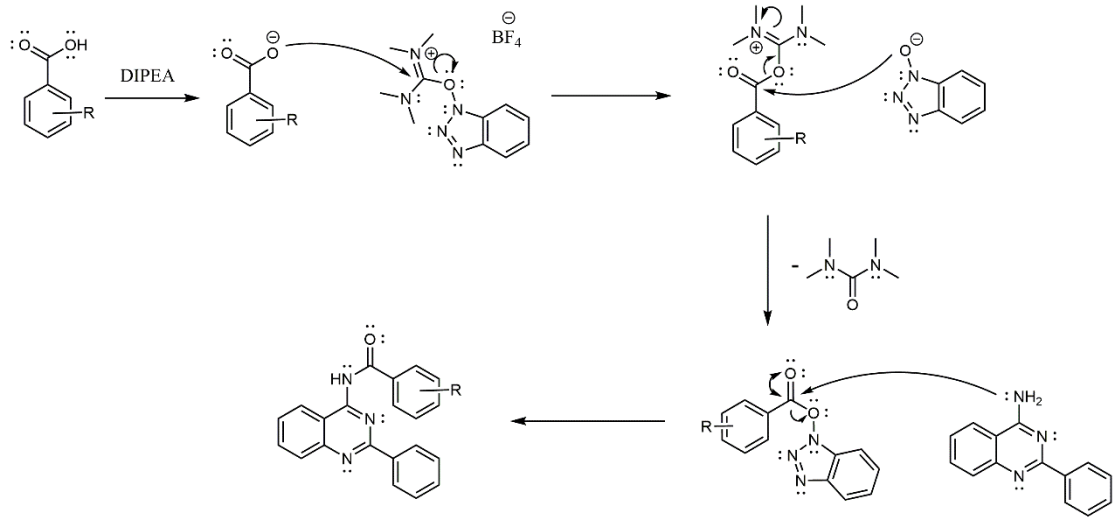

Scheme 5: Mechanism of forming amide bond which was adapted from Valeur et al.[141]

The coupling mechanism is depicted in Scheme 5. Substituted benzoic acid was deprotonated by organic base to afford benzonate anion which attacks uronium center of TBTU. A novel uronium intermediate is obtained. Subsequently, the left 1H-

benzotriazole-1-hydroxy ion attacks back to carbonyl center but not uronium center of the intermediate to afford 1-benzoyloxybenzotriazole. This intermediate ester is similar to TBTU. They both contained 1H-benzo[d][1,2,3]triazol-1-ol which is a good leaving group. Therefore, it could easily be attacked by amine group of 4-amino-2-phenylquinazoline to obtain final product. The driving force of whole reaction is the generation of the urea by-product.

4.2.3. Formation of urea linker.

Except amide linker, several compounds with urea as linker at position 4 were synthesized. 2-phenyl-4-aminoquinazoline and substituted phenyl isocyanate reacted in anhydrous THF at room temperature overnight. After filtration and recrystallization, final products were obtained. The low solubility of the products in THF simplified the isolation and purification.

The mechanism is displayed in Scheme 6. Due to higher electronegativity of N and O, isocyanate is an electrophile group with C as electrophile center. As such, it is reactive to a variety of nucleophiles including alcohols, amines, and even water. Therefore, amine group of 2-phenyl-4-aminoquinazoline could easily attack isocyanate resulting in an intermediate which finally afford urea products.

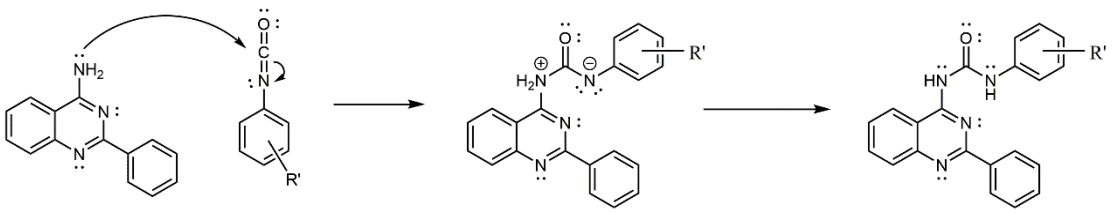

Scheme 6: Proposed mechanism of urea linker formation.

4.3. Results and discussion

The inhibitory potency of synthesized quinazoline derivatives was investigated in Hoechst 33342 accumulation and pheophorbide A assays. ABCG2 overexpressing MDCK II BCRP and parental cell line were used. More information about Hoechst 33342 accumulation and pheophorbide A assay is described in introduction chapter. The activity data of quinazoline derivatives are summarized in Table 9. The potency of compounds was evaluated not only by IC_{50} value, but also by maximal inhibition which was discussed in introduction chapter. When the maximal plateau of a partial inhibitor is low enough, it is not worth to report IC_{50}. Therefore, to simplify discussion, all compounds with I_{max} less than 50% are regarded as inactive.

Due to the poor solubility of substances with urea linker at position 4, they are not able to be tested *in vitro*. Hence, only the activity results of compounds with amide linker are shown here (Table 9).

3,4-OMe and 3-OMe were introduced as substituents at first. In Hoechst 33342 assay, compound **30** (3,4-OMe) was found emitting strong fluorescence in high concentration, and its emitting spectrum was overlapped with Hoechst 33342 emitting spectrum. Therefore, the determined I_{max} was not accurate. This phenomenon was also observed in compound **32** (4-OC_2H_5), but not in compound **31** (3-OMe). So it is reasonable to assume that *para* position in aniline ring contribute more to strong fluorescence. Although the accurate I_{max} was not accessible in Hoechst 33342 assay for compound **30** and **32**, it could be used for primary screening. When both of their maximal inhibition were set as 100% which meant the top plateau of positive control, the IC_{50} value of compound **32** was about 10-fold higher than compound **30**. It indicated compound **32** was apparently less active than compound **30**. On the contrary, compound **31** exhibited no substantial difference in potency in comparison to compound **30**. Both of them displayed higher affinity to ABCG2 than corresponding phthalazine derivatives (compound **19** and **20**).

Table 9: Inhibitory potencies of synthesized quinazoline derivatives against ABCG2 in the Hoechst 33342 and pheophorbide A accumulation assays.

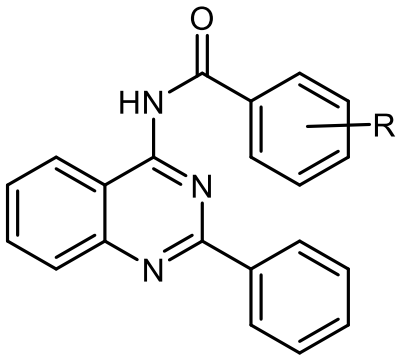

No.	R	Hoechst 33342		pheophorbide A	
		IC_{50} ± SD* [µM]	I_{max} ± SD# [%]	IC_{50} ± SD* [µM]	I_{max} ± SD# [%]
30	3,4-OCH_3	0.743 ± 0.056	100 [a]	0.830 ± 0.152	87 ± 12
31	3-OCH_3	0.909 ± 0.181	87 ± 16	1.040 ± 0.032	75 ± 14
32	4-OC_2H_5	7.066 ± 2.426	100 [a]	-	-
33	4-OCH_3, 3-NO_2	n.a.	< 30%	-	-
34	3-Br	n.a.	< 30%	-	-
35	4-CF_3	n.a.	< 30%	-	-
36	4-CN	n.a.	< 30%	-	-
37	3-CN	0.239 ± 0.033	75 ± 9	0.585 ± 0.036	58 ± 4
Ko143	-	0.221 ± 0.024	100	0.276 ± 0.040	100

**: Data are expressed as mean ± SD (n = 3)*

#: Percentage of inhibition with regard to Ko143

[a]: plateau of curve was fixed to top of Ko143

n.a. = not active

Hence, 5 more compounds were synthesized containing different substituents at *meta* and *para* position of aniline ring. Unfortunately, compounds **33** to **36** did not exert satisfying inhibitory effect against ABCG2 even up to a concentration of 10 µM. However, when the cyano group was moved to *meta* position, compound **37** (3-CN) which shared similar chemical property with compound **36** (4-CN) turned out to be a

good ABCG2 modulator. This observation is opposite to what was described in phthalazine chapter. In bis-substituted phthalazine derivatives, compound **28** (4-CN) was a moderate ABCG2 inhibitor, but compound **27** (3-CN) was inactive.

To accurately measure the activity, pheophorbide A assay was performed for compounds **30**, **31** and **37**, which showed IC_{50} values below 1 µM in Hoechst 33342 assay. The emitting wavelength range of pheophorbide A was not overlapping with emitting wavelength range of them. Therefore, I_{max} values would be accurately displayed. By comparison to Hoechst 33342 assay, all these three compounds demonstrated slightly decreased maximal response and slightly increased IC_{50} value in pheophorbide A assay. No significant difference in activity results in both assays were observed.

Table 10: Comparative study of selected quinazoline derivatives with NH or amide linker at position 4 against ABCG2 in the Hoechst 33342 accumulation assay.

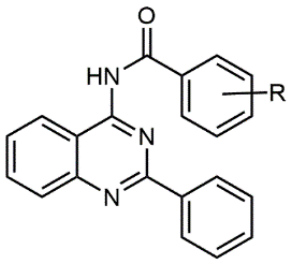

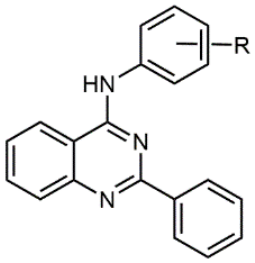

R	IC_{50} ± SD (µM)	IC_{50} ± SD[#] (µM)
3,4-OCH_3	0.743 ± 0.056	0.19 ± 0.01
3-OCH_3	0.909 ± 0.181	1.32 ± 0.10
4-CF_3	1.70 ± 0.18	1.53 ± 0.13
3-Br	n.a.	0.57 ± 0.04
3-CN	0.239 ± 0.033	0.14 ± 0.04

[#]: IC_{50} value taken from reference[118].

In table 10, the potency of selected compounds is compared to corresponding 4-anilino-2-phenylquinazoline derivatives in the Hoechst 33342 accumulation assay. When R was

3-OCH_3, amide linker slightly improved the inhibitory effect. But all of other compounds with amide linker at position 4 were less potent than corresponding compounds with NH linker. Therefore, replacing NH linker by amide at position 4 might not be an effective strategy for improving ABCG2 inhibitory effect.

Despite the general decreased activity, there is an interesting phenomenon that is worth to notice. In phthalazine derivatives, we observed 4-CN bis-substituted compound **28** was moderately active, but 3-CN was inactive. In 2-phenyl-4-anilinoquinazoline series, both 3-CN and 4-CN were highly potent derivatives. In this series, compound **37** (3-CN) was a potent ABCG2 inhibitor, while compound **36** (4-CN) was inactive. Altering position of CN group in aniline moiety leads to significant difference in activity. It is interesting for us to explain.

In 2004, Chang et.al reported that when 4-amido-2,6-diphenylpyrimidine derivatives were synthesized, a ^1H signal in 16 ppm region was seen in NMR($CDCl_3$) spectra.[142] They reasonably speculated that amide bond might have two tautomers. ^1H peak at 16 and 10 ppm region might be attributed to iminol and amide form respectively. Interestingly, in our $CDCl_3$ NMR spectra, a 16 ppm signal was also observed. We thought intramolecular bond between H of amide and N at position 3 was formed. This resulted in an unusual deshielding effect on H of amide group. Correspondingly, the 10 ppm area was empty. Therefore, our compounds may only exist in iminol form in $CDCl_3$. To further confirm this assumption, IR spectroscopy of compounds **30**, **31**, **36** and **37** were tested. In all spectral, no peak could be seen in 1605-2000 cm^{-1} area. Whereas, in IR spectral of some 4-quinolinamide derivatives,[143] typical strong peak caused by carbonyl stretch vibration could be observed in range 1650-1720 cm^{-1}. This might suggest that carbonyl group was not existing in solid phase. Meanwhile, in our spectral, the peaks at 3423-3427 cm^{-1} area (X-H stretching) were all medium and broad. It might indicate the existence of hydrogen bond. Hence, it is reasonable to postulate that the iminol form, but not amide form, might be the dominating tautomer in solid phase. This

assumption is also consistent with what was reported in synthesis of 1-substituted-3-(2-phenylquinazolin-4-yl)-thioureas.[144]

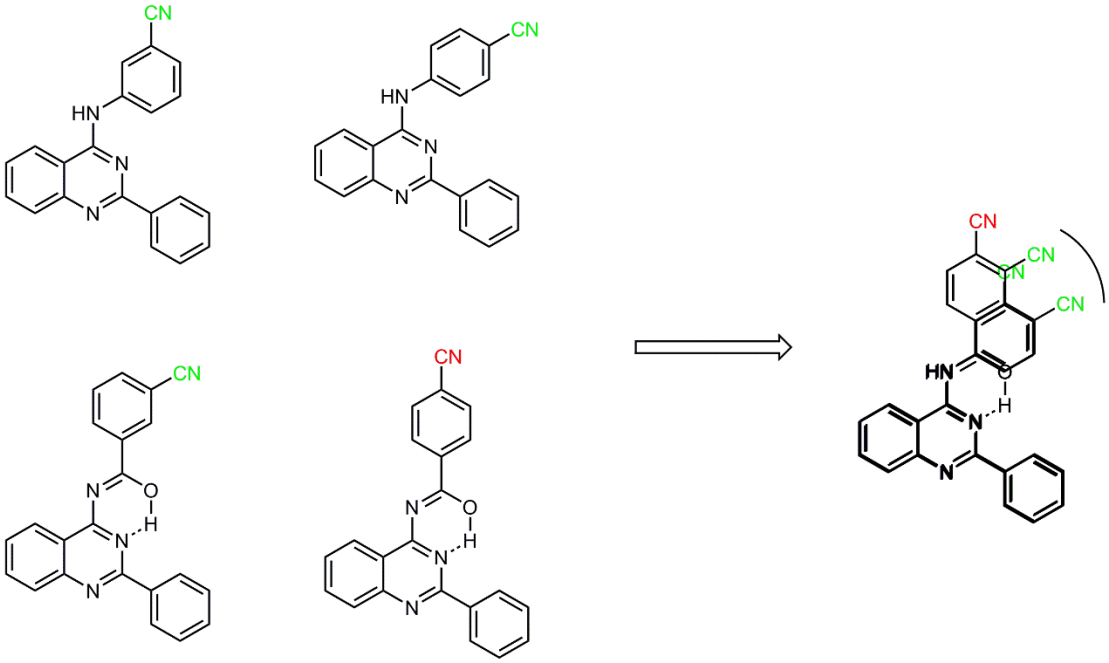

Figure 15: Illustration of potential steric hinderance for quinazoline derivatives.

Based on all of these information, a hypothesis was generated. In Figure 15, the cyano group of inactive compound (36) is red. Three other substances demonstrated high-affinity to ABCG2, and their cyano substituents are green. If we overlap all of them, the red CN group occupies a unique region, this might mean an area with steric hindrance.

Despite the unambiguous experimental evidence supporting the existence of iminol form, it should still be noted that this is just a way to help us to explain the interesting phenomenon which happened on 3-CN and 4-CN substituted derivatives. When ligand is dissolved for biological test and bounded to ABCG2, which tautomer and conformation is used? It still remains to be determined.

In summary, the biological data of this series of compounds generally demonstrated decreased activity of ABCG2 inhibition compared to 4-anilino-2-phenylquinazoline derivatives. Therefore, the original assumption of increasing planarity at position 4

might not be effective. Although planarity is an important descriptor, molecules with absolute planarity in 3D conformation might also not be favorable for ABCG2 inhibition.

5 Project III: Pyrimidine derivatives as ABCG2 inhibitors

5.1 Overview

In the last chapter, we investigated the function of linker at position 4 of quinazoline scaffold. Increasing planarity by replacing NH by amide or urea did not show positive effect on activity. Therefore, we decided to maintain NH as linker at position 4 and explore modification in other area.

Pyrimidine is the right six-membered aromatic ring of quinazoline. Krapf et al. replaced left benzene ring of quinazoline by methyl group and synthesized several pyrimidine derivatives as ABCG2 inhibitors.[121] The preliminary results showed removing the left benzne ring of quinazoline scaffold slightly improved potency of ABCG2 inhibition. IC_{50} value of 3-((2-phenylquinazolin-4-yl)amino)benzonitrile and 3-((6-methyl-2-phenylpyrimidine-4-yl)amino)benzonitrile in Hoechst 33342 assay were 140 nM and 122 nM respectively. The other advantage of pyrimidine in comparison to quinazoline is the improved solubility. Several quinazoline derivatives possessed poor aqueous solubility limiting their further application. In this chapter, we continue to investigate pyrimidine derivatives as potential ABCG2 inhibitors.

5.2 Synthesis

As in Scheme 7 depicted, 4-anilino-6-methyl-2-phenylpyrimidine derivatives were synthesized in three steps. In step 1, benzamidine is condensed with ethyl acetoacetate in freshly prepared sodium ethoxide solution to form pyrimidine scaffold. In step 2, 4-hydroxyl-6-methyl-2-phenylprimidine was chlorinated to yield 4-chloro-6-methyl-2-

phenylprimidine. In step 3, the chlorinated pyrimidine was treated with different substituted aniline to afford final products.

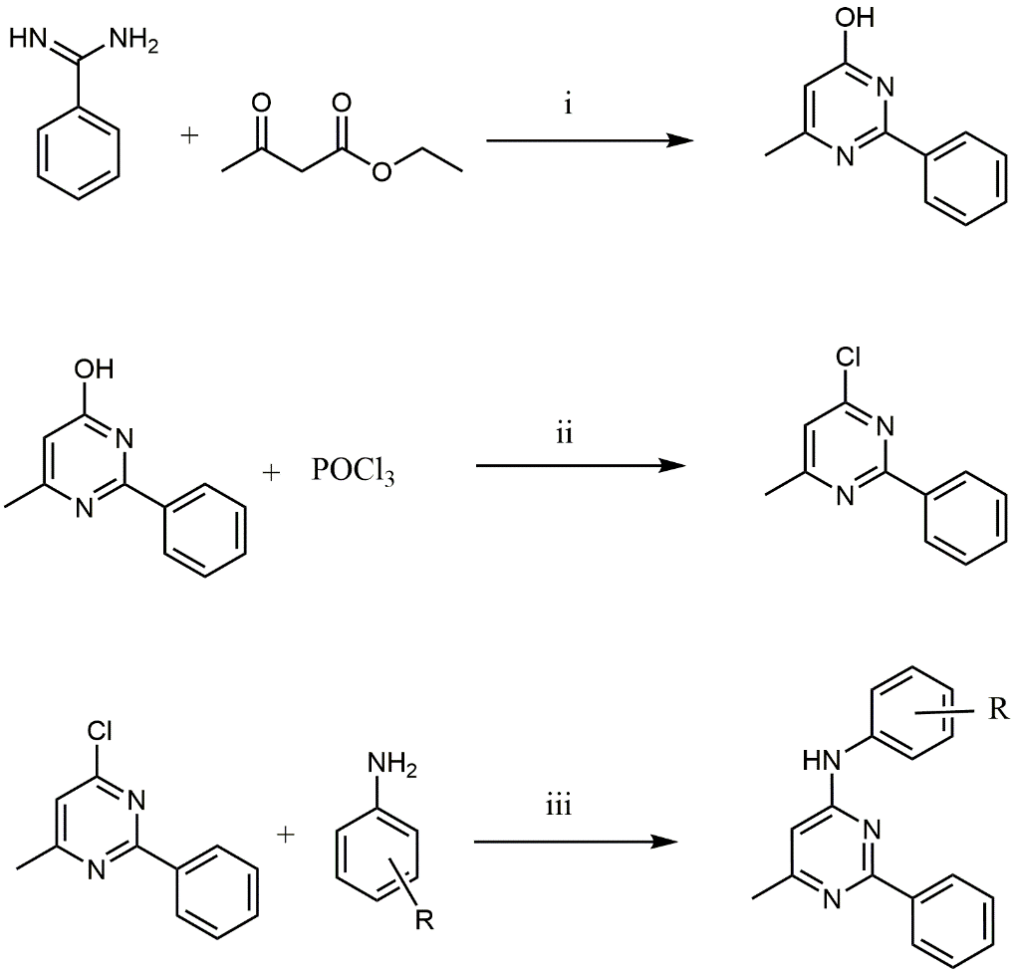

Scheme 7: Synthesis scheme of pyrimidine derivatives. [*]

[*]: Reagents and conditions for synthesis of pyrimidine derivatives: (i) NaOEt/EtOH, reflux, overnight. (ii) reflux, 8-9 h. (iii) *i*-PrOH, microwave, 110 °C, 30 min.

5.2.1 Pinner pyrimidine synthesis

In the 1880s, Pinner performed different condensation reactions of substituted amidines with acetoacetic ester to afford 2-substituted-6-hydroxy-4-methylpyrimidine.[145] Afterwards, numerous variations were developed such as reactions of amidines with *β*-keto esters, malonic esters, and *β*-diketones. In this chapter, 4-hydroxyl-6-methyl-2-phenylpyrimidine was synthesized by classical condensation approach. The details

about experimental procedures and factors which affect yield of reaction were described in experimental section.

Although Pinner pyrimidine synthesis has been widely used in synthesis of pyrimidine derivatives, the reaction mechanism is still not fully elucidated. Katritzky and Yousaf have done nuclear magnetic resonances studies to reveal the detailed mechanistic pathways of reactions including condensation of methyl acetoacetate with benzamidine.[146] But the reaction mechanism they proposed was not based on basic reaction system. Fandrick et al. conducted react-IR to analyze the condensation of amidines and activated olefins in the presence of alkoxide.[147] In their proposed mechanism, aromatization was addressed as rate-limiting step. We combined both of their research work and proposed possible mechanism in synthesis of 4-hydroxyl-6-methyl-2-phenylpyrimidine (Scheme 8).

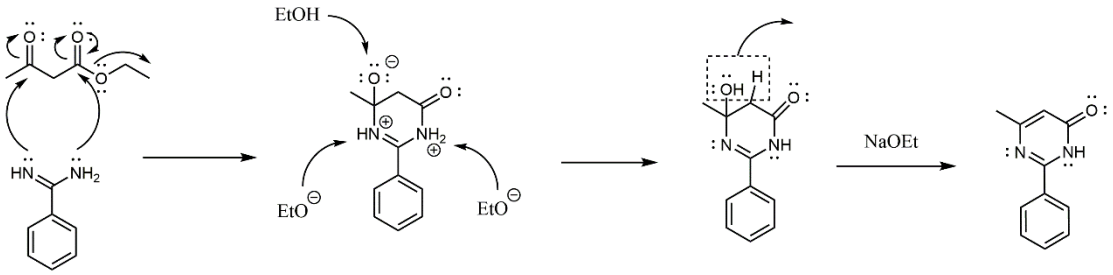

Scheme 8: Possible mechanism in synthesis of 4-hydroxyl-6-methyl-2-phenylpyrimidine

Sodium was dissolved in ethanol to prepare fresh alkoxide which neutralized benzamidine hydrochloride to afford free benzamidine. The established pK_a values of ethanol and benzamidine in DMSO are 29.8[148] and 26.7[149] respectively, the equilibrium should be towards benzamidine anion with ethoxide in DMSO. But, when solvent was altered to methanol, Fandrick et al. revealed through spectroscopy assessment that the free base amidine was dominating in the presence of tert-butoxide, amidine anion was only observable. Therefore, it is reasonable to postulate the nucleophilic reagent which condensed with ethyl acetoactetate in our reaction system was benzamidine but not

benzamidine anion. The nucleophilic addition between benzamidine and ethyl acetoacetate leads to an intermediate with a six-member ring. It would be quickly neutralized to hydroxypyrimidinone which is already observed in NMR study. At last, water is easily eliminated by base to give pyrimidine aromatic ring which is more stable and 4-hydroxyl-6-methyl-2-phenylpyrimidine is obtained.

5.2.2 Chlorination of 4-hydroxyl-6-methyl-2-phenylpyrimidine

The hydroxyl group at position 4 of 4-hydroxyl-6-methyl-2-phenylpyrimidine is substituted by chlorine via a chlorination reaction using $POCl_3$. The reaction mechanism is analogous to what described in phthalazine chapter.

5.2.3 Amination of 4-chlorine-6-methyl-2-phenylpyrimidine

Final compounds were obtained via nucleophilic aromatic substitution of 4-chlorine-6-methyl-2-phenylpyrimidine by different substituted anilines. The reaction mechanism is analogous to what described in phthalazine chapter. If the reaction was not initiated, a little hydrochloride acid was added to the mixture to catalyze reaction.

5.3 Results and discussion

The inhibitory potency of synthesized pyrimidine derivatives was investigated in Hoechst 33342 accumulation and pheophorbide A assays. ABCG2 overexpressing MDCK II BCRP and parental cell line were used. More information about Hoechst 33342 accumulation and pheophorbide A assay is described in introduction chapter. The activity data of pyrimidine derivatives are shown in Table 11 and 12. The potency of compounds was evaluated not only by IC_{50} value, but also by maximal inhibition.

Table 11: Inhibitory potencies of synthesized pyrimidine derivatives against ABCG2 in the Hoechst 33342 and pheophorbide A accumulation assays.

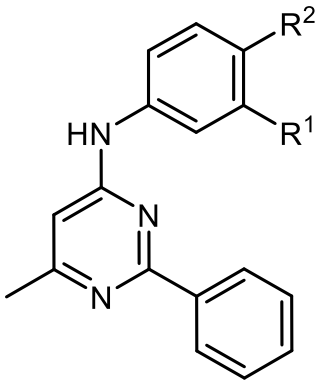

No.	R^1	R^2	Hoechst 33342		pheophorbide A	
			$IC_{50} \pm SD^*$ [µM]	$I_{max} \pm SD^\#$ [%]	$IC_{50} \pm SD^*$ [µM]	$I_{max} \pm SD^\#$ [%]
45 [b]	H	H	0.648 ± 0.149	80-110	n.t.	n.t.
46	H	CH_2CN	2.54 ±0.47	100 [a]	3.64 ± 0.50	100 [a]
47 [b]	H	CN	0.128 ± 0.032	80-110	n.t.	n.t.
48	CH_2OH	H	4.31 ± 0.99	100 [a]	2.52 ± 0.19	100 [a]
49	OH	H	0.257 ± 0.055	74 ± 13	0.518 ± 0.055	59 ± 5
50	F	H	1.14 ± 0.32	100 [a]	n.t.	n.t.
51	Cl	H	0.823 ± 0.164	100 [a]	n.t.	n.t.
52	Br	H	0.902 ± 0.166	100 [a]	0.391 ± 0.078	83 ± 5
53	OCH_3	H	n.t.	n.t.	0.506 ± 0.081	100 [a]
54	OCH_3	Br	0.287 ± 0.075	100 [a]	0.330 ± 0.045	53 ± 5
55	F	OCH_3	0.865 ± 0.105	100 [a]	1.32 ± 0.20	100 [a]
56	CF_3	OCH_3	n.t.	n.t.	0.547 ± 0.061	83 ± 8

57 [b]	CN	H	0.122 ± 0.024	80-110	n.t.	n.t.
58	CN	CN	0.188 ± 0.017	117 ± 18	0.551 ± 0.076	100 [a]
59	CN	F	0.307 ± 0.014	100 [a]	0.086 ± 0.008	59 ± 10
60	Br	CN	0.119 ± 0.011	90 ± 10	0.060 ± 0.006	40 ± 9
61	CH_3	CN	0.097 ± 0.033	106 ± 19	0.176 ± 0.021	76 ± 20
62	CF_3	CN	0.069 ± 0.001	114 ± 12	0.391 ± 0.084	92 ± 7
63	NO_2	H	0.133 ± 0.029	80 ± 8	0.146 ± 0.016	68 ± 11
64	H	NO_2	0.053 ± 0.008	79 ± 8	0.156 ± 0.029	67 ± 17
65 [b]	NO_2	OH	0.099 ± 0.017	80-110	n.t.	n.t.
66	NO_2	F	1.02 ± 0.20	100 [a]	n.t.	n.t.
67	COOH	NO_2	> 10 µM	-	> 10 µM	-
68	Cl	NO_2	0.059 ± 0.004	76 ± 16	n.t.	n.t.
Ko143	-	-	0.221 ± 0.024	100	0.276 ± 0.040	100

[*]: Data are expressed as mean ± SD (n = 3)

[#]: Percentage of inhibition with regard to Ko143

[a]: plateau of curve was fixed to top of Ko143

[b]: data taken from reference[121].

n.t. = not tested

As described above, substitution was only carried out at *meta* and/or *para* position of anline ring. The effect of inserting a methylene group between aniline ring and the substituent was investigated initially. It is obvious to notice that compounds **47** (4-CN) and **49** (3-OH) displayed excellent potency as ABCG2 inhibitors (128 nM and 257 nM), but compound **46** (4-CH_2CN) and **48** (3-CH_2OH) showed about 20-fold lower activity. Therefore, insertion of a methylene group at *meta* or *para* position of aniline ring appeared to be unfavorable for ABCG2 inhibition.

Next, different halogen were introduced at *meta* position. In Hoechst 33342 assay, they showed similar efficacy. In the sequence of 3-F, 3-Br, 3-Cl, the activity of corresponding derivative was slightly increasing from 1.136 µM to 0.823 µM.

Table 12: Inhibitory potency of synthesized pyrimidine derivatives against ABCG2 in the Hoechst 33342 and pheophorbide A accumulation assays.

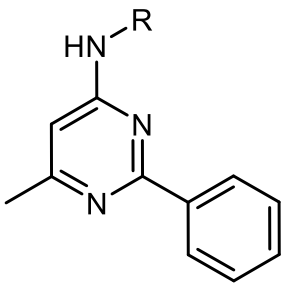

No.	R	Hoechst 33342		pheophorbide A	
		IC_{50} ± SD* [µM]	I_{max} ± SD# [%]	IC_{50} ± SD* [µM]	I_{max} ± SD# [%]
69	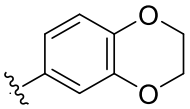	0.815 ± 0.112	100 [a]	n.t.	n.t.
70	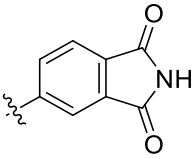	0.253 ± 0.012	105 ± 7	n.t.	n.t.
71	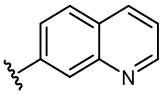	fluo	-	0.152 ± 0.026	79 ± 16
72	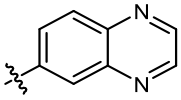	fluo	-	0.321 ± 0.095	96 ± 6
Ko143	-	0.221 ± 0.024	100	0.276 ± 0.040	100

**: Data are expressed as mean ± SD (n = 3)*

#: Percentage of inhibition with regard to Ko143

a: plateau of curve was fixed to top of Ko143

n.t. = not tested

fluo: compound showed strong fluorescence in Hoechst 33342 assay.

However, taking into account the standard deviations, all three compounds were equally active. So the size of halogen at *meta* position of aniline moiety did not influence inhibitory potency. All of them were less potent than the unsubstituted compound **45** in Hoechst 33342 assay. It might indicate halogens at position 3 exhibit negative effects on inhibiting Hoechst 33342 efflux. But, in pheophorbide A assay, an interesting result was observed. The inhibitory efficacy of compound **52** (3-Br) was even comparable with positive control, only a little lower than Ko143. This inspired us to continue the exploration of halogens.

Given the positive impact of methoxy group in some scaffolds on ABCG2 inhibition, compound **53** (3-OCH_3) was synthesized at first and reached similar inhibitory effect as compound **52** in pheophorbide A assay. Owing to positive effects of 3-Br and 3-OCH_3 on inhibiting pheophorbide A efflux, the strategy of combining methoxy group and halogen was applied. In Hoechst 33342 assay, IC_{50} value of compound **54** (3-OCH_3, 4-Br) was 0.287 μM, which was comparable to compound **49** (3-OH). But, in pheophorbide A assay, it produced only partial inhibition of pheophorbide A efflux. Its maximal plateau was only half of Ko143's. This might suggest Br is an unfavorable group at position 4. Next, the position of halogen and methoxyl group was swapped. The 3-F, 4-OCH_3 disubstituted compound **55** yielded increased IC_{50} values in both assays. After comparison with 3-F monosubstituted compound **50**, 4-OCH3 contributed slightly positive to inhibitory activity. Therefore, it might be 3-F resulting in decreased potency. Subsequently, fluorine at position 3 was replaced by CF_3. Compound **56** (3-CF_3, 4-OCH_3) showed more potent activity than **55** in pheophorbide A assay. It might indicate that CF_3 is a more preferred substituent at position 3 than F and 3-F might exhibit negative effect on inhibition. Although compounds **49** and **54** displayed higher activity towards ABCG2 than unsubstituted compound **45**, they were still only half as potent as compounds **57** (3-CN) and **47** (4-CN). Introducing both methoxy and halogen together might not a very effective strategy for improving inhibitory potency. Therefore, we continued to explore substances containing cyano and nitro group.

Initially, 3,4-CN was introduced at aniline moiety. In contrast to the monosubstituted 3-CN and 4-CN compounds, no improvement was obtained. In Hoechst 33342 assay, its increased maximal inhibitory plateau was accompanied by decreased IC_{50} value. Subsequently, pyrimidine analogs with combination of cyano and other substituents were examined. In comparison to compounds **49** and **54**, compound **59** (3-CN, 4-F) demonstrated slightly decreased potency (IC_{50} = 0.307 μM) in Hoechst 33342 assay, but reached slightly improved activity in pheophorbide A assay. This phenomenon happened more obviously to compound **60** (3-Br, 4-CN). It was 2-fold more potent than compounds **49**, **54** and **59** in inhibiting efflux of Hoechst 33342, but less active and was only as partial inhibitor in pheophorbide A assay. When R^1 residue of compound **49** was altered to Br or *para* position as in compound **52** was substituted by CN, the inhibitory activity against ABCG2 was modulated to opposite direction in these two assays. This observation might be attributed to different binding sites of Hoechst 33342 and pheophorbide A on ABCG2.

Compounds **57**, **58** and **59** shared the same R^1 residue — CN, but different substituents at R^2. When H and CN occupied *para* position, similar inhibitory effect was observed. Both of them were more active than fluorine in Hoechst 33342 assay. Similarly, R^1 of compounds **52** and **60** were both bromine, but compound **60** containing CN as R^2 was apparently more active in Hoechst 33342 assay than compound **52** which had no substituent at *para* position. Thus, it is reasonable to presume that both R^1 and R^2 contribute to the interaction with ABCG2 in Hoechst 33342 assay. And this conclusion could also be applied in pheophorbide A assay (comparing compounds **49**, **52** and **60**). Therefore, we decided to investigate more substances with *meta* and *para* disubstituted combinations at aniline moiety.

Considering the positive effect of CN at *para* position of aniline ring in Hoechst 33342 assay, compounds **61** and **62** were synthesized. In comparison to compound **60**, R^2 was kept as CN, but R^1 was replaced by CH3 and CF3 respectively. In sequence of compounds **47** (3-H, 4-CN), **60** (3-Br, 4-CN), **61** (3-CH_3, 4-CN) and **62** (3-CF_3, 4-CN),

the inhibitory activity was improved from 0.122 μM to 0.069 μM and accompanied by increased I_{max} in Hoechst 33342 assay. Compound **62** was about 3-fold more potent than Ko143. In pheophorbide A assay, the maximal response was also dramatically increased from 40% for compound **60** to 92% in case of compound **62**, and the inhibitory efficacy of compounds **61** and **62** were comparable to Ko143 in the pheophorbide A assay.

Next, owing to the excellent ABCG2 inhibitory activity of nitro group in case of quinazoline derivatives, some pyrimidine analogs with nitro group as R^1 or R^2 were also investigated. Monosubstituted derivatives were synthesized at first. Compound **63** (3-NO_2) and **64** (4-NO_2) demonstrated almost the same maximal response (80% in Hoechst 33342, 68% in pheophorbide A assay). But the affinity results against ABCG2 were different. In pheophord A assay, they were equipotent. But in Hoechst 33342 assay, compound **64** was about 2.5-fold more potent than compound **63**, which was slightly less potent than compounds **57** (3-CN) and **65** (3-NO_2, 4-OH). To further improve the activity, fluorine was introduced as R^2 residue in compound **66**. However, this modification led to a drastic decrease of the modulatory potency against ABCG2. Therefore, fluoro might be an unfavorable group at *para* position of anline moiety. The other evidence was from the results of compounds **59** (3-CN, 4-F; IC_{50} = 0.307 μM) and **57** (3-CN, 4-H; IC_{50} = 0.122 μM),

Afterwards, R^2 was kept as nitro group and modification was only done at *meta* position. To improve the solubility of compounds containing nitro group, COOH was introduced as R^1. However, compound **67** was totally inactive. But when Cl was introduced instead, compound **68** was as potent as **64**, and the solubility was obviously improved. Despite their excellent IC_{50} values, the maximal inhibition of compounds bearing a nitro group were all lower than I_{max} of Ko143.

The high activity of compounds **61**, **62** and **68** showed that the disubstituted strategy was applicable. Furthermore, R^1 and R^2 were connected by a ring. Initially, 1,4-dioxane ring was introduced. Compound **69** was less active than **45** (unsubstituted aniline

moiety). The decreased activity might be attributed to the broken planarity of 1,4-dioxane moiety. Subsequently, only planar rings were introduced. Compound **70** with phthalimide moiety (IC_{50} = 0.253 μM) was equipotent to Ko143 in Hoechst 33342 assay. Pyridine and pyrazine ring were introduced at last. In Hoechst 33342 assay, they were found to show fluorencence and maximal inhibition was not accessible. In pheophorbide A assay, compounds **71** and **72** demonstrated similar inhibitory effects as compounds **61** and **62** respectively. They both displayed comparable inhibitory activity to Ko143. Removing one nitrogen of pyrazine moiety resulted in a decreased IC_{50} value and I_{max}.

In summary, a series of compounds with 2-phenylpyrimidine scaffold were synthesized. Several compounds demonstrated excellent inhibitory potency against ABCG2. Cyano, and nitro were favorable substituents at both *meta* and *para* position of aniline ring. Different halogen applied at *meta* position as substituents produced similar inhibitory effects. Introducing 3-CH_2R, 3-F, 4-CH_2R, 4-F and 4-Br at aniline ring resulted in decreased activity. Both R^1 and R^2 are essential parts for interacting with ABCG2 in Hoechst 33342 and pheophorbide A assay, but the same variation in structure might lead to obviously different potency in two assays. Modifying aniline ring with disubstitutes and introducing an aromatic ring at R^1 and R^2 might be effective strategies for development of potent ABCG2 inhibitors. In the next chapter, we further explored some compounds with 2-phenylpyrimidine scaffold as potent ABCG2 inhibitors.

6 Project IV: Novel pyrimidine derivatives as ABCG2 inhibitors

6.1 Introduction

In the last chapter, we synthesized and evaluated dozens of 4-anilino-6-methyl-2-phenylpyrimidine derivatives as ABCG2 inhibitors. Several of them displayed excellent inhibitory activities. Therefore, we continued to explore potent pyrimidine derivatives in this chapter.

As described before, Pick et al. had investigated 6 TKIs with quinazoline scaffold as ABCG2 inhibitors, and an interesting result was observed. PD153035 and PD158780 shared similar chemical structure. Both of them contain pyrimidine core and 3-bromaniline at position 4. However, their activities were different. PD158780 was approximately 7-fold more potent than PD153035 as ABCG2 inhibitor in both Hoechst 33342 and pheophorbide A assays. This could only be attributed to the different component of structure at position 6 and 7 of quinazoline ring (red bold bond in Figure 16). It might indicate potential interaction of this area with ABCG2. Thus, modification at position 5 or 6 of pyrimidine ring might be worth to be investigated.

For the compounds investigated in this chapter, the critical features of quinazoline and pyrimidine derivatives for ABCG2 inhibition were preserved. Pyrimidine core and phenyl at position 2 were not modified. Due to easy availability and high potency, 4-cyanoaniline was substituted at position 4. Considering the difficulty of synthesis, modification was finally focused on position 6. The methyl group of 4-anilino-6-methyl-2-phenylpyrimidine scaffold was replaced by chlorine, phenyl, various amines or anilines.

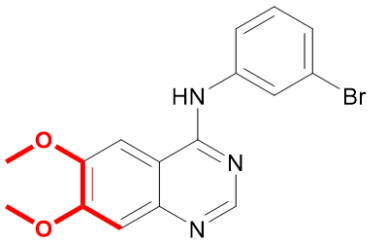

PD153035

Hoechst 33342: 2.50 ± 0.42 uM

Pheophorbide A: 1.62 ± 0.95 uM

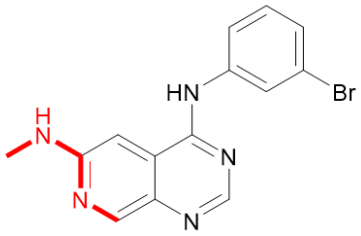

PD158780

Hoechst 33342: 0.36 ± 0.07 uM

Pheophorbide A: 0.25 ± 0.09 uM

Figure 16: Inhibitory potencies of PD153035 and PD158780 against ABCG2 (data from Pick et al.)[117]

6.2 Synthesis

As depicted in Scheme 9, novel 4-anilino-2-phenylpyrimidine derivatives were synthesized in four steps. In step 1, benzamidine was condensed with diethyl malonate in freshly prepared sodium ethoxide solution to form pyrimidine scaffold. In step 2, 2-phenylpyrimidine-4,6-diol was chlorinated to yield 4,6-dichloro-2-phenylpyrimidine. In step 3, chlorinated 2-phenylpyrimidine was treated with 1 equivalent of 4-cyanoaniline to afford monosubstituted product 4-((6-chloro-2-phenylpyrimidin-4-yl)amino)benzonitrile. In step 4, 4-((6-chloro-2-phenylpyrimidin-4-yl)amino)benzonitrile was first reacted with various amines to produce 6-amin-4-anilino-2-phenylpyrimidine derivatives. Afterwards, it was treated with phenylboronic acid via Suzuki coupling to produce 4-((2,6-diphenylpyrimidin-4-yl)amino)benzonitrile. Lastly, different aminophenols reacted with it to afford 4-((6-((hydroxyphenyl)amino)-2-phenylpyrimidin-4-yl)amino)benzonitriles. The mechanism of each step is illustrated below.

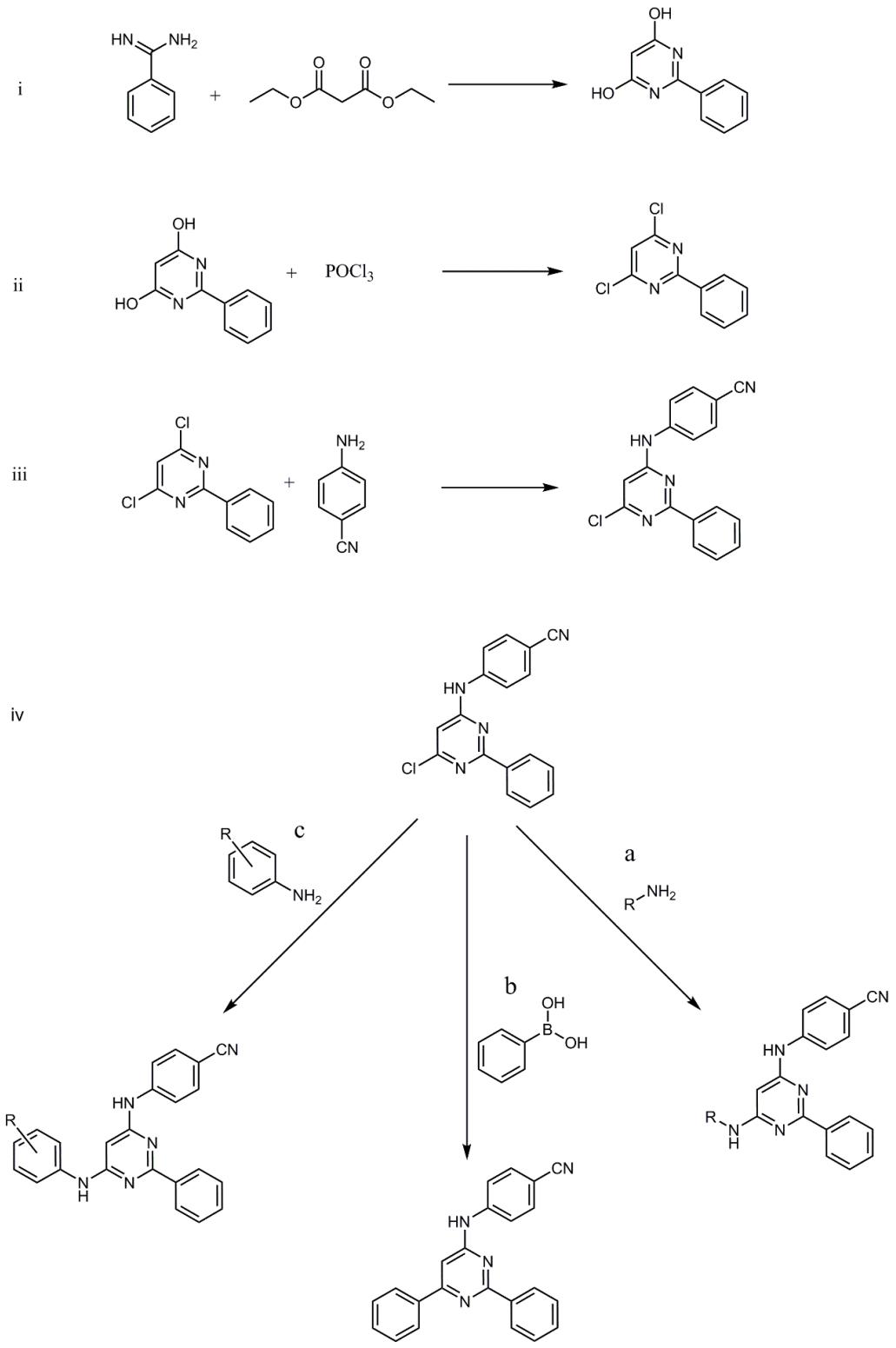

Scheme 9: Synthesis scheme of novel pyrimidine derivatives.[*]

[*]*: Reagents and conditions for synthesis of pyrimidine derivatives: (i) NaOEt/EtOH, reflux, overnight. (ii) reflux, 8-9 h. (iii) i-PrOH, reflux, HCl (catalyst), ratio = 1:1 (iv) a: i-PrOH , 120 °C, 0.5 h; b: Pd(t-Bu$_3$P)$_2$, dioxane:2M K$_2$CO$_3$ = 3:1, 90 °C, 7 h, argon; c: i-PrOH, 110 °C, HCl (catalyst).*

6.2.1 Pinner pyrimidine synthesis

The reaction mechanism of Pinner pyrimidine synthesis is analogous to what described in last chapter and illustrated below. The *β*-keto ester which reacted with the benzamidine was replaced by malonic ester. Thus, a six-membered ring with double amide bonds were obtained after deprotonation. Owing to stability issue, this six-membered ring is prone to rearrangement to pyrimidine ring. Therefore, 2-phenylpyrimidine-4,6-diol was obtained finally.

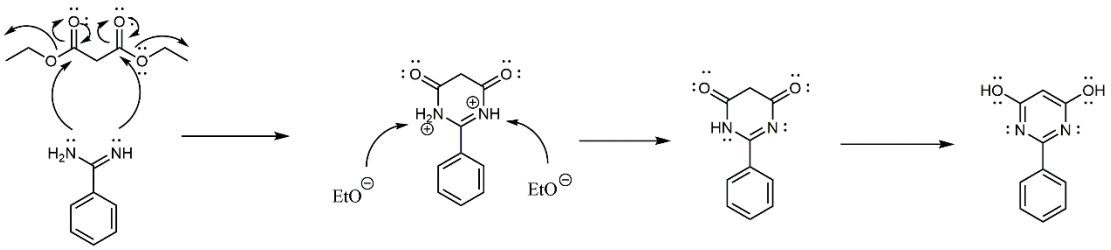

Scheme 10: Possible mechanism in synthesis of 2-phenylpyrimidine-4,6-diol

6.2.2 Chlorination of 2-phenylpyrimidine-4,6-diol

The two hydroxyl groups at position 4 and 6 of 2-phenylpyrimidine-4,6-diol were substituted by chlorines via a chlorination reaction using POCl3. The reaction mechanism is analogous to what is described in phthalazine chapter.

6.2.3 Amination of 4,6-dichloro-2-phenylpyrimidine

4-((6-chloro-2-phenylpyrimidin-4-yl)amino)benzonitrile was obtained via nucleophilic aromatic substitution of 4,6-dichloro-2-phenylpyrimidine with 4-cyanoaniline in ratio 1:1. The reaction mechanism is analogous to what is described in phthalazine chapter. If the reaction was not initiated, a little hydrochloride acid was added to the mixture to catalyze reaction.

6.2.4 Modification at position 6 of 4-((6-chloro-2-phenylpyrimidin-4-yl)amino)benzonitrile

6.2.4.1 Amination at position 6

Various 4-((6-amino-2-phenylpyrimidin-4-yl)amino)benzonitriles were obtained via nucleophilic aromatic substitution of 4-((6-chloro-2-phenylpyrimidin-4-yl)amino)benzonitrile by corresponding amines. The reaction mechanism is analogous to previous amination steps. But due to the high nucleophilicity of applied amines, hydrochloride acid was not necessary to be used as catalyst.

6.2.4.2 Suzuki coupling

4-((2,6-diphenylpyrimidin-4-yl)amino)benzonitrile was synthesized via Suzuki cross-coupling. The Suzuki reaction involves an organohalide with an organoborane to produce coupled product in the presence of a palladium catalyst and base. It has been widely used in formation of aryl-aryl bond. The catalyst and base in this reaction are bis(tri-tert-butylphosphine)palladium(0) and potassium hydroxide respectively. The mechanism is illustrated below. It starts with oxidation addition of Cl-pyrimidine bond at position 6 to the catalyst Pd(0) to give a Pd(II) complex. This step is probably the rate-determining step. Subsequently, the hydroxide base attacks this complex and replaces chloride to give more reactive organopalladium hydroxide complex. On the other hand, phenylboronic acid is basified by another hydroxide ion to form borate which makes phenyl more nucleophilic. Afterwards, trans*meta*lation follows. Phenyl group on borate replaces hydroxyl group on organopalladium hydroxide complex to give a diorganopalladium complex. This complex undergoes reductive elimination in which palladium catalyst is regenerated leading to restart of the catalytic cycle and the final coupled product 4-((2,6-diphenylpyrimidin-4-yl)amino)benzonitrile is obtained.

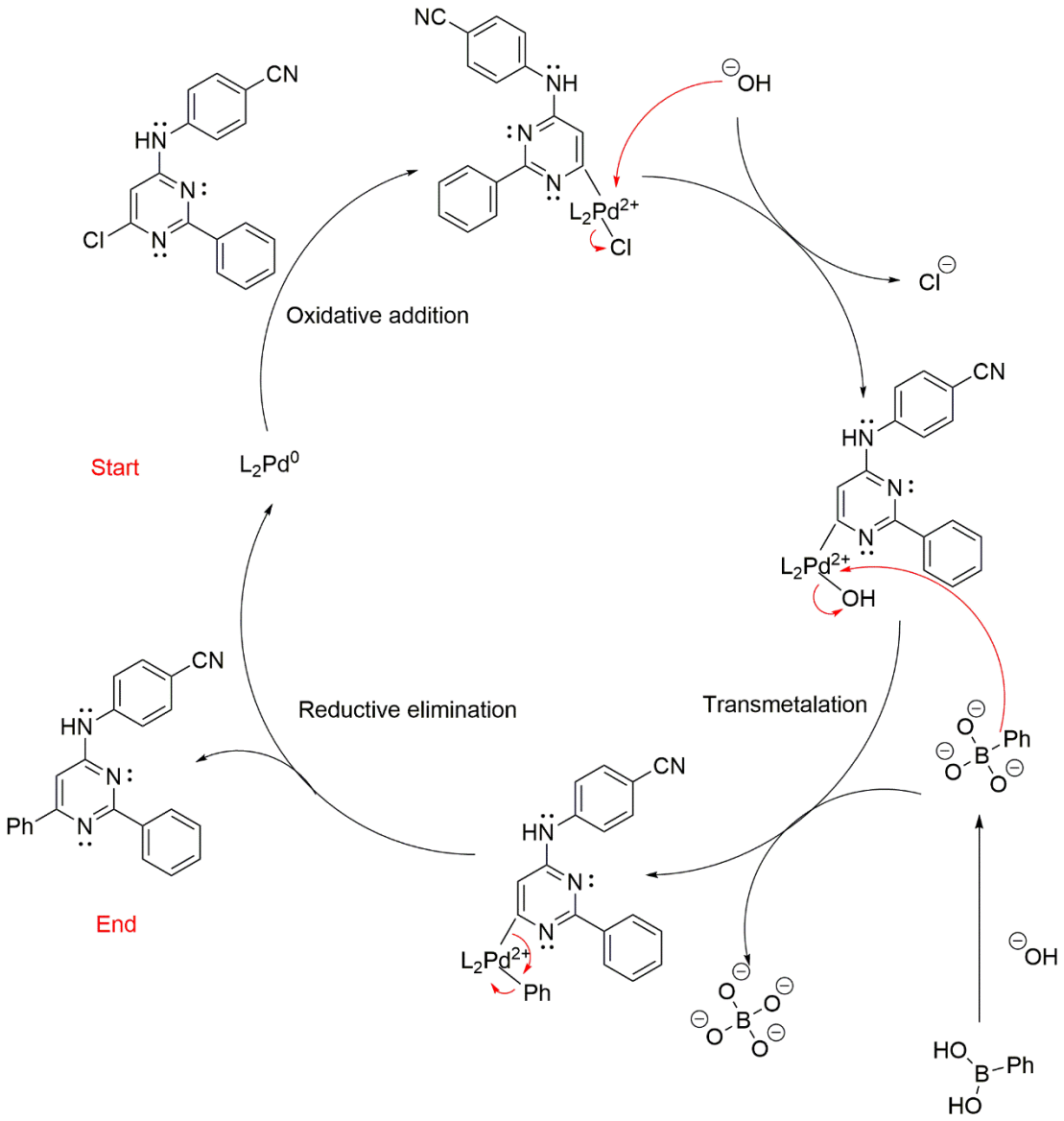

Scheme 11: Possible mechanism in synthsis of 4-((2,6-diphenylpyrimidin-4-yl)amino)benzonitrile.

6.2.4.3 Synthesis of three 4-((6-((hydroxyphenyl)amino)-2-phenylpyrimidin-4-yl)amino)benzonitriles

Three 4-((6-((hydroxyphenyl)amino)-2-phenylpyrimidin-4-yl)amino)benzonitriles were obtained via nucleophilic aromatic substitution of 4-((6-chloro-2-phenylpyrimidin-4-yl)amino)benzonitrile by 2, 3 or 4-aminophenol (ratio 1:1) in the presence of catalytic amounts of hydrochloride acid. The reaction mechanism is analogous to what is described in previous amination steps.

6.3 Results and discussion

The inhibitory potency of novel synthesized pyrimidine derivatives was investigated in Hoechst 33342 and pheophorbide A accumulation assays. ABCG2 overexpressing MDCK II BCRP and parental cell line were used. More information about Hoechst 33342 and pheophorbide A assays is described in introduction chapter. The activity data of pyrimidine derivatives are shown in Table 13 and 14. The potency of compounds was evaluated not only by IC_{50} value, but also by maximal inhibition.

Table 13: Inhibitory potencies of compound 75 and 47 against ABCG2 in the Hoechst 33342 accumulation assay.

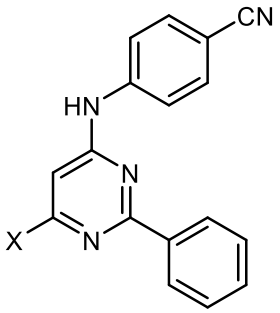

No.	X	Hoechst 33342	
		$IC_{50} \pm SD^{*}$ [μM]	$I_{max} \pm SD^{\#}$ [%]
75	Cl	0.105 ± 0.029	81 ± 11
47[a]	CH_3	0.128 ± 0.032	80-110
Ko143	-	0.221 ± 0.024	100

[a]: data taken from literature.[121]

[*]: Data are expressed as mean ± SD (n = 3)

[#]: Percentage of inhibition with regard to Ko143

Firstly, compound **75** was investigated in Hoechst 33342 assay and demonstrated slightly better inhibitory activity than compound **47** which contains methyl group at position 6. It indicated the applicability of modification at position 6. Next, we tried to investigated activities of several other derivatives with NH linker as X in Hoechst

Table 14: Inhibitory potenciy of synthesized novel pyrimidine derivatives against ABCG2 in the pheophorbide A accumulation assay.

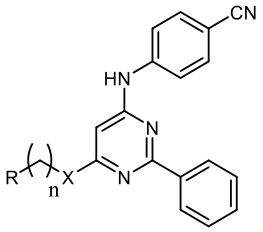

No.	X	n	R	pheophorbide A	
				$IC_{50} \pm SD^{*}$ [μM]	$I_{max} \pm SD^{\#}$ [%]
76	NH	0	CH_3	0.147 ± 0.054	68 ± 13
77	NH	1	$(CH_3)_2$	0.777 ± 0.180	101 ± 11
78	NH	2	CH_3	0.299 ± 0.077	89 ± 13
79	NH	3	CH_3	0.502 ± 0.060	73 ± 15
80	-	0	Ph	n.e.	n.e.
81	NH	0	Ph	0.170 ± 0.018	84 ± 24
82	NH	1	Ph	0.285 ± 0.044	99 ± 20
83	NH	3	Ph	0.099 ± 0.029	61 ± 12
84	NH	4	Ph	0.150 ± 0.037	61 ± 3
85	NH	1	2-Pyridiyl	0.210 ± 0.006	88 ± 8
86	NH	1	3-Pyridiyl	0.375 ± 0.041	91 ± 7
87	NH	1	4-Pyridiyl	0.435 ± 0.003	78 ± 19
88	NH	0	2-OH Ph	0.224 ± 0.023	86 ± 17
89	NH	0	3-OH Ph	0.610 ± 0.049	66 ± 16
90	NH	0	4-OH Ph	0.392 ± 0.073	76 ± 7
91	NH	0	4-CN Ph	0.135 ± 0.025	60 ± 5
Ko143	-	-	-	0.276 ± 0.040	100

**: Data are expressed as mean ± SD (n = 3)*

#: Percentage of inhibition with regard to Ko143

n.e. = no effect

33342 assay, but all of them displayed strong fluorescence which might lead to inaccurate results. Therefore, we investigated all of the remaining compounds only in pheophorbide A assay.

Because methyl was the starting point of our investigation at position 6, the influence of various aliphatic alkyl chains on potency was explored. Compound **76** (methylamino) and **78** (n-propylamino) displayed low IC_{50} values (lower than 0.3 μM). High maximal inhibition (higher than 80%) was reached by compounds **77** and **78**. Hence, compound **78** is a potent ABCG2 inhibitor. Next, the terminal group of aliphatic chain was replaced by phenyl to improve potential lipophilic interactions. Compound **80** with no linker between phenyl and pyrimidine scaffold exhibited no inhibitory effect. Whereas, compound **81** containing the NH linker at position 6 displayed higher potency than **78**. This difference suggested the importance of linker between pyrimidine ring and phenyl moiety. Afterwards, 1 to 4 CH_2 were inserted between NH and phenyl to explore the best length of linker. As a result, compounds **81** (n=0) and **82** (n=1) possessed high potency against ABCG2. But maximal inhibition of compounds **83** (n=3) and **84** (n=4) only reached 61%. As observed for purely aliphatic compounds (**79**), it might indicate that long aliphatic chains (n>2) lead to decreased maximal inhibition. The most effective distance between Ph and NH might be one or two bonds. Therefore, n was chosen as 0 and 1 in the following investigation. In last chapter, we have explored the effects of various lipophilic substituents on aniline ring at position 4, and it is easy to observe the symmetry of position 4 and 6 in chemical structure. Therefore, we did not focus on investigation of lipophilic interaction at position 6 again, but on potential polar interaction. 2, 3 and 4-picolylamino group were tested at first. The results showed compound **85** (2-picolylamino) was the most potent one amongst them and 4-picolylamino (**87**) least. Afterwards, they were replaced by 2, 3, and 4-hydroxylanilino moieties. Here, 2-hydroxylanilino was the most potent residue, and 3-hydroxylanilino least. It is inconsistent with the observation at position 4, the results of these 6 compounds might suggest *ortho* area, but not *meta* and *para*, is more favorable for polar

residue of phenyl ring at position 6 of these compounds for ABCG2 inhibition. In addition, bis-4-cyano substituted compound **91** was also tested. Although the IC_{50} value was lower, the maximal inhibition was also decreased. The final seven compounds possess more hydrophilic properties than compounds **81** and **82**, but the inhibitory effects were not improved. Hence, improved polarity of moiety at position 6 lead to higher solubility, but might not lead to higher activity against ABCG2.

In summary, the influence of different moieties at position 6 of pyrimidine scaffold was investigated. Chlorine, methyl and appropriate amines displayed high activity against ABCG2. When position 6 was substituted by amines, the length between NH and end residue of chain is critical. Increased polar potential at this position might not result in improved inhibitory effect. By comparison to the most potent four compounds in last chapter, compound **81** was comparable with **71** and more active than **61**. Compound **82** demonstrated higher efficacy than compounds **62** and **72** in inhibition of pheophorbide A efflux. Although the improvement of activity was not significant, modification at position 6 was still beneficial.

7 Summary

In the current study, we synthesized dozens of structurally different series of compounds which were biologically evaluated as potential selective ABCG2 inhibitors. These substances were all phthalazine, quinazoline or pyrimidine derivatives and divided into four projects. Hoechst 33342 and pheophorbide A accumulation assays were carried out by my colleague Katja Silbermann to determine their inhibitory efficacy to reverse multi-drug resistance mediated by ABCG2. A brief summary of results from each project is given below.

7.1 Project 1

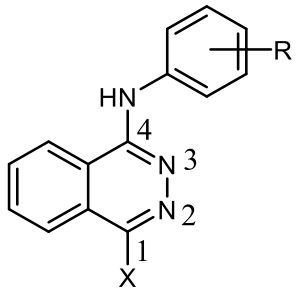

Project 1

In the first project, the critical features of 4-anilinoquinazonine derivatives for ABCG2 inhibition were preserved and a series of phthalazine derivatives were synthesized to investigate the potential influence of variation at position 1. At first, position 4 was aminated by various anilines which showed good activity in case of quinazoline derivatives and position 1 was unsubstituted. Unfortunately, all of this first series of compounds did not only show difficulty in synthesis, but also displayed low maximal inhibition (less than 20%). Afterwards, position 1 was also included in modification. It was substituted by chlorine or phenyl. Simultaneously, position 4 was aminated by 3-methoxyl or 3,4-dimethoxylaniline. As a result, the combination of Ph, 3,4-OCH_3 and Cl, 3,4-OCH_3 displayed moderate inhibitory effects, the latter one being more active. Therefore, several more compounds with Cl at position 1 and substituted aniline at

position 4 were also synthesized. But all of them were inactive. At this point, it is reasonable to presume variation at position 1 is crucial for ABCG2 inhibition, but Cl is not a favorable substituent. Instead of replacing Cl by other atoms, we decided to elongate the length of substituent at position 1 and synthesized bis-anilinosubstituted derivatives whose aniline moiety at position 1 might serve as a replacement of critical phenyl ring at position 2 of 4-anilino-2-phenylquinazoline derivatives. Finally, compounds **19**, **20** and **25** demonstrated moderate inhibitory activity. The potency of compound **26** was even comparable with standard inhibitor WK-X-24.

In this series of compounds, we also discovered two phenomena which were also observed elsewhere. (i) Methoxyl is a favorable substituent. (ii) lipophilicity and steric effect, but not electrostatic properties, were essential descriptors. However, the comparative study showed that phthalazine derivatives were generally less active than corresponding quinazoline derivatives. It might indicate swapping N (position 1) and C (position 2) of quinazoline scaffold is not an effective strategy. Therefore, we turned our direction back to quinazoline in next project.

7.2 Project 2

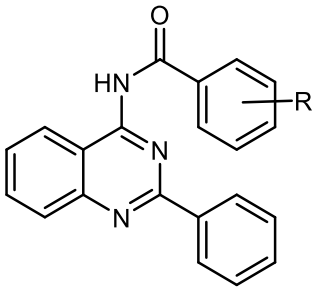

Project 2

The previous studies suggested variation at 2-phenylquinazoline scaffold might not result in improved activity. Therefore, this scaffold was preserved. Planarity has been shown as an essential feature of potent ABCG2 inhibitors with various scaffolds. So, in the second project, the NH linker at position 4 of 4-anilino-2-phenylquinazoline scaffold was replaced by amide or urea moiety leading to increased planarity of

molecular conformation. Due to the solubility problem, compounds with urea linker could not biologically evaluated. Eight compounds containing amide linker at position 4 were tested in Hoechst 33342 and pheophorbide A assays, but the results were disappointing. Half of them were inactive (I_{max} < 30%), the other half showed moderate activity, but none of them was comparable to Ko143. By comparison to corresponding 4-anilino-2-phenylquinazoline derivatives, they were generally less active. Therefore, improving molecular conformation to absolute planarity might not be an effective strategy, certain conformational flexibility might also be necessary for designing potent inhibitors.

In addition, an interesting phenomenon was observed: altering the position of cyano substituents on aniline moiety resulted in obviously different inhibitory effects. After collecting spectral evidence, we presumed that a steric hindrance area might exist for this series of compounds.

7.3 Project 3

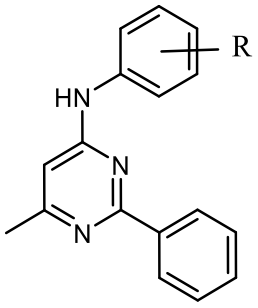

Project 3

In project 3, we continued the investigations of Krapf et al. on pyrimidine derivatives as potential ABCG2 inhibitors. 2-phenylpyrimidine ring which contains critical features was preserved. Position 6 of pyrimidine core was substituted as methyl and a variety of substituents was introduced on aniline moiety at position 4. Removing the left benzene ring of quinazoline scaffold improved aqueous solubility. All of the

derivatives were evaluated in both Hoechst 33342 accumulation and pheophorbide A assays.

At first, when CH_2 was inserted at *meta* or *para* position of aniline moiety, the activities were significantly decreased. Afterwards, halogen was inserted at *meta* position. Bromine displayed excellent inhibitory potency in pheophorbide A assay. Inspired by this result, combination of halogen and methoxy was applied. All of the 4 compounds containing OCH_3 at *meta* or *para* position did not show improved activity. Therefore, we turned our direction back to CN and NO_2 substituents. Most of compounds with cyano substituent demonstrated excellent inhibitory effects as well as nitro derivatives. But the latter series of compounds did not reach full inhibition. The most potent substances were compounds **61** and **62**. In comparison to Ko143, they are 2-3 fold more potent in Hoechst 33342 assay and displayed comparable efficiency to inhibit pheophorbide A efflux.

Due to the importance of both R^1 and R^2 for interacting with ABCG2, we applied a strategy to fuse R^1 and R^2 substituents into a 5- or 6-membered ring. As a result, compounds **71** (pyridine moiety) and **72** (pyrazine moiety) showed comparable inhibitory activities as Ko143 in pheophorbide A assay. These active compounds promoted us to continue the exploration of 2-phenylpyrimidine derivatives.

7.4 Project 4

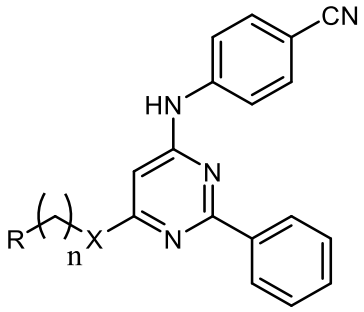

Project 4

The different inhibitory potency of PD153035 and PD158780 inspired us to investigate the potential influence of area around position 5 and 6 of pyrimidine ring. Due to the easy availability and high activity, position 4 was preserved as 4-cyanoaniline. Considering the difficulty of synthesis, position 6 was selected as the modification point. The methyl group in last series of derivatives was replaced by chlorine, phenyl and various amines or anilines.

In the beginning, 4 aliphatic amino residues with various lengths were introduced at position 6. Compound **78** (n-propylamino) displayed slightly decreased potency than Ko143. To improve the potential lipophilic interaction, phenyl was introduced in the end of various aliphatic chains. As a result, compound **80** in which phenyl was directly attached to pyrimidine ring showed no inhibitory effect. But compound **81** and **82** in which phenyl was connected to pyrimidine scaffold via NH and $NHCH_2$ respectively demonstrated comparable inhibitory activities as Ko143. Therefore, the efficient number of n might be 0 or 1. Next, X was preserved as NH and n was decided as 0 or 1, the phenyl group was replaced by pyridines and phenols to investigate potential polar interactions. However, none of them showed increased potency which might indicate the disadvantage of polar modification. By comparison to results of 4-anilino-6-methyl-2-phenylpyrimidine derivatives, certain modification at position 6 of pyrimidine core might slightly improve the inhibitory potency.

ABCG2 is one of important proteins which are associated with multi-drug resistance. All of these four projects involving various phthalazine, quinazoline and pyrimidine derivatives were aiming to find potent ABCG2 inhibitors. The biological data show pyrimidine is a promising scaffold which might be more potent than quinazoline and it is worth to further investigation. Other biological investigations such as cytotoxicity of compounds in this study are on the way.

8 Experimental section

8.1 Materials and methods

Chemicals: All chemicals were purchased from Acros Organics (Belgium), Alfa Aesar (Germany), Sigma-Aldrich (Germany) or Merck (Germany).

Chromatography:

Thin layer chromatography (TLC): The reaction progress was monitored by analytical thin layer chromatography (TLC) on silica gel plates (Silica Gel 60 F254, Merck). For detection, 254 nm and 366 nm UV light were used.

Column chromatography: For certain compounds, column chromatography was performed for final purification. Silica gel 60 (40-63 µm) obtained from Merck was used as stationary phase. Eluting system is described in corresponding synthesis step.

NMR-Spectroscopy: Structures of all compounds were confirmed by NMR. NMR spectra were recorded in DMSO-d_6 or $CDCl_3$. All ^{1}H NMR spectra and ^{13}C NMR were obtained on a Bruker Advance 500 (500 MHz in ^{1}H spectra and 126 MHz in ^{13}C spectra) or Bruker Advance 600 (600 MHz in ^{1}H spectra and 151 MHz in ^{13}C spectra).

Fourier-transform infrared spectroscopy (FTIR): For certain compounds, IR spectra were recorded with a FTIR spectrometer ALPHA from Bruker in ATR mode. The spectra were subsequently evaluated with the Opus software and converted into transmission spectra.

Microwave synthesis: The microwave syntheses were performed in microwave Discover SP produced by CEM.

Liquid chromatography–mass spectrometry (LC-MS): The purities of selected compounds were determined by ESI−mass spectra obtained on an LC-MS instrument (Applied Biosystems API 2000 LC-MS/MS, HPLC Agilent 1100).

8.2 Synthesis procedures

8.2.1.1: Synthesis of 1-chlorophthalazine (1)

450 mg 1(2H)-phthalazinone and 1.5 ml phosphorus oxychloride were filled into a 10 ml microwave vessel. The slurry was slowly heated up to 80 °C and maintained at that temperature for 30 min in microwave reactor. When TLC indicated reaction was completed, the mixture was allowed to cool to room temperature and was transferred carefully onto crushed ice portion by portion. After ice had melt, the solution was stirred for 0.5 hour and slowly basified with saturated sodium carbonate solution until no bubbles were observed (pH = 8-9). The temperature of solution should always be kept under 10 °C. Yellow precipitate fell out, and was extracted by 50 ml dichloromethane 3 times. The organic layer was washed with brine, dried over Na_2SO_4 and concentrated under reduced pressure at 40 °C. Further purification was performed by column chromatography with DCM/MeOH = 20:1 as eluent to yield pale yellow crystals (197 mg; 39 %).

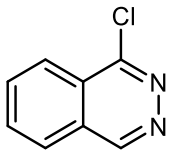

Molecular Weight: 164.59

^{1}H NMR (600 MHz, $CDCl_3$) δ: 9.45 (d, *J* = 0.9 Hz, 1H), 8.32 (ddd, *J* = 1.3, 2.2, 7.8 Hz, 1H), 8.05 – 7.98 (m, 3H).

^{13}C NMR (151 MHz, $CDCl_3$) δ: 155.60, 151.37, 133.98, 133.69, 128.34, 126.84, 126.27, 125.31.

In work-up process, hydrolysis and reversion of 1-chlorophthalazine may be observed at high temperature and aqueous acidic conditions as well as dimerization and

oligomerization. Moreover, degradation may also take place at room temperature. This inherent instability was also described elsewhere.[150, 151] Therefore, it is advised to use freshly purified 1-chlorophthalazine for next step.

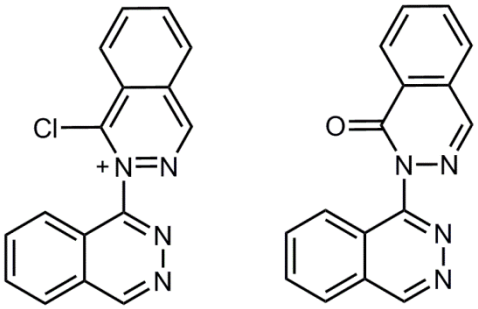

Figure 17: Proposed dimers adapted from Achmatowicz et al.[150]

8.2.1.2: Synthesis of 1-anilinephthalazine or 1-aniline-4-phenylphthalazine derivatives

1-Chloro-4-phenylphthalazine was bought from commercial source and 1-chlorophthalazine was freshly prepared. A mixture of 1 mmol phthalazine and 1 mmol substituted aniline was dissolved in 3 ml isopropanol. The mixture was heated to 70 °C at 60 W irradiation and maintained for 10 mins in microwave reactor. After cooling, the precipitate was filtered off and washed with acetonitrile 3 times. Subsequently, it was washed with saturated sodium carbonate solution and distilled water for 3 times respectively. Further purification was performed by recrystallization or column chromatography.

N-(3,4-dimethoxyphenyl)phthalazin-1-amine (2)

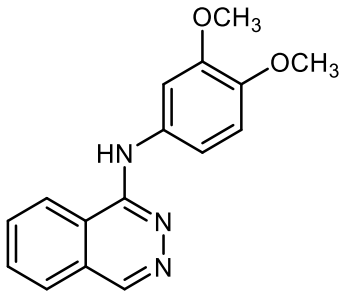

Molecular Weight: 281.32

The title compound was synthesized from 1-chloroquinazoline (156 mg, 0.95 mmol) and 3,4-dimethoxyaniline (155 mg, 1.01 mmol) as described in the general procedure above. Further purification was performed by column chromatography with DCM to DCM/MeOH = 50:1 as eluent, yellow solid (44 mg, 16.5 %).

^{1}H NMR (500 MHz, DMSO-d_6) δ: 9.07 (s, 1H), 8.99 (s, 1H), 8.56 (d, J = 8.0 Hz, 1H), 8.03 – 7.90 (m, 3H), 7.58 – 7.50 (m, 2H), 6.96 (d, J = 8.7 Hz, 1H), 3.79 (s, 3H), 3.76 (s, 3H).

^{13}C NMR (126 MHz, DMSO) δ: 152.35, 148.47, 144.81, 144.45, 134.12, 131.83, 131.66, 127.09, 126.42, 121.92, 118.00, 113.31, 112.09, 106.76, 55.85, 55.50.

N-(3-bromophenyl)phthalazin-1-amine (3)

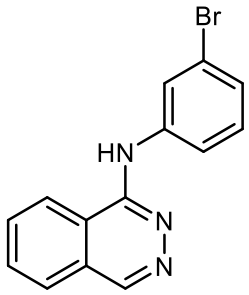

Molecular Weight: 300.16

The title compound was synthesized from 1-chloroquinazoline (152 mg, 0.93 mmol) and 3-bromoaniline (196 mg, 1.14 mmol) as described in the general procedure above. Further purification was performed by recrystallization from EtOH/H_2O, beige solid (68.5 mg, 24.6 %).

^{1}H NMR (500 MHz, DMSO-d_6) δ: 9.30 (s, 1H), 9.19 (d, J = 1.0 Hz, 1H), 8.59 (dd, J = 1.0, 8.2 Hz, 1H), 8.37 (t, J = 2.0 Hz, 1H), 8.08 – 7.97 (m, 3H), 7.94 (ddd, J = 1.0, 2.2, 8.4 Hz, 1H), 7.32 (t, J = 8.1 Hz, 1H), 7.21 (ddd, J = 0.9, 2.0, 7.9 Hz, 1H).

^{13}C NMR (126 MHz, DMSO) δ: 152.05, 145.95, 142.35, 132.23, 132.07, 130.29, 127.19, 126.67, 124.42, 122.52, 122.04, 121.26, 119.13, 118.21.

3-(phthalazin-1-ylamino)benzonitrile (4)

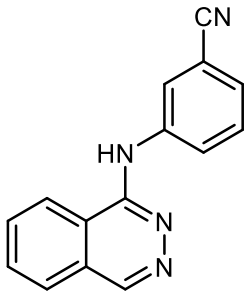

Molecular Weight: 246.27

The title compound was synthesized from 1-chloroquinazoline (96 mg, 0.58 mmol) and 3-cyanoaniline (130 mg, 1.10 mmol) as described in the general procedure above. Further purification was performed by column chromatography with DCM to DCM/MeOH = 50:1 as eluent, beige solid (11.7 mg, 8.2 %).

^{1}H NMR (500 MHz, DMSO-d_6) δ: 9.48 (s, 1H), 9.22 (d, J = 0.9 Hz, 1H), 8.59 (d, J = 8.8 Hz, 1H), 8.54 (t, J = 1.9 Hz, 1H), 8.22 (ddd, J = 8.4, 2.3, 1.1 Hz, 1H), 8.10 – 7.98 (m, 3H), 7.58 (t, J = 8.0 Hz, 1H), 7.47 (dt, J = 7.6, 1.3 Hz, 1H).

^{13}C NMR (126 MHz, DMSO) δ: 152.00, 146.20, 141.53, 132.31, 132.13, 129.78, 127.20, 126.69, 125.22, 124.82, 122.88, 122.01, 119.01, 118.20, 111.18.

N-(4-fluorophenyl)phthalazin-1-amine (5)

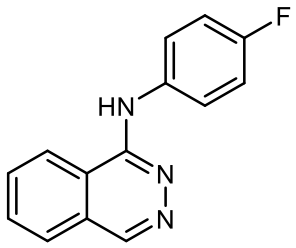

Molecular Weight: 239.25

The title compound was synthesized from 1-chloroquinazoline (299 mg, 1.82 mmol) and 4-fluoroaniline (248 mg, 2.23 mmol) as described in the general procedure above. Further purification was performed by recrystallization from EtOH/H_2O, beige solid (15.5 mg, 3.6 %).

^{1}H NMR (500 MHz, DMSO-d_6) δ: 9.17 (s, 1H), 9.12 (s, 1H), 8.58 – 8.55 (m, 1H), 8.06 – 7.90 (m, 5H), 7.24 – 7.15 (m, 2H).

^{13}C NMR (126 MHz, DMSO) δ: 157.53 (d, J = 238.8 Hz), 152.19, 145.34, 136.88, 132.00, 131.82, 127.14, 126.50, 122.72 (d, J = 7.7 Hz), 122.00, 118.01, 114.80 (d, J = 22.1 Hz).

N-(4-nitrophenyl)phthalazin-1-amine (6)

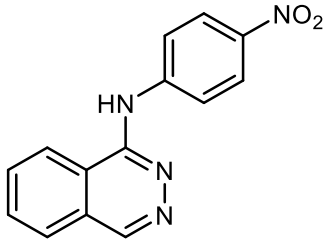

Molecular Weight: 266.26

The title compound was synthesized from 1-chloroquinazoline (77 mg, 0.47 mmol) and 4-nitroaniline (77 mg, 0.56 mmol) as described in the general procedure above. Further purification was performed by column chromatography with DCM to DCM/MeOH = 50:1 as eluent, yellow solid (13.3 mg, 10.6 %).

^{1}H NMR (500 MHz, DMSO-d_6) δ: 9.86 (s, 1H), 9.32 (s, 1H), 8.62 (d, J = 8.5 Hz, 1H), 8.29 – 8.22 (m, 4H), 8.13 (dd, J = 7.9, 1.3 Hz, 1H), 8.09 – 8.01 (m, 2H).

^{13}C NMR (126 MHz, DMSO) δ: 147.39, 147.05, 140.67, 139.99, 132.56, 132.35, 127.33, 126.79, 124.80, 122.22, 118.98, 118.64.

N-(3,4-dimethoxyphenyl)-4-phenylphthalazin-1-amine (7)

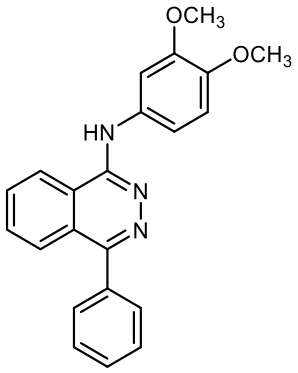

Molecular Weight: 357.41

The title compound was synthesized from 1-chloro-4-phenylphthalazine (47 mg, 0.20 mmol) and 3,4-dimethoxyaniline (46 mg, 0.30 mmol) as described in the general procedure above. Further purification was performed by recrystallization from EtOH/H_2O, dark grey solid (15.5 mg, 3.6 %).

^{1}H NMR (500 MHz, DMSO-d_6) δ: 9.10 (s, 1H), 8.64 (d, J = 8.2 Hz, 1H), 8.01 (ddd, J = 8.3, 6.9, 1.4 Hz, 1H), 7.92 (ddd, J = 8.2, 6.9, 1.2 Hz, 1H), 7.86 (dd, J = 8.3, 1.4 Hz, 1H), 7.68 – 7.61 (m, 3H), 7.60 – 7.50 (m, 4H), 6.98 (d, J = 8.7 Hz, 1H), 3.80 (s, 3H), 3.77 (s, 3H).

^{13}C NMR (126 MHz, DMSO) δ: 152.86, 151.91, 148.49, 144.49, 136.82, 134.16, 131.95, 131.39, 129.59, 128.40, 128.32, 125.65, 125.62, 122.47, 118.25, 113.33, 112.09, 106.80, 55.86, 55.52.

3-((4-phenylphthalazin-1-yl)amino)phenol (8)

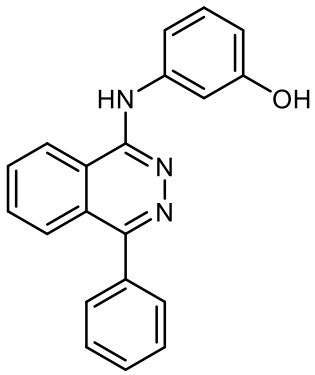

Molecular Weight: 313.36

The title compound was synthesized from 1-chloro-4-phenylphthalazine (45 mg, 0.19 mmol) and 3-aminophenol (22 mg, 0.20 mmol) as described in the general procedure above. Further purification was performed by recrystallization from ethyl acetate/cyclohexane, yellow solid (8.1 mg, 13.6 %).

^{1}H NMR (500 MHz, DMSO-d_6) δ: 9.32 (s, 1H), 9.13 (s, 1H), 8.66 (d, J = 8.4 Hz, 1H), 8.01 (ddd, J = 8.3, 6.9, 1.3 Hz, 1H), 7.93 (ddd, J = 8.1, 6.9, 1.1 Hz, 1H), 7.89 – 7.87 (m, 1H), 7.68 – 7.65 (m, 2H), 7.61 (t, J = 2.2 Hz, 1H), 7.60 – 7.53 (m, 3H), 7.31 (ddd, J = 8.1, 2.1, 0.9 Hz, 1H), 7.13 (t, J = 8.1 Hz, 1H), 6.46 (ddd, J = 8.0, 2.4, 0.9 Hz, 1H).

^{13}C NMR (126 MHz, DMSO) δ: 157.45, 153.25, 151.83, 141.68, 136.78, 132.08, 131.49, 129.62, 128.89, 128.50, 128.38, 125.69, 125.68, 122.70, 118.48, 111.63, 109.36, 107.95.

8.2.1.3: Synthesis of 1,4-dicholorphthalazine

15 g 2,3-dihydrophthalazine-1,4-dione was added into 30 ml $POCl_3$. The reaction was refluxed for 8-9 hours until it was complete. Excess $POCl_3$ was removed under reduced pressure. The oily residue was transfer onto crushed ice portion by portion, while keeping the temperature of solution below 10 °C. Subsequently, 1 M NaOH was added until pH = 8-9 and a yellow solid precipitated. After filtering off the precipitate, it was washed with 100 ml distilled water 3 times. Further purification was performed by column chromatography with DCM as eluent to yield pale yellow or white needle crystals (4.23g, 22 %).

Different from 1-chlorophthalazine, 1,4-dicholorphthalazine was stored under no special condition, no stability issues were displayed in the first few weeks. The right pure product should be pale yellow or white needle crystals. Nevertheless, red products with little impurity inside might also be applicable for next step.

1,4-dichlorophthalazine (9)

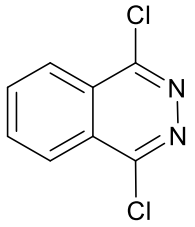

Molecular Weight: 199.03

^{1}H NMR (500 MHz, DMSO-d_6) δ: 8.39 – 8.35 (m, 2H), 8.30 – 8.26 (m, 2H).

^{13}C NMR (126 MHz, DMSO) δ: 154.83, 135.80, 126.81, 125.79.

8.2.1.2: Synthesis of 1-chloro-4-anilinophthalazine derivatives.

1 equivalent 1,4-dichlorophthalazine was added into 5 ml isopropanol. The mixture was heated up to 70 °C and no solid was visible. On the other hand, 1 equivalent of substituted aniline was dissolved in 10-15 ml isopropanol. Aniline solution was added to hot 1,4-dichlorophthalazine solution drop by drop. If initiation of reaction was not observed, 0.1 equivalent of conc. HCl was added as catalyst. After the completion of reaction which was monitored by TLC, the precipitate was filtered off and washed with saturated sodium bicarbonate solution 3 times and distilled water 3 times. Further purification was performed by column chromatography.

Tip: A little amount of hydrochloric acid (0.1 equi.) catalyzes and speeds up reaction, especially when aniline was substituted by electro withdrawing group. This observation was consistent with what was described by Banks.[125] He performed various condensation reactions between haloheterocycles with aniline, and it was found that condensation occurred only under acidic conditions, while little or no reaction was noticed under alkaline conditions. In addition, this was also a proof that the rate determining step of this reaction was addition but not elimination step.

In 1-chlorophthalazine synthesis, we described acidic aqueous condition would lead to hydrolysis and oligomerization. But here, acid could also catalyze the desired reaction between chlorinated phthalazine and substituted aniline. Hydrogen ion seemed a two-

edged sword. To lead reaction to our desired direction, the amount of acid in reaction system should always be taken into account as well as temperature. High concentration of acid may easily result in unexpected products.

4-chloro-N-(3,4-dimethoxyphenyl)phthalazin-1-amine (10)

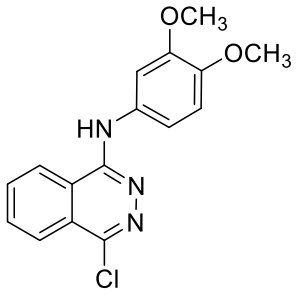

Molecular Weight: 315.76

The title compound was synthesized from 1,4-dichlorophthalazine (259 mg, 1.30 mmol) and 3,4-dimethoxylaniline (199 mg, 1.30 mmol) as described in the general procedure above. Green solid (294.1 mg, 71.6 %).

^{1}H NMR (500 MHz, DMSO-d_6) δ: 9.20 (s, 1H), 8.64 (d, J = 7.6 Hz, 1H), 8.15 (dd, J = 7.5, 1.9 Hz, 1H), 8.11 – 8.05 (m, 2H), 7.50 (d, J = 2.5 Hz, 1H), 7.44 (dd, J = 8.6, 2.5 Hz, 1H), 6.97 (d, J = 8.6 Hz, 1H), 3.78 (s, 3H), 3.77 (s, 3H).

^{13}C NMR (126 MHz, DMSO) δ: 152.91, 148.47, 145.80, 144.90, 133.38, 133.21, 132.88, 125.55, 124.67, 123.05, 120.37, 113.80, 111.96, 107.08, 55.80, 55.51.

4-chloro-N-(3-methoxyphenyl)phthalazin-1-amine (11)

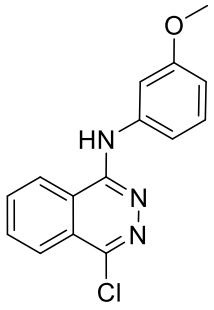

Molecular Weight: 285.73

The title compound was synthesized from 1,4-dichlorophthalazine (104 mg, 0.52 mmol) and 3-methoxylaniline (67.4 mg, 0.44 mmol) as described in the general procedure above. Further purification was performed by column chromatography with ethyl acetate/petroleum ether (40-60 °C) = 1:2 as eluent, beige solid (38.3 mg, 53.5 %).

^{1}H NMR (500 MHz, DMSO-d_6) δ: 9.28 (s, 1H), 8.67 – 8.64 (m, 1H), 8.18 – 8.15 (m, 1H), 8.12 – 8.06 (m, 2H), 7.57 (t, J = 2.2 Hz, 1H), 7.48 (ddd, J = 0.9, 2.2, 8.2 Hz, 1H), 7.26 (t, J = 8.2 Hz, 1H), 6.65 (ddd, J = 0.9, 2.5, 8.2 Hz, 1H), 3.77 (s, 3H).

^{13}C NMR (126 MHz, DMSO) δ: 159.61, 152.96, 146.68, 141.37, 133.53, 133.17, 129.29, 125.79, 124.90, 123.36, 120.69, 113.63, 108.31, 107.15, 55.19.

N-(3-bromophenyl)-4-chlorophthalazin-1-amine (12)

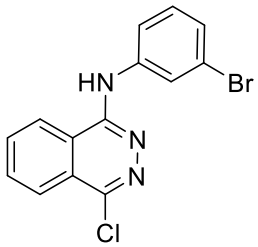

Molecular Weight: 334.60

The title compound was synthesized from 1,4-dichlorophthalazine (231 mg, 1.16 mmol) and 3-bromoaniline (210 mg, 1.22 mmol) as described in the general procedure above. Further purification was performed by recrystallization from isopropanol, white solid (90.5 mg, 27.1 %).

^{1}H NMR (500 MHz, DMSO-d_6) δ: 9.46 (s, 1H), 8.68 – 8.64 (m, 1H), 8.26 (t, J = 2.0 Hz, 1H), 8.20 (dd, J = 1.6, 7.8 Hz, 1H), 8.16 – 8.08 (m, 2H), 7.88 (ddd, J = 0.9, 2.0, 8.2 Hz, 1H), 7.34 (t, J = 8.0 Hz, 1H), 7.24 (ddd, J = 1.0, 2.0, 8.1 Hz, 1H).

^{13}C NMR (126 MHz, DMSO) δ: 152.58, 147.07, 141.74, 133.55, 133.18, 130.34, 125.68, 125.04, 124.83, 123.17, 123.03, 121.24, 120.52, 119.59.

4-chloro-N-(4-fluorophenyl)phthalazin-1-amine (13)

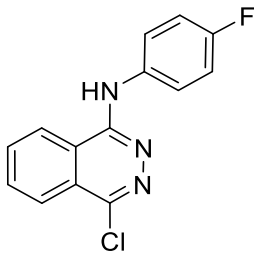

Molecular Weight: 273.70

The title compound was synthesized from 1,4-dichlorophthalazine (101 mg, 0.51 mmol) and 4-fluoroaniline (56 mg, 0.51 mmol) as described in the general procedure above. Further purification was performed by column chromatography with ethyl acetate/petroleum ether (40-60 °C) = 1:1 as eluent, pale yellow solid (60.0 mg, 43.0 %).
^{1}H NMR (500 MHz, DMSO-d_6) δ: 11.26 (s, 1H), 9.10 (dd, J = 2.0, 7.3 Hz, 1H), 8.28 – 8.18 (m, 3H), 7.76 – 7.71 (m, 2H), 7.37 – 7.31 (m, 2H).
^{13}C NMR (126 MHz, DMSO) δ: 160.14 (d, J = 242.9 Hz), 152.08, 145.49, 135.40, 134.00, 133.08, 126.40 (d, J = 8.2 Hz), 126.31, 125.63, 125.24, 121.62, 116.15 (d, J = 22.6 Hz).

3-((4-chlorophthalazin-1-yl)amino)benzonitrile (14)

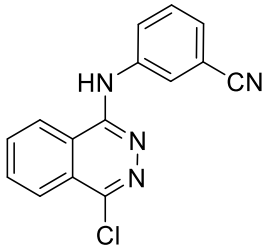

Molecular Weight: 280.72

The title compound was synthesized from 1,4-dichlorophthalazine (135 mg, 0.68 mmol) and 3-cyanoaniline (89 mg, 0.76 mmol) as described in the general procedure above. Further purification was performed by recrystallization from isopropanol, white solid (73.4 mg, 38.6 %).

^{1}H NMR (500 MHz, DMSO-d_6) δ: 9.61 (s, 1H), 8.64 (dd, J = 7.7, 1.6 Hz, 1H), 8.42 (t, J = 1.9 Hz, 1H), 8.21 – 8.18 (m, 1H), 8.16 – 8.09 (m, 3H), 7.58 (t, J = 7.9 Hz, 1H), 7.49 (dt, J = 7.6, 1.3 Hz, 1H).

^{13}C NMR (126 MHz, DMSO) δ: 152.72, 147.55, 141.16, 133.84, 133.43, 130.04, 126.01, 125.89, 125.46, 125.06, 123.59, 123.34, 120.69, 119.06, 111.44.

4-chloro-N-(4-nitrophenyl)phthalazin-1-amine (15)

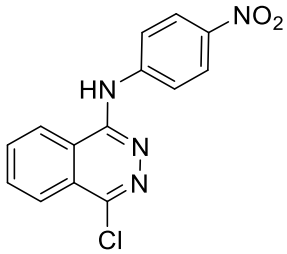

Molecular Weight: 300.70

The title compound was synthesized from 1,4-dichlorophthalazine (205 mg, 1.03 mmol) and 4-nitroaniline (145 mg, 1.05 mmol) as described in the general procedure above. Yellow solid (167.1 mg, 53.9 %).

^{1}H NMR (500 MHz, DMSO-d_6) δ: 9.96 (s, 1H), 8.68 (dd, J = 1.6, 7.6 Hz, 1H), 8.28 – 8.21 (m, 3H), 8.19 – 8.12 (m, 4H).

^{13}C NMR (126 MHz, DMSO) δ: 152.37, 148.34, 146.87, 141.06, 133.88, 133.42, 125.83, 124.94, 124.74, 123.41, 120.93, 119.44.

4-chloro-N-(3-nitrophenyl)phthalazin-1-amine (16)

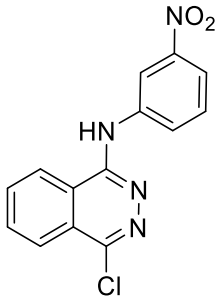

Molecular Weight: 300.70

The title compound was synthesized from 1,4-dichlorophthalazine (108 mg, 0.54 mmol) and 3-nitroaniline (75 mg, 0.54 mmol) as described in the general procedure above. Further purification was performed by column chromatography with ethyl acetate/petroleum ether (40-60 °C) = 1:3 as eluent, yellow solid (8.7 mg, 5.4 %).

^{1}H NMR (500 MHz, DMSO-d_6) δ: 9.78 (s, 1H), 8.95 (t, J = 2.2 Hz, 1H), 8.71 – 8.69 (m, 1H), 8.36 (ddd, J = 0.7, 2.1, 8.2 Hz, 1H), 8.24 – 8.21 (m, 1H), 8.20 – 8.12 (m, 2H), 7.91 (ddd, J = 0.8, 2.3, 8.1 Hz, 1H), 7.67 (t, J = 8.2 Hz, 1H).

^{13}C NMR (126 MHz, DMSO) δ: 152.54, 147.92, 147.54, 141.38, 133.70, 133.30, 129.72, 126.56, 125.72, 124.91, 123.17, 120.53, 116.79, 114.60.

3-((4-chlorophthalazin-1-yl)amino)phenol (17)

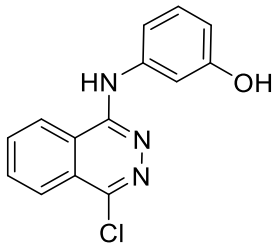

Molecular Weight: 271.70

The title compound was synthesized from 1,4-dichlorophthalazine (200 mg, 1.00 mmol) and 3-aminophenol (117 mg, 1.07 mmol) as described in the general procedure above. Pale yellow solid (102.5 mg, 37.7 %).

^{1}H NMR (500 MHz, DMSO-d_6) δ: 9.37 (s, 1H), 9.21 (s, 1H), 8.68 – 8.65 (m, 1H), 8.19 – 8.15 (m, 1H), 8.12 – 8.06 (m, 2H), 7.47 (t, J = 2.2 Hz, 1H), 7.25 (dd, J = 8.4, 1.1 Hz, 1H), 7.14 (t, J = 8.0 Hz, 1H), 6.49 (ddd, J = 8.1, 2.5, 0.9 Hz, 1H).

^{13}C NMR (126 MHz, DMSO) δ: 157.45, 152.80, 146.31, 141.02, 133.31, 132.96, 128.97, 125.62, 124.70, 123.26, 120.53, 112.00, 109.95, 108.35.

4-((4-chlorophthalazin-1-yl)amino)benzonitrile (18)

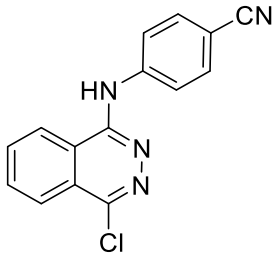

Molecular Weight: 280.72

The title compound was synthesized from 1,4-dichlorophthalazine (154 mg, 0.77 mmol) and 4-cyanoaniline (98 mg, 0.83 mmol) as described in the general procedure above. Further purification was performed by column chromatography with ethyl acetate/petroleum ether (40-60 °C) = 1:2 as eluent, beige solid (28.3 mg, 13.1 %).

^{1}H NMR (500 MHz, DMSO-d_6) δ: 9.76 (s, 1H), 8.67 (d, J = 7.4 Hz, 1H), 8.23 (dd, J = 1.6, 7.7 Hz, 1H), 8.18 – 8.13 (m, 2H), 8.13 – 8.09 (m, 2H), 7.83 – 7.79 (m, 2H).

^{13}C NMR (126 MHz, DMSO) δ: 152.47, 147.98, 144.64, 133.83, 133.39, 132.92, 125.82, 124.95, 123.36, 120.82, 120.18, 119.36, 103.58.

8.2.1.4: Synthesis of 1,4-bisanilinophthalazine derivatives

A mixture of 200 mg 1,4-dichlorophthalazine, 2 equivalent of substituted aniline in 3 ml isopropanol was heated to 110 °C in microwave for 15-30 mins. If reaction did not initiate, 0.1 equivalent of conc. HCl was added as catalyst. The precipitate was filtered off and washed with saturated sodium bicarbonate solution 3 times followed by distilled water 3 times. Further purification for certain compounds was performed by recrystallization or column chromatography.

N1,N4-bis(3,4-dimethoxyphenyl)phthalazine-1,4-diamine (19)

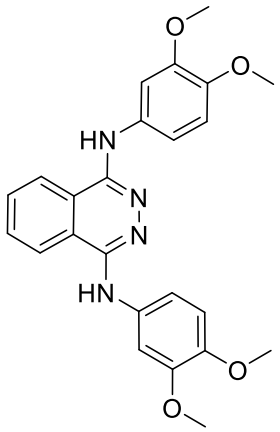

Molecular Weight: 432.48

The title compound was synthesized from 1,4-dichlorophthalazine (126 mg, 0.63 mmol) and 3,4-dimethoxylaniline (241 mg, 1.57 mmol) as described in the general procedure above. Pale green solid (105 mg, 38.4 %).

^{1}H NMR (500 MHz, DMSO-d_6) δ: 8.55 (s, 2H), 8.49 – 8.44 (m, 2H), 7.98 – 7.94 (m, 2H), 7.46 – 7.42 (m, 4H), 6.90 (d, J = 8.5 Hz, 2H), 3.76 (s, 6H), 3.74 (s, 6H).

^{13}C NMR (126 MHz, DMSO) δ: 148.61, 148.46, 143.53, 135.64, 131.13, 122.65, 120.47, 112.41, 111.78, 105.60, 55.97, 55.48.

N1,N4-bis(3-methoxyphenyl)phthalazine-1,4-diamine (20)

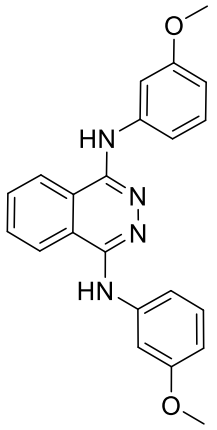

Molecular Weight: 372.43

The title compound was synthesized from 1,4-dichlorophthalazine (106 mg, 0.53 mmol) and 3-methoxylaniline (147 mg, 1.20 mmol) as described in the general procedure

above. Further purification was performed by column chromatography with ethyl acetate/petroleum ether (40-60 °C) = 1:1 as eluent, pale yellow solid (150.6 mg, 76.0 %).

^{1}H NMR (500 MHz, DMSO-d_6) δ: 8.78 (s, 2H), 8.50 (dd, J = 3.3, 6.2 Hz, 2H), 7.99 (dd, J = 3.1, 6.2 Hz, 2H), 7.50 (t, J = 2.4 Hz, 2H), 7.45 (dd, J = 2.0, 7.9 Hz, 2H), 7.20 (t, J = 8.1 Hz, 2H), 6.53 (dd, J = 2.5, 8.1 Hz, 2H), 3.76 (s, 6H).

^{13}C NMR (126 MHz, DMSO) δ: 159.52, 148.58, 143.01, 131.39, 129.01, 122.80, 120.65, 111.84, 106.10, 105.23, 54.91.

N1,N4-bis(4-fluorophenyl)phthalazine-1,4-diamine (21)

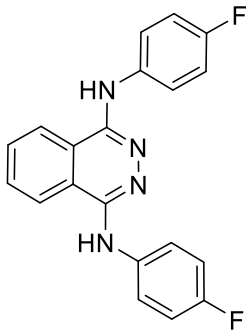

Molecular Weight: 348.36

The title compound was synthesized from 1,4-dichlorophthalazine (125 mg, 0.63 mmol) and 4-fluoroaniline (195 mg, 1.76 mmol) as described in the general procedure above. Pale yellow solid (209 mg, 79.0 %).

^{1}H NMR (500 MHz, DMSO-d_6) δ: 8.83 (s, 2H), 8.51 (dd, J = 6.2, 3.3 Hz, 2H), 7.99 (dd, J = 6.2, 3.2 Hz, 2H), 7.87 (dd, J = 9.1, 4.8 Hz, 4H), 7.17 – 7.11 (m, 4H).

^{13}C NMR (126 MHz, DMSO) δ: 156.79 (d, J = 237.2 Hz), 148.49, 138.09, 131.40, 122.78, 121.16 (d, J = 7.7 Hz), 120.45, 114.70 (d, J = 22.0 Hz).

N1,N4-bis(3-nitrophenyl)phthalazine-1,4-diamine (22)

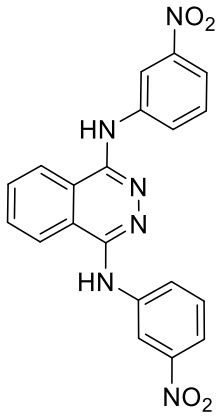

Molecular Weight: 402.37

The title compound was synthesized from 1,4-dichlorophthalazine (149 mg, 0.75 mmol) and 3-nitroaniline (253 mg, 1.83 mmol) as described in the general procedure above. Red solid (90 mg, 29.9 %).

^{1}H NMR (500 MHz, DMSO-d_6) δ: 9.42 (s, 2H), 8.58 (dd, J = 3.4, 6.2 Hz, 2H), 8.34 (d, J = 8.3 Hz, 2H), 8.08 (dd, J = 3.5, 6.3 Hz, 2H), 7.82 – 7.78 (m, 4H), 7.61 (t, J = 8.2 Hz, 2H).

^{13}C NMR (126 MHz, DMSO) δ: 148.70, 148.05, 142.76, 132.01, 129.66, 125.24, 122.86, 120.55, 115.27, 113.10.

N1,N4-bis(4-nitrophenyl)phthalazine-1,4-diamine (23)

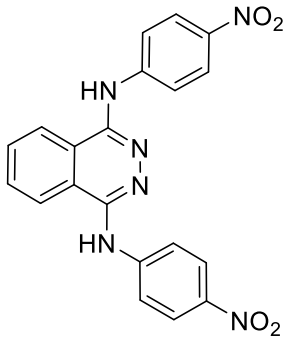

Molecular Weight: 402.37

The title compound was synthesized from 1,4-dichlorophthalazine (140 mg, 0.70 mmol) and 4-nitroaniline (242 mg, 1.75 mmol) as described in the general procedure above. Pale grey solid (80 mg, 28.3 %).

^{1}H NMR (500 MHz, DMSO-d_6) δ: 9.77 (s, 2H), 8.57 (dd, J = 6.2, 3.3 Hz, 2H), 8.24 (d, J = 8.9 Hz, 4H), 8.12 – 8.08 (m, 6H).

^{13}C NMR (126 MHz, DMSO) δ: 148.87, 148.12, 140.00, 132.28, 124.98, 123.04, 120.85, 117.95.

3,3'-(phthalazine-1,4-diylbis(azanediyl))diphenol (24)

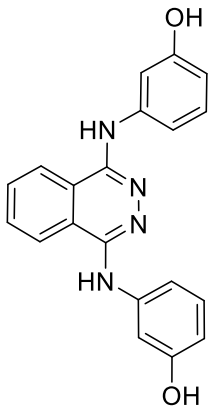

Molecular Weight: 344.37

The title compound was synthesized from 1,4-dichlorophthalazine (120 mg, 0.60 mmol) and 3-aminophenol (168 mg, 1.54 mmol) as described in the general procedure above. Further purification was performed by column chromatography with $CHCl_3$/MeOH = 3:1 as eluent, yellow solid (62.7 mg, 30.3 %).

^{1}H NMR (500 MHz, DMSO-d_6) δ: 9.19 (s, 2H), 8.65 (s, 2H), 8.49 (dd, J = 3.3, 6.2 Hz, 2H), 7.97 (dd, J = 3.2, 6.2 Hz, 2H), 7.50 (t, J = 2.2 Hz, 2H), 7.16 (ddd, J = 1.0, 2.1, 8.1 Hz, 2H), 7.06 (t, J = 8.0 Hz, 2H), 6.35 (ddd, J = 1.0, 2.4, 8.0 Hz, 2H).

^{13}C NMR (126 MHz, DMSO) δ: 157.45, 148.50, 142.93, 131.29, 128.82, 122.85, 120.66, 110.31, 108.01, 106.42.

N1,N4-bis(3-(trifluoromethyl)phenyl)phthalazine-1,4-diamine (25)

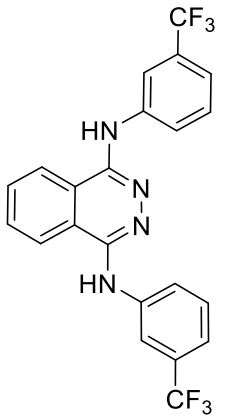

Molecular Weight: 448.37

The title compound was synthesized from 1,4-dichlorophthalazine (112 mg, 0.56 mmol) and 3-trifluoroamine (250 mg, 1.55 mmol) as described in the general procedure above. Further purification was performed by recrystallization from DMF/H_2O, yellow solid (45.5 mg, 18.0 %).

^{1}H NMR (500 MHz, DMSO-d_6) δ: 9.99 (s, 2H), 8.76 (s, 2H), 8.21 – 8.14 (m, 4H), 8.07 (d, J = 8.2 Hz, 2H), 7.63 (t, J = 8.0 Hz, 2H), 7.44 (d, J = 5.9 Hz, 2H).

^{13}C NMR (126 MHz, DMSO) δ: 162.23, 148.34, 140.37, 133.35, 130.01, 129.62 (q, J = 32.0 Hz), 124.11, 121.65, 124.17 (q, J = 272.5 Hz), 119.62, 117.54.

N1,N4-bis(3-bromophenyl)phthalazine-1,4-diamine (26)

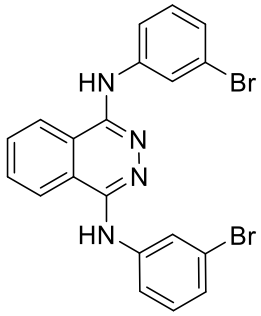

Molecular Weight: 470.17

The title compound was synthesized from 1,4-dichlorophthalazine (142 mg, 0.71 mmol) and 3-bromoaniline (376 mg, 2.19 mmol) as described in the general procedure above. Further purification was performed by recrystallization from 75% EtOH, white solid (41.0 mg, 12.3 %).

^{1}H NMR (500 MHz, DMSO-d_6) δ: 9.02 (s, 2H), 8.51 (dd, J = 6.2, 3.3 Hz, 2H), 8.19 (t, J = 2.0 Hz, 2H), 8.04 – 8.01 (m, 2H), 7.83 (ddd, J = 8.3, 2.1, 0.9 Hz, 2H), 7.27 (t, J = 8.1 Hz, 2H), 7.11 (ddd, J = 7.9, 1.9, 0.9 Hz, 2H).

^{13}C NMR (126 MHz, DMSO) δ: 148.72, 143.49, 131.93, 130.47, 123.47, 122.99, 121.51, 121.43, 120.73, 118.21, 40.24, 39.78, 39.63, 39.34.

3,3'-(phthalazine-1,4-diylbis(azanediyl))dibenzonitrile (27)

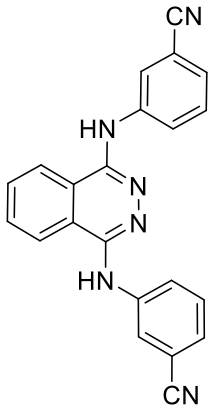

Molecular Weight: 362.40

The title compound was synthesized from 1,4-dichlorophthalazine (201 mg, 1.01 mmol) and 3-cyanoaniline (300 mg, 2.54 mmol) as described in the general procedure above. Further purification was performed by recrystallization from DMF/H_2O, yellow solid (215.1 mg, 59.4 %).

^{1}H NMR (500 MHz, DMSO-d_6) δ: 9.23 (s, 2H), 8.53 (dd, J = 6.2, 3.2 Hz, 2H), 8.38 (t, J = 2.0 Hz, 2H), 8.15 (dd, J = 8.4, 2.4 Hz, 2H), 8.06 (dd, J = 6.3, 3.2 Hz, 2H), 7.53 (t, J = 8.0 Hz, 2H), 7.38 (d, J = 7.6 Hz, 1H).

^{13}C NMR (126 MHz, DMSO) δ: 148.64, 142.39, 131.91, 129.79, 124.17, 123.78, 122.82, 121.66, 120.53, 119.16, 111.18.

4,4'-(phthalazine-1,4-diylbis(azanediyl))dibenzonitrile (28)

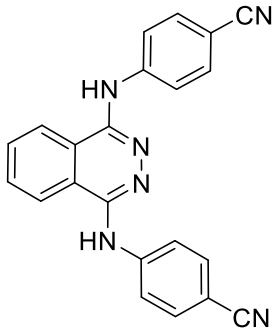

Molecular Weight: 362.40

The title compound was synthesized from 1,4-dichlorophthalazine (194 mg, 0.98 mmol) and 4-cyanoaniline (294 mg, 2.49 mmol) as described in the general procedure above. Yellow solid (226 mg, 64.0 %).

^{1}H NMR (500 MHz, DMSO-d_6) δ: 9.47 (s, 2H), 8.54 (dd, J = 6.2, 3.3 Hz, 2H), 8.09 – 8.04 (m, 6H), 7.77 – 7.74 (m, 4H).

^{13}C NMR (126 MHz, DMSO) δ: 148.75, 145.96, 132.92, 132.11, 122.98, 120.80, 119.70, 118.70, 101.81.

8.2.2.1: Synthesis of 2-phenylquinazolin-4-amine (29)

A mixture of anthranilonitrile (2.316g, 19.6 mmol), benzonitrile (2.127g, 20.6 mmol) and potassium tert-butoxide (209 mg, 1.86 mmol) was added in 10 ml microwave vial and heated to 170 °C in microwave reactor (300 W) until no starting materials were observed by TLC. The crude product was purified by recrystallization from methanol (1.496g, 34.5 %).

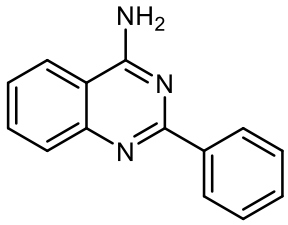

Molecular Weight: 221.26

^{1}H NMR (500 MHz, DMSO-d_6) δ: 8.48 – 8.44 (m, 2H), 8.24 (dt, J = 0.8, 8.2 Hz, 1H), 7.83 – 7.74 (m, 4H), 7.52 – 7.44 (m, 4H).

^{13}C NMR (126 MHz, DMSO) δ: 162.04, 159.68, 150.34, 138.55, 132.89, 129.85, 128.08, 127.77, 127.62, 125.06, 123.53, 113.22.

8.2.2.2: Synthesis of quinazoline derivatives with amide linker

To a stirred solution of 1 eq benzoic acid in DMF (0.5 M final concentration) was added 1.1 eq TBTU and 5 eq DIPEA. The reaction mixture was stirred for 10 mins at room temperature. Afterwards, 1 eq 2-phenyl-4-aminoquinazoline was added. The solution was stirred at 85°C overnight. After the completion of reaction which was monitored by TLC, the mixture was quenched with water, extracted by DCM, and washed with aqueous $NaHCO_3$, 10% w/v aqueous citric acid and brine sequentially. The organic layer was dried with Na_2SO4 and evaporated under reduced pressure to afford the crude product. Further purification was performed by column chromatography.

3,4-dimethoxy-N-(2-phenylquinazolin-4-yl)benzamide (30)

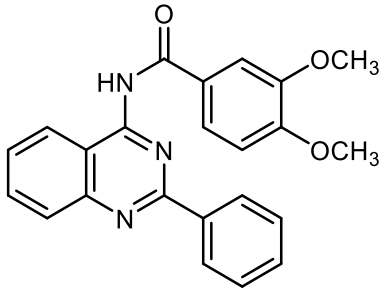

Molecular Weight: 385.42

The title compound was synthesized from 2-phenylquinazolin-4-amine (79 mg, 0.36 mmol) and 3,4-dimethoxybenzoic acid (59 mg, 0.33 mmol) as described in the general procedure above. Further purification was performed by column chromatography with DCM as eluent, beige solid (19.9 mg, 15.8 %).

^{1}H NMR (600 MHz, Chloroform-*d*) δ: 16.03 (s, 1H), 8.70 (s, 1H), 8.28 (s, 2H), 8.16 (s, 1H), 7.94 – 7.84 (m, 3H), 7.60 – 7.56 (m, 4H), 6.95 (d, *J* = 8.4 Hz, 1H), 4.01 (s, 3H), 3.96 (s, 3H).

^{13}C NMR (126 MHz, DMSO) δ 166.70, 159.31, 159.13, 152.42, 151.73, 148.37, 137.20, 134.37, 130.77, 128.56, 128.04, 126.89, 125.90, 125.58, 122.29, 117.67, 111.65, 111.02, 79.12, 55.74, 55.66.

3-methoxy-N-(2-phenylquinazolin-4-yl)benzamide (31)

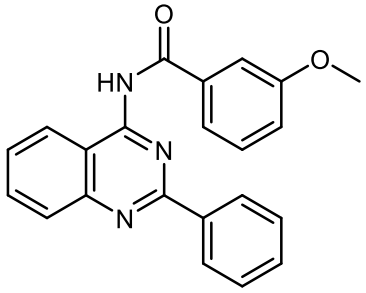

Molecular Weight: 355.40

The title compound was synthesized from 2-phenylquinazolin-4-amine (173 mg, 0.78 mmol) and 3-methoxybenzoic acid (107 mg, 0.70 mmol) as described in the general procedure above. Further purification was performed by column chromatography with DCM as eluent, yellow solid (52.9 mg, 21.1 %).

^{1}H NMR (600 MHz, Chloroform-*d*) δ 16.02 (s, 1H), 8.69 (s, 1H), 8.30 (s, 2H), 8.04 (s, 1H), 7.93 (s, 2H), 7.87 (t, *J* = 6.9 Hz, 1H), 7.62 – 7.54 (m, 4H), 7.41 (t, *J* = 7.9 Hz, 1H), 7.12 (dd, *J* = 8.1, 2.7 Hz, 1H), 3.91 (s, 3H).

^{13}C NMR (151 MHz, DMSO) δ: 158.64, 157.93, 148.45, 134.37, 131.00, 128.30, 128.23, 126.97, 126.51, 126.29, 125.19, 121.10, 117.99, 112.90, 76.20, 75.98, 75.77, 54.47.

4-ethoxy-N-(2-phenylquinazolin-4-yl)benzamide (32)

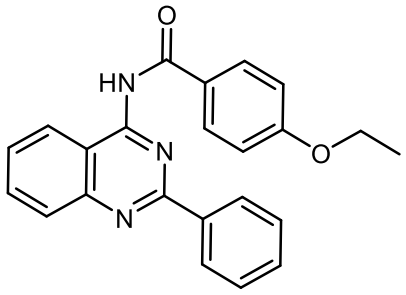

Molecular Weight: 369.42

The title compound was synthesized from 2-phenylquinazolin-4-amine (177 mg, 0.80 mmol) and 4-ethoxybenzoic acid (124 mg, 0.74 mmol) as described in the general procedure above. Further purification was performed by column chromatography with DCM as eluent, beige solid (20.1 mg, 7.3 %).

^{1}H NMR (600 MHz, Chloroform-*d*) δ 16.05 (s, 1H), 8.67 (s, 1H), 8.36 (s, 2H), 8.27 (s, 2H), 7.90 (s, 1H), 7.84 (t, *J* = 6.9 Hz, 1H), 7.57 – 7.54 (m, 4H), 6.95 (d, *J* = 8.6 Hz, 2H), 4.10 (q, *J* = 7.0 Hz, 2H), 1.44 (t, *J* = 7.0 Hz, 3H).

^{13}C NMR (151 MHz, $CDCl_3$) δ 161.65, 157.60, 148.52, 134.11, 130.85, 130.72, 128.18, 127.02, 126.34, 126.23, 126.21, 125.17, 118.90, 112.98, 62.65, 13.73.

4-methoxy-3-nitro-N-(2-phenylquinazolin-4-yl)benzamide (33)

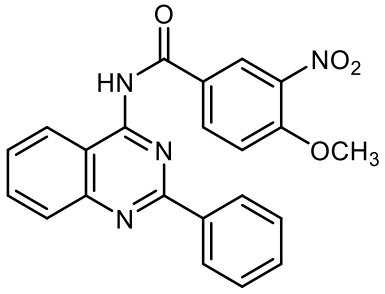

Molecular Weight: 400.39

The title compound was synthesized from 2-phenylquinazolin-4-amine (286 mg, 1.29 mmol) and 4-methoxy-3-nitrobenzoic acid (218 mg, 1.10 mmol) as described in the general procedure above. Further purification was performed by column chromatography with DCM as eluent, white solid (26.4 mg, 6.0 %).

^{1}H NMR (500 MHz, DMSO-d_6) δ: 11.44 (s, 1H), 8.63 (s, 1H), 8.44 (s, 2H), 8.35 (d, *J* = 7.3 Hz, 1H), 8.21 (s, 1H), 8.08 – 7.98 (m, 2H), 7.68 (t, *J* = 7.6 Hz, 1H), 7.57 – 7.51 (m, 4H), 4.05 (s, 3H).

^{13}C NMR (126 MHz, DMSO) δ: 165.45, 159.21, 158.90, 154.98, 151.93, 139.00, 137.30, 134.73, 131.00, 128.76, 128.26, 128.15, 127.18, 125.89, 125.67, 117.48, 114.46, 57.42.

3-bromo-N-(2-phenylquinazolin-4-yl)benzamide (34)

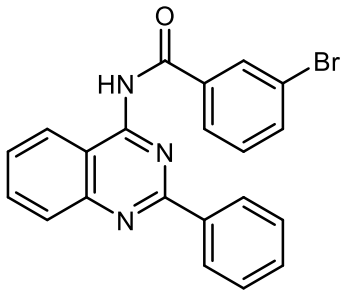

Molecular Weight: 404.27

The title compound was synthesized from 2-phenylquinazolin-4-amine (305 mg, 1.38 mmol) and 3-bromobenzoic acid (246 mg, 1.23 mmol) as described in the general procedure above. Further purification was performed by column chromatography with DCM as eluent, white solid (122.3 mg, 24.7 %).

^{1}H NMR (600 MHz, Chloroform-*d*) δ: 15.99 (s, 1H), 8.77 (s, 1H), 8.61 (s, 1H), 8.37 (d, *J* = 7.5 Hz, 1H), 8.27 (d, *J* = 4.4 Hz, 2H), 7.94 – 7.89 (m, 2H), 7.69 (d, *J* = 8.1 Hz, 1H), 7.65 – 7.58 (m, 4H), 7.38 (t, *J* = 7.8 Hz, 1H).

^{13}C NMR (151 MHz, $CDCl_3$) δ 178.02, 158.31, 148.45, 148.07, 138.46, 134.58, 134.09, 131.80, 131.09, 131.00, 128.73, 128.34, 127.30, 127.21, 126.68, 125.95, 125.28, 121.40, 118.85.

N-(2-phenylquinazolin-4-yl)-4-(trifluoromethyl)benzamide (35)

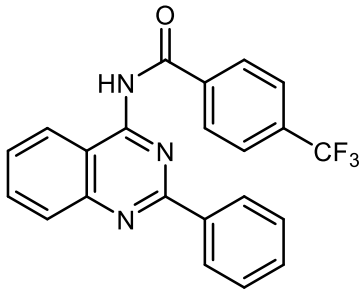

Molecular Weight: 393.37

The title compound was synthesized from 2-phenylquinazolin-4-amine (158 mg, 0.72 mmol) and 4-trifluorobenzoic acid (122 mg, 0.64 mmol) as described in the general procedure above. Further purification was performed by column chromatography with DCM as eluent, white solid (26.3 mg, 10.4 %).

^{1}H NMR (600 MHz, Chloroform-*d*) δ 15.85 (s, 1H), 8.63 (d, *J* = 8.0 Hz, 1H), 8.43 (d, *J* = 8.0 Hz, 2H), 8.15 – 8.10 (m, 2H), 7.81 – 7.74 (m, 2H), 7.62 (d, *J* = 8.1 Hz, 2H), 7.52 – 7.44 (m, 4H).

^{13}C NMR (151 MHz, $CDCl_3$) δ 178.11, 158.44, 148.50, 148.03, 139.58, 134.64, 132.50 (q, *J* = 32.3 Hz), 131.13, 130.93, 128.99, 128.35, 127.29, 127.25, 126.70, 125.93, 125.21, 124.33 (q, *J* = 272.6 Hz), 124.11 (q, *J* = 3.8 Hz), 118.81.

4-cyano-N-(2-phenylquinazolin-4-yl)benzamide (36)

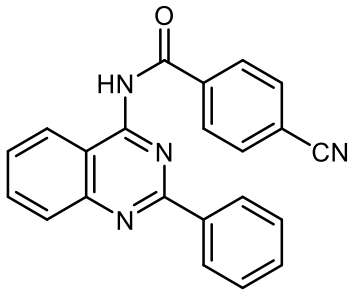

Molecular Weight: 350.38

The title compound was synthesized from 2-phenylquinazolin-4-amine (198 mg, 0.89 mmol) and 4-cyanobenzoic acid (126 mg, 0.85 mmol) as described in the general procedure above. Further purification was performed by column chromatography with DCM as eluent, white solid (16.5 mg, 5.5 %).

^{1}H NMR (500 MHz, DMSO-d_6) δ: 11.83 (s, 1H), 8.37 – 8.33 (m, 2H), 8.24 – 8.19 (m, 3H), 7.93 – 7.89 (m, 2H), 7.87 – 7.79 (m, 2H), 7.51 – 7.43 (m, 4H).

^{13}C NMR (126 MHz, DMSO) δ: 167.42, 164.55, 159.19, 151.22, 142.80, 138.42, 132.97, 131.90, 130.02, 129.12, 128.16, 127.91, 127.45, 125.99, 125.46, 118.80, 118.75, 112.37.

3-cyano-N-(2-phenylquinazolin-4-yl)benzamide (37)

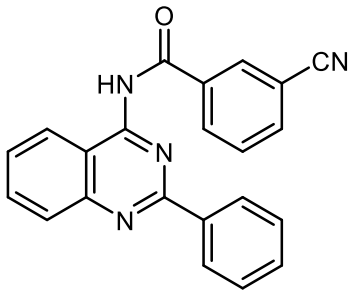

Molecular Weight: 350.38

The title compound was synthesized from 2-phenylquinazolin-4-amine (289 mg, 1.31 mmol) and 3-cyanobenzoic acid (182 mg, 1.24 mmol) as described in the general procedure above. Further purification was performed by column chromatography with DCM as eluent, white solid (16.5 mg, 5.5 %).

^{1}H NMR (500 MHz, DMSO-*d*6) δ 11.52 (s, 1H), 8.51 (s, 1H), 8.37 (d, J = 6.8 Hz, 2H), 8.29 (s, 2H), 8.12 (dt, J = 1.3, 7.8 Hz, 1H), 8.08 – 7.99 (m, 2H), 7.78 (td, J = 0.6, 7.8 Hz, 1H), 7.69 (t, J = 7.4 Hz, 1H), 7.53 (s, 3H).

^{13}C NMR (126 MHz, DMSO) δ: 166.22, 158.89, 158.39, 151.73, 137.06, 135.42, 134.55, 132.95, 132.07, 130.81, 129.83, 128.53, 128.09, 127.92, 127.04, 125.49, 118.16, 116.93, 111.60.

8.2.2.3: Synthesis of quinazoline derivatives with urea linker

Corresponding phenyl isocyanate was dissolved in 3-5 ml anhydrous THF. Afterwards, the solution was added dropwise to a solution of 1 equivalent 2-phenyl-4-aminoquinazoline in 10 ml anhydrous THF at room temperature. The reaction mixture was stirred at room temperature overnight. The precipitate was filtered off and washed with THF 3 times to give crude product. Further purification was performed by recrystallizaion from DMF/MeOH.

1-phenyl-3-(2-phenylquinazolin-4-yl)urea (38)

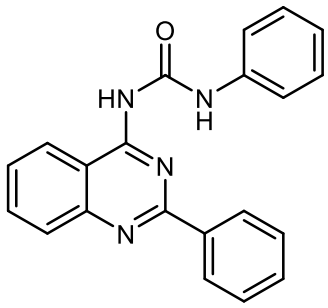

Molecular Weight: 340.39

The title compound was synthesized from 2-phenylquinazolin-4-amine (197 mg, 0.89 mmol) and phenyl isocyanate (116 mg, 0.98 mmol) as described in the general procedure above. White solid (47.5 mg, 15.7 %).

^{1}H NMR (500 MHz, DMSO-d_6) δ: 12.22 (s, 1H), 10.57 (s, 1H), 8.75 (d, J = 8.3 Hz, 1H), 8.43 – 8.38 (m, 2H), 8.00 – 7.96 (m, 2H), 7.71 – 7.59 (m, 6H), 7.43 (t, J = 7.8 Hz, 2H), 7.14 (tt, J = 1.2, 7.3 Hz, 1H).

^{13}C NMR (126 MHz, DMSO) δ: 157.63, 157.52, 151.62, 150.58, 138.16, 137.46, 134.48, 130.84, 129.13, 128.79, 128.29, 127.77, 127.10, 123.60, 123.48, 119.53, 113.55.

1-(3-methoxyphenyl)-3-(2-phenylquinazolin-4-yl)urea (39)

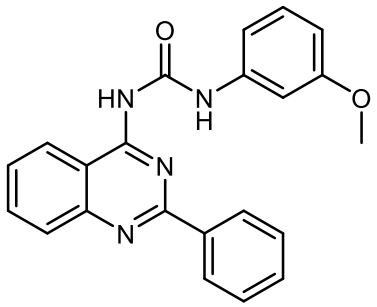

Molecular Weight: 370.41

The title compound was synthesized from 2-phenylquinazolin-4-amine (133 mg, 0.60 mmol) and 3-methoxyphenyl isocyanate (91 mg, 0.61 mmol) as described in the general procedure above. White solid (81.2 mg, 36.3 %).

^{1}H NMR (500 MHz, DMSO-d_6) δ: 12.24 (s, 1H), 10.56 (s, 1H), 8.75 (d, J = 8.3 Hz, 1H), 8.42 – 8.39 (m, 2H), 7.99 (d, J = 3.7 Hz, 2H), 7.70 – 7.66 (m, 1H), 7.63 – 7.60 (m, 3H), 7.33 (t, J = 8.1 Hz, 1H), 7.28 (t, J = 2.2 Hz, 1H), 7.25 (ddd, J = 1.0, 2.0, 7.9 Hz, 1H), 6.72 (ddd, J = 1.0, 2.5, 8.2 Hz, 1H), 3.79 (s, 3H).

^{13}C NMR (126 MHz, DMSO) δ: 159.81, 157.62, 157.46, 151.47, 150.59, 139.28, 137.47, 134.53, 130.88, 129.96, 128.76, 128.31, 127.80, 127.15, 123.58, 113.46, 111.71, 109.09, 105.27, 55.06.

1-(3-bromophenyl)-3-(2-phenylquinazolin-4-yl)urea (40)

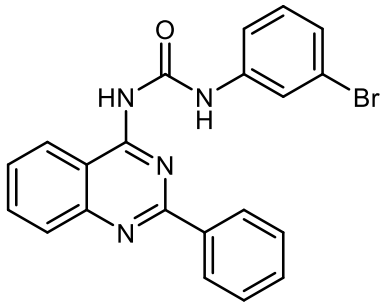

Molecular Weight: 419.28

The title compound was synthesized from 2-phenylquinazolin-4-amine (104 mg, 0.47 mmol) and 3-bromophenyl isocyanate (97 mg, 0.49 mmol) as described in the general procedure above. White solid (24.8 mg, 12.6 %).

^{1}H NMR (500 MHz, DMSO-d_6) δ: 12.34 (s, 1H), 10.64 (s, 1H), 8.72 (d, J = 8.4 Hz, 1H), 8.40 (dd, J = 3.0, 6.7 Hz, 2H), 7.99 (s, 3H), 7.68 (dt, J = 4.1, 8.3 Hz, 1H), 7.64 – 7.56 (m, 4H), 7.41 – 7.30 (m, 2H).

1-(3-cyanophenyl)-3-(2-phenylquinazolin-4-yl)urea (41)

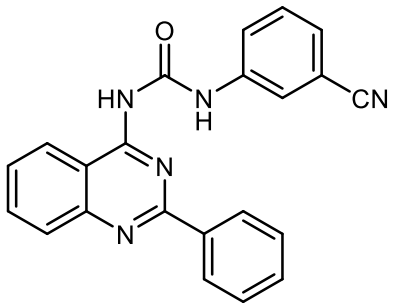

Molecular Weight: 365.40

The title compound was synthesized from 2-phenylquinazolin-4-amine (100 mg, 0.45 mmol) and 3-cyanophenyl isocyanate (65 mg, 0.45 mmol) as described in the general procedure above. White solid (27.0 mg, 16.4 %).

^{1}H NMR (500 MHz, DMSO-d_6) δ: 12.35 (s, 1H), 10.71 (s, 1H), 8.73 (d, J = 8.3 Hz, 1H), 8.42 – 8.39 (m, 2H), 8.16 (t, J = 1.8 Hz, 1H), 8.00 (d, J = 3.9 Hz, 2H), 7.86 (d, J = 8.0 Hz, 1H), 7.71 – 7.58 (m, 6H).

1-(2-nitrophenyl)-3-(2-phenylquinazolin-4-yl)urea (42)

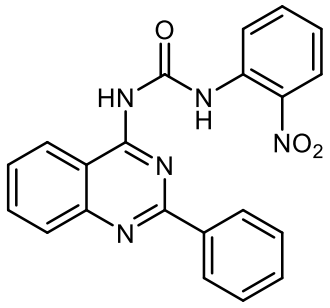

Molecular Weight: 385.38

The title compound was synthesized from 2-phenylquinazolin-4-amine (105 mg, 0.48 mmol) and 2-nitrophenyl isocyanate (81 mg, 0.49 mmol) as described in the general procedure above. Yellow solid (16.8 mg, 9.2 %).

^{1}H NMR (500 MHz, DMSO-d_6) δ: 12.42 (s, 1H), 10.81 (s, 1H), 8.71 (d, J = 8.4 Hz, 1H), 8.39 – 8.35 (m, 2H), 8.16 (dd, J = 1.3, 8.3 Hz, 1H), 8.12 (dd, J = 1.5, 8.2 Hz, 1H), 8.02 – 7.98 (m, 2H), 7.82 (ddd, J = 1.6, 7.4, 8.6 Hz, 1H), 7.69 (ddd, J = 3.3, 4.9, 8.3 Hz, 1H), 7.55 – 7.47 (m, 3H), 7.43 (ddd, J = 1.4, 7.3, 8.5 Hz, 1H).

8.2.3.1: Synthesis of 6-methyl-2-phenylpyrimidin-4-ol (43)

0.304 g (13.2 mmol) sodium was dissolved in 50 ml ethanol to afford sodium ethoxide solution. Subsequently, 1.31 g (10.88 mmol) benzamidine which was dissolved in 10 ml ethanol and 1.428 g (10.97 mmol) ethyl acetoacetate were added into sodium ethoxide solution respectively. The resulting mixture was heated to reflux overnight and cooled down to room temperature. After solvent was removed under reduced pressure, 20 ml water was added to the solid and the mixture was acidified with concentrated

HCl to pH 5-6. The formed precipitate was vacuum filtered and washed with water 3 times. Finally, the obtained crude residue was recrystallized from DMF/H2O to give 6-methyl-2-phenylpyrimidin-4-ol as white solid (1.22 g; 60.1 %).

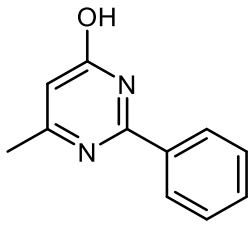

Molecular Weight: 186.21

^{1}H NMR (500 MHz, DMSO-d_6) δ: 12.49 (s, 1H), 8.13 – 8.09 (m, 2H), 7.58 – 7.55 (m, 1H), 7.53 – 7.49 (m, 2H), 6.20 (s, 1H), 2.28 (d, J = 0.9 Hz, 3H).
^{13}C NMR (126 MHz, DMSO) δ: 164.56, 163.59, 156.92, 132.71, 131.42, 128.51, 127.68, 109.87, 23.45.

8.2.3.2: Synthesis of 4-chloro-6-methyl-2-phenylpyrimidine (44)

1.035 g (5.07 mmol) 6-methyl-2-phenylpyrimidin-4-ol was added into 20 ml $POCl_3$. The reaction was refluxed until the reaction was complete. Excess $POCl_3$ was removed under reduced pressure. The oily residue was transfer onto crushed ice portion by portion, while keeping the temperature of solution below 10 °C. Ethyl acetate was used to extract products 3 times. The organic layer was washed with saturated $NaHCO_3$, saturated NaCl solution and dried over magnesium sulfate. After filtration, ethyl acetate was removed under reduced pressure. Final purification was performed by column chromatography with ethyl acetate/petroleum ether (40-60 °C) = 1:8 as eluent to yield white crystals (yield: 0.782 g; 75.4 %).

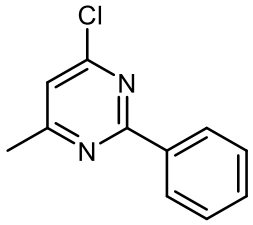

Molecular Weight: 204.66

^{1}H NMR (600 MHz, Chloroform-*d*) δ: 8.47 – 8.44 (m, 2H), 7.52 – 7.47 (m, 3H), 7.11 (s, 1H), 2.60 (s, 3H).
^{13}C NMR (126 MHz, DMSO) δ: (151 MHz, $CDCl_3$) δ 169.02, 165.05, 161.69, 136.27, 131.53, 128.75, 128.73, 118.59, 24.14.

8.2.3.3: Synthesis of 4-anilino-6-methyl-2-phenylpyrimidine derivatives

A mixture of 1 equivalent 4-chloro-6-methyl-2-phenylpyrimidine, 1 equivalent of substituted aniline in 3 ml isopropanol was heated to 110 °C in microwave for 15-30 mins. If reaction did not initiate, 0.1 equivalent of conc. HCl was added as catalyst. The precipitate was filtered off and washed with saturated sodium bicarbonate solution 3 times followed by distilled water 3 times. Further purification for certain compounds was performed by recrystallization or column chromatography.

2-(4-((6-methyl-2-phenylpyrimidin-4-yl)amino)phenyl)acetonitrile (46)

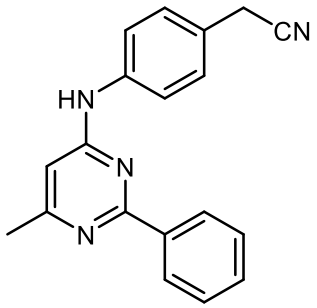

The title compound was synthesized from 4-chloro-6-methyl-2-phenylpyrimidine (105 mg, 0.51 mmol) and 2-(4-aminophenyl)acetonitrile (65 mg, 0.49 mmol) as described in the general procedure above. White solid (113.4 mg, 76.6 %).

^{1}H NMR (500 MHz, DMSO-d_6) δ: 9.58 (s, 1H), 8.37 – 8.33 (m, 2H), 7.81 – 7.76 (m, 2H), 7.53 – 7.48 (m, 3H), 7.36 (d, J = 8.6 Hz, 2H), 6.58 (d, J = 0.8 Hz, 1H), 3.99 (s, 2H), 2.39 (s, 3H).

^{13}C NMR (126 MHz, DMSO) δ: 164.87, 162.40, 160.59, 139.46, 137.89, 130.24, 128.51, 128.35, 127.61, 124.50, 120.02, 119.37, 103.46, 23.77, 21.77.

LC-MS (m/z) Calcd. for $C_{19}H_{16}N_4$ $[M+1]^+$: 301.14, Found: 301.0, Purity: 98.6 %.

(3-((6-methyl-2-phenylpyrimidin-4-yl)amino)phenyl)methanol (48)

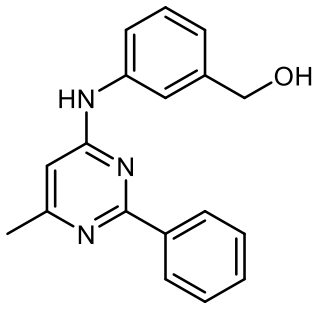

The title compound was synthesized from 4-chloro-6-methyl-2-phenylpyrimidine (103 mg, 0.50 mmol) and (4-aminophenyl)methanol (62 mg, 0.50 mmol) as described in the general procedure above. White solid (83.1 mg, 56.9 %).

^{1}H NMR (500 MHz, DMSO-d_6) δ: 9.81 (s, 1H), 8.39 – 8.33 (m, 2H), 7.82 (s, 1H), 7.61 (dt, J = 1.6, 8.0 Hz, 1H), 7.55 – 7.49 (m, 3H), 7.33 (t, J = 7.8 Hz, 1H), 7.01 (d, J = 7.5 Hz, 1H), 6.63 (s, 1H), 5.21 (s, 1H), 4.55 (s, 2H), 2.42 (s, 3H).

^{13}C NMR (126 MHz, DMSO) δ: 163.23, 161.78, 160.76, 143.34, 139.43, 136.70, 130.70, 128.42, 127.86, 120.65, 118.33, 118.18, 103.38, 62.84, 22.98.

LC-MS (m/z) Calcd. for $C_{18}H_{17}N_3O$ $[M+1]^+$: 292.14, Found: 292.1, Purity: 98.6 %.

3-((6-methyl-2-phenylpyrimidin-4-yl)amino)phenol (49)

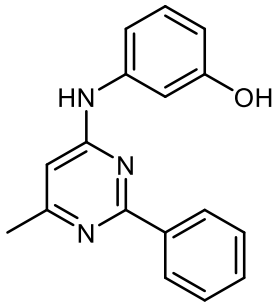

The title compound was synthesized from 4-chloro-6-methyl-2-phenylpyrimidine (210 mg, 1.03 mmol) and 3-bromoaniline(113 mg, 1.04 mmol) as described in the general procedure above. Further purification was performed by recrystallization from chloroform/n-Hexane, white solid (122.9 mg, 43.3 %).

^{1}H NMR (500 MHz, DMSO-d_6) δ: 9.36 (s, 2H), 8.39 – 8.34 (m, 2H), 7.52 – 7.46 (m, 3H), 7.26 (dd, J = 1.6, 2.7 Hz, 1H), 7.17 – 7.11 (m, 2H), 6.56 (d, J = 0.7 Hz, 1H), 6.45 (dt, J = 2.3, 6.6 Hz, 1H), 2.38 (d, J = 0.6 Hz, 3H).

^{13}C NMR (126 MHz, DMSO) δ: 164.64, 162.45, 160.74, 157.74, 141.03, 137.99, 130.16, 129.36, 128.28, 127.68, 110.55, 109.47, 106.88, 103.32, 23.79.

LC-MS (m/z) Calcd. for $C_{17}H_{15}N_3O$ $[M+1]^+$: 278.12, Found: 278.1, Purity: 99.2 %.

N-(3-fluorophenyl)-6-methyl-2-phenylpyrimidin-4-amine (50)

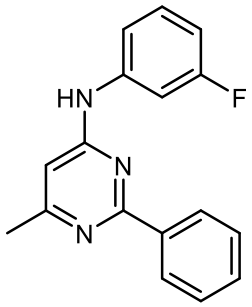

The title compound was synthesized from 4-chloro-6-methyl-2-phenylpyrimidine (193 mg, 0.94 mmol) and 3-fluoroaniline(108 mg, 0.97 mmol) as described in the general

procedure above. Further purification was performed by recrystallization from n-hexane, white solid (134.1 mg, 50.9 %).

^{1}H NMR (500 MHz, DMSO-d_6) δ: 9.73 (s, 1H), 8.37 – 8.32 (m, 2H), 7.86 (dt, J = 2.3, 12.2 Hz, 1H), 7.55 – 7.48 (m, 3H), 7.46 (ddd, J = 1.0, 2.0, 8.3 Hz, 1H), 7.39 (td, J = 6.9, 8.2 Hz, 1H), 6.84 (tdd, J = 0.9, 2.6, 8.5 Hz, 1H), 6.61 (d, J = 0.8 Hz, 1H), 2.41 (d, J = 0.6 Hz, 3H).

^{13}C NMR (126 MHz, DMSO) δ: 165.17, 162.44, 161.76 (d, J = 240.6 Hz), 160.47, 142.00, 137.86, 130.35, 130.26 (d, J = 9.6 Hz), 128.41, 127.54, 115.12, 108.19 (d, J = 21.5 Hz), 106.05 (d, J = 26.2 Hz),

103.91, 23.80.

LC-MS (m/z) Calcd. for $C_{17}H_{14}FN_3$ $[M+1]^+$: 280.12, Found: 280.1, Purity: 97.9 %.

N-(3-chlorophenyl)-6-methyl-2-phenylpyrimidin-4-amine (51)

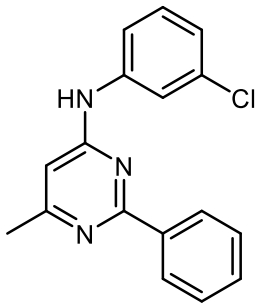

The title compound was synthesized from 4-chloro-6-methyl-2-phenylpyrimidine (168 mg, 0.82 mmol) and 3-chloroaniline(102 mg, 0.80 mmol) as described in the general procedure above. Further purification was performed by recrystallization from n-hexane, white solid (148.7 mg, 62.7 %).

^{1}H NMR (500 MHz, DMSO-d_6) δ: 9.72 (s, 1H), 8.39 – 8.31 (m, 2H), 8.11 (t, J = 2.1 Hz, 1H), 7.62 (ddd, J = 0.9, 2.1, 8.3 Hz, 1H), 7.56 – 7.46 (m, 3H), 7.39 (t, J = 8.1 Hz, 1H), 7.07 (ddd, J = 0.9, 2.2, 8.0 Hz, 1H), 6.60 (d, J = 0.8 Hz, 1H), 2.41 (d, J = 0.6 Hz, 3H).

^{13}C NMR (126 MHz, DMSO) δ: 165.22, 162.37, 160.40, 141.64, 137.82, 133.03, 130.38, 130.34, 128.39, 127.54, 121.42, 118.90, 117.69, 103.93, 23.80.

LC-MS (m/z) Calcd. for $C_{17}H_{14}ClN_3$ $[M+1]^+$: 296.09, Found: 296.2, Purity: 98.8 %.

N-(3-bromophenyl)-6-methyl-2-phenylpyrimidin-4-amine (52)

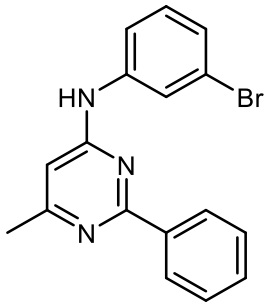

The title compound was synthesized from 4-chloro-6-methyl-2-phenylpyrimidine (123 mg, 0.60 mmol) and 3-bromoaniline(102 mg, 0.60 mmol) as described in the general procedure above. Further purification was performed by recrystallization from n-hexane, white solid (44.7 mg, 22.1 %).

^{1}H NMR (500 MHz, DMSO-d_6) δ: 9.71 (s, 1H), 8.38 – 8.32 (m, 2H), 8.29 (t, J = 2.0 Hz, 1H), 7.65 (ddd, J = 0.9, 2.1, 8.2 Hz, 1H), 7.56 – 7.47 (m, 3H), 7.33 (t, J = 8.1 Hz, 1H), 7.20 (ddd, J = 0.9, 1.9, 7.9 Hz, 1H), 6.59 (d, J = 0.7 Hz, 1H), 2.41 (d, J = 0.7 Hz, 3H).

^{13}C NMR (126 MHz, DMSO) δ: 165.22, 162.34, 160.36, 141.78, 137.80, 130.63, 130.39, 128.38, 127.55, 124.28, 121.83, 121.53, 118.04, 103.93, 23.81.

LC-MS (m/z) Calcd. for $C_{17}H_{14}BrN_3$ $[M+1]^+$: 340.04, Found: 340.0, Purity: 98.6 %.

N-(3-methoxyphenyl)-6-methyl-2-phenylpyrimidin-4-amine (53)

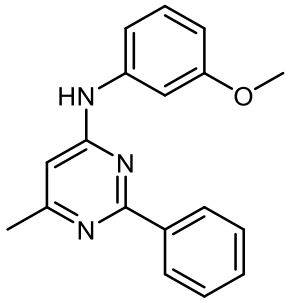

The title compound was synthesized from 4-chloro-6-methyl-2-phenylpyrimidine (182 mg, 0.89 mmol) and 3-methoxyaniline(186 mg, 1.51 mmol) as described in the general procedure above. Further purification was performed by recrystallization from isopropanol, white solid (23.6 mg, 9.1 %).

^{1}H NMR (500 MHz, DMSO-d_6) δ: 9.51 (s, 1H), 8.38 – 8.34 (m, 2H), 7.59 (t, J = 2.1 Hz, 1H), 7.53 – 7.47 (m, 3H), 7.29 – 7.22 (m, 2H), 6.61 (ddd, J = 1.7, 2.5, 7.6 Hz, 1H), 6.58 (d, J = 0.8 Hz, 1H), 3.80 (s, 3H), 2.39 (d, J = 0.6 Hz, 3H).

^{13}C NMR (126 MHz, DMSO) δ: 164.81, 162.41, 160.67, 159.62, 141.31, 138.00, 130.24, 129.46, 128.31, 127.55, 111.83, 107.86, 105.12, 103.59, 54.94, 23.79.

LC-MS (m/z) Calcd. for $C_{18}H_{17}N_3O$ $[M+1]^+$: 292.14, Found: 292.0, Purity: 99.5 %

N-(4-bromo-3-methoxyphenyl)-6-methyl-2-phenylpyrimidin-4-amine (54)

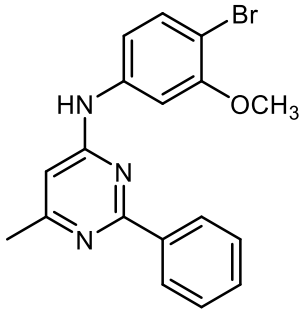

The title compound was synthesized from 4-chloro-6-methyl-2-phenylpyrimidine (148 mg, 0.72 mmol) and 4-bromo-3-methoxyaniline(146 mg, 0.72 mmol) as described in the general procedure above. Further purification was performed by recrystallization from isopropanol/H_2O, white solid (34.4 mg, 12.9 %).

^{1}H NMR (500 MHz, DMSO-d_6) δ: 9.67 (s, 1H), 8.39 – 8.34 (m, 2H), 7.87 (d, J = 2.4 Hz, 1H), 7.53 – 7.48 (m, 4H), 7.18 (dd, J = 2.4, 8.6 Hz, 1H), 6.60 (d, J = 0.8 Hz, 1H), 2.41 (d, J = 0.6 Hz, 3H).

^{13}C NMR (126 MHz, DMSO) δ: 165.21, 162.58, 160.62, 155.49, 141.23, 138.05, 132.73, 130.48, 128.50, 127.75, 112.90, 104.26, 104.08, 102.49, 56.06, 23.95.

LC-MS (m/z) Calcd. for $C_{18}H_{16}BrN_3O$ $[M+1]^+$: 370.05, Found: 370.0, Purity: 99.3 %.

N-(3-fluoro-4-methoxyphenyl)-6-methyl-2-phenylpyrimidin-4-amine (55)

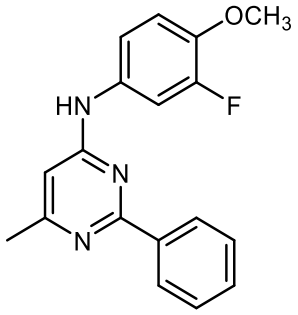

The title compound was synthesized from 4-chloro-6-methyl-2-phenylpyrimidine (91 mg, 0.45 mmol) and 3-fluoro-4-methoxyaniline (60 mg, 0.42 mmol) as described in the general procedure above. White solid (84.0 mg, 64.1 %).

^{1}H NMR (500 MHz, DMSO-d_6) δ: 9.49 (s, 1H), 8.35 – 8.30 (m, 2H), 7.76 (dd, J = 2.6, 13.9 Hz, 1H), 7.53 – 7.47 (m, 3H), 7.41 (ddd, J = 1.4, 2.6, 8.9 Hz, 1H), 7.19 (dd, J = 8.9, 9.8 Hz, 1H), 6.52 (d, J = 0.7 Hz, 1H), 3.84 (s, 3H), 2.38 (d, J = 0.6 Hz, 3H).

^{13}C NMR (126 MHz, DMSO) δ: 164.77, 162.40, 160.56, 151.04 (d, J = 241.9 Hz), 142.23 (d, J = 10.6 Hz), 137.97, 133.56 (d, J = 9.6 Hz), 130.24, 128.34, 127.52, 115.69, 114.37 (d, J = 3.0 Hz), 108.33 (d, J = 22.7 Hz), 103.16, 56.28, 23.77.

LC-MS (m/z) Calcd. for $C_{18}H_{16}FN_3O$ $[M+1]^+$: 310.13, Found: 310.1, Purity: 99.6 %.

N-(4-methoxy-3-(trifluoromethyl)phenyl)-6-methyl-2-phenylpyrimidin-4-amine (56)

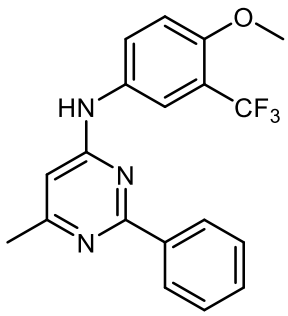

The title compound was synthesized from 4-chloro-6-methyl-2-phenylpyrimidine (53 mg, 0.26 mmol) and 3-trifluoro-4-methoxyaniline (49 mg, 0.26 mmol) as described in the general procedure above. Brown solid (73.8 mg, 80.6 %).

^{1}H NMR (500 MHz, DMSO-d_6) δ: 11.13 (s, 1H), 8.29 – 8.22 (m, 3H), 7.91 (d, J = 8.8 Hz, 1H), 7.67 (t, J = 7.4 Hz, 1H), 7.61 (t, J = 7.6 Hz, 2H), 7.37 (d, J = 9.0 Hz, 1H), 6.81 (s, 1H), 3.91 (s, 3H), 2.53 (s, 3H).

^{13}C NMR (126 MHz, DMSO) δ: 160.64, 160.60, 159.88, 153.61, 132.52, 130.88, 128.80, 128.42, 126.71, 123.50 (q, J = 272.5 Hz), 119.89, 116.78 (q, J = 27.5, 28.3 Hz), 113.69, 104.01, 56.39, 20.31.

LC-MS (m/z) Calcd. for $C_{19}H_{16}F_3N_3O$ $[M+1]^+$: 360.12, Found: 360.0, Purity: 98.3 %.

4-((6-methyl-2-phenylpyrimidin-4-yl)amino)phthalonitrile (58)

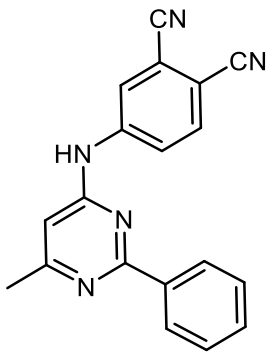

The title compound was synthesized from 4-chloro-6-methyl-2-phenylpyrimidine (145 mg, 0.71 mmol) and 3,4-dicyanoaniline (101 mg, 0.70 mmol) as described in the

general procedure above. Further purification was performed by recrystallization from ethanol/H_2O, white solid (13.6 mg, 6.2 %).

^{1}H NMR (500 MHz, DMSO-d_6) δ: 10.35 (s, 1H), 8.54 (d, J = 2.2 Hz, 1H), 8.33 – 8.30 (m, 2H), 8.15 (dd, J = 2.2, 8.8 Hz, 1H), 8.05 (d, J = 8.7 Hz, 1H), 7.53 – 7.50 (m, 3H), 6.69 (s, 1H), 2.45 (s, 3H).

^{13}C NMR (126 MHz, DMSO) δ: 166.44, 162.47, 159.77, 144.84, 137.38, 134.88, 130.68, 128.51, 127.64, 122.81, 122.53, 116.41, 116.05, 115.29, 105.28, 105.11, 23.86.

LC-MS (m/z) Calcd. for $C_{19}H_{13}N_5$ $[M+1]^+$: 312.12, Found: 312.2, Purity: 92.2 %.

2-fluoro-5-((6-methyl-2-phenylpyrimidin-4-yl)amino)benzonitrile (59)

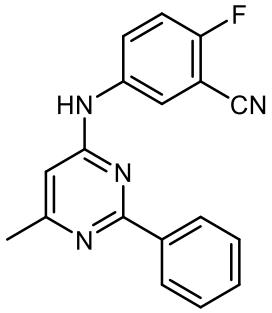

The title compound was synthesized from 4-chloro-6-methyl-2-phenylpyrimidine (101 mg, 0.49 mmol) and 3-cyano-4-fluoroaniline(66 mg, 0.48 mmol) as described in the general procedure above. White solid (117.6 mg, 80.1 %).

^{1}H NMR (500 MHz, DMSO-d_6) δ: 9.84 (s, 1H), 8.34 – 8.29 (m, 3H), 8.02 (ddd, J = 2.8, 4.8, 9.2 Hz, 1H), 7.56 – 7.47 (m, 4H), 6.59 (s, 1H), 2.41 (s, 3H).

^{13}C NMR (126 MHz, DMSO) δ: 165.45, 162.35, 160.21, 157.34 (d, J = 250.7 Hz), 137.71, 137.31 (d, J = 2.4 Hz), 130.42, 128.38, 127.56, 126.67 (d, J = 7.8 Hz), 123.15, 116.98 (d, J = 20.6 Hz), 114.13, 103.77, 99.77 (d, J = 16.1 Hz), 23.80.

LC-MS (m/z) Calcd. for $C_{18}H_{13}FN_4$ $[M+1]^+$: 305.11, Found: 305.1, Purity: 97.6 %.

2-bromo-4-((6-methyl-2-phenylpyrimidin-4-yl)amino)benzonitrile (60)

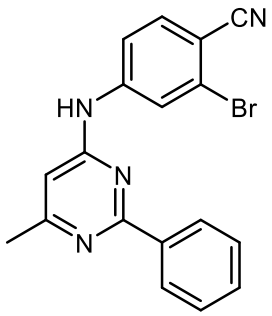

The title compound was synthesized from 4-chloro-6-methyl-2-phenylpyrimidine (102 mg, 0.50 mmol) and 3-bromo-4-cyanoaniline (97 mg, 0.49 mmol) as described in the general procedure above. White solid (93.4 mg, 52.1 %).

^{1}H NMR (500 MHz, DMSO-d_6) δ: 10.94 (s, 1H), 8.57 (s, 1H), 8.32 – 8.29 (m, 2H), 7.93 – 7.87 (m, 2H), 7.63 – 7.55 (m, 3H), 6.85 (s, 1H), 2.51 (s, 3H).

^{13}C NMR (126 MHz, DMSO) δ: 163.28, 161.39, 160.27, 144.78, 135.29, 131.57, 128.71, 128.05, 124.86, 122.84, 118.61, 117.65, 106.71, 105.29, 22.41.

LC-MS (m/z) Calcd. for $C_{18}H_{13}BrN_4$ $[M+1]^+$: 365.03, Found: 365.0, Purity: 97.7 %.

2-methyl-4-((6-methyl-2-phenylpyrimidin-4-yl)amino)benzonitrile (61)

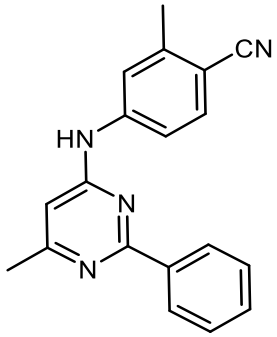

The title compound was synthesized from 4-chloro-6-methyl-2-phenylpyrimidine (149 mg, 0.73 mmol) and 4-cyano-3-methylaniline (95 mg, 0.72 mmol) as described in the general procedure above. Further purification was performed by recrystallization from ethanol, white solid (103.9 mg, 48.3 %).

^{1}H NMR (500 MHz, DMSO-d_6) δ: 9.94 (s, 1H), 8.38 – 8.33 (m, 2H), 7.92 (d, J = 1.7 Hz, 1H), 7.81 (dd, J = 2.2, 8.6 Hz, 1H), 7.73 (d, J = 8.5 Hz, 1H), 7.55 – 7.49 (m, 3H), 6.66 (s, 1H), 2.43 (s, 3H).

^{13}C NMR (126 MHz, DMSO) δ: 165.68, 162.46, 160.22, 144.37, 142.29, 137.65, 133.41, 130.46, 128.47, 127.64, 119.74, 118.50, 116.60, 104.60, 103.65, 23.83, 20.34.

LC-MS (m/z) Calcd. for $C_{19}H_{16}N_4$ $[M+1]^+$: 301.14, Found: 301.1, Purity: 99.1 %

4-((6-methyl-2-phenylpyrimidin-4-yl)amino)-2-(trifluoromethyl)benzonitrile (62)

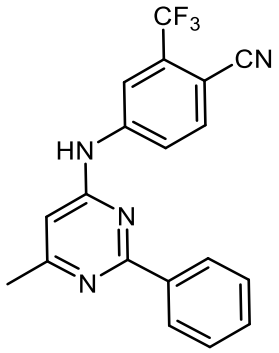

The title compound was synthesized from 4-chloro-6-methyl-2-phenylpyrimidine (153 mg, 0.75 mmol) and 4-cyano-3-trifluoroaniline (139 mg, 0.74 mmol) as described in the general procedure above. Further purification was performed by recrystallization from ethanol, white solid (59.0 mg, 22.4 %).

^{1}H NMR (500 MHz, DMSO-d_6) δ: 10.41 (s, 1H), 8.84 (s, 1H), 8.37 – 8.31 (m, 2H), 8.09 (d, J = 8.7 Hz, 1H), 8.02 (d, J = 8.8 Hz, 1H), 7.57 – 7.47 (m, 3H), 6.70 (s, 1H), 2.46 (s, 3H).

^{13}C NMR (126 MHz, DMSO) δ: 166.32, 162.41, 159.90, 144.95, 137.36, 136.19, 131.70 (q, J = 31.6 Hz), 130.69, 128.46, 127.57, 122.26 (q, J = 273.2 Hz), 121.41, 116.16, 116.10, 105.15, 99.16, 23.86.

LC-MS (m/z) Calcd. for $C_{19}H_{13}F_3N_4$ $[M+1]^+$: 355.11, Found: 355.1, Purity: 99.0 %.

6-methyl-N-(3-nitrophenyl)-2-phenylpyrimidin-4-amine (63)

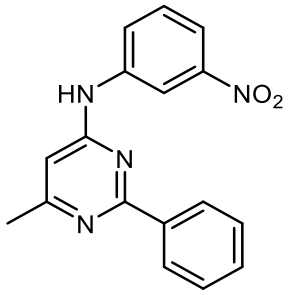

The title compound was synthesized from 4-chloro-6-methyl-2-phenylpyrimidine (71 mg, 0.35 mmol) and 3-nitroaniline(49 mg, 0.35 mmol) as described in the general procedure above. Further purification was performed by recrystallization from isopropanol/H_2O, yellow solid (22.5 mg, 21.2 %).

^{1}H NMR (500 MHz, DMSO-d_6) δ: 10.06 (s, 1H), 9.24 (t, J = 2.2 Hz, 1H), 8.46 – 8.42 (m, 2H), 7.95 (ddd, J = 0.9, 2.2, 8.2 Hz, 1H), 7.86 (ddd, J = 0.9, 2.3, 8.1 Hz, 1H), 7.64 (t, J = 8.1 Hz, 1H), 7.56 – 7.48 (m, 3H), 6.64 (d, J = 0.8 Hz, 1H), 4.30 (d, J = 4.3 Hz, 0H), 2.44 (d, J = 0.6 Hz, 3H),

^{13}C NMR (126 MHz, DMSO) δ: 13C NMR (126 MHz, DMSO) δ 165.51, 162.35, 160.30, 148.09, 141.44, 137.60, 130.52, 129.97, 128.41, 127.69, 124.95, 116.05, 113.24, 104.30, 23.83.

LC-MS (m/z) Calcd. for $C_{17}H_{14}N_4O_2$ $[M+1]^+$: 307.11, Found:307.1, Purity: 99.5 %.

6-methyl-N-(4-nitrophenyl)-2-phenylpyrimidin-4-amine (64)

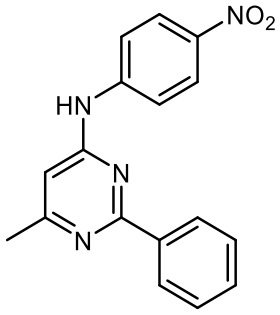

The title compound was synthesized from 4-chloro-6-methyl-2-phenylpyrimidine (100 mg, 0.49 mmol) and 4-nitroaniline(68 mg, 0.49 mmol) as described in the general

procedure above. Further purification was performed by recrystallization from isopropanol/H_2O, yellow solid (18.7 mg, 12.5 %).

^{1}H NMR (500 MHz, DMSO-d_6) δ: 10.25 (s, 1H), 8.41 – 8.37 (m, 2H), 8.32 – 8.28 (m, 2H), 8.09 – 8.05 (m, 2H), 7.57 – 7.51 (m, 3H), 6.72 (d, J = 0.7 Hz, 1H), 2.46 (d, J = 0.6 Hz, 3H).

^{13}C NMR (126 MHz, DMSO) δ: 166.03, 162.55, 160.03, 146.72, 140.70, 137.47, 130.55, 128.52, 127.78, 125.15, 118.39, 105.00, 23.86.

LC-MS (m/z) Calcd. for $C_{17}H_{14}N_4O_2$ $[M+1]^+$: 307.11, Found: 307.2, Purity: 99.3 %.

N-(4-fluoro-3-nitrophenyl)-6-methyl-2-phenylpyrimidin-4-amine (66)

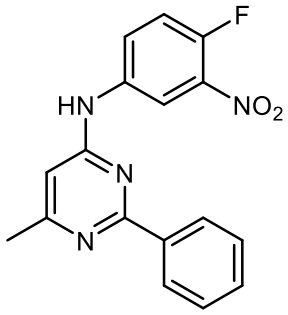

The title compound was synthesized from 4-chloro-6-methyl-2-phenylpyrimidine (98 mg, 0.48 mmol) and 4-fluoro-3-nitroaniline (68 mg, 0.44 mmol) as described in the general procedure above. Yellow solid (96.5 mg, 68.1 %).

^{1}H NMR (500 MHz, DMSO-d_6) δ: 9.99 (s, 1H), 9.11 (dd, J = 2.8, 6.9 Hz, 1H), 8.43 – 8.38 (m, 2H), 7.90 (ddd, J = 2.8, 3.8, 9.1 Hz, 1H), 7.58 (dd, J = 9.0, 11.2 Hz, 1H), 7.54 – 7.48 (m, 3H), 6.60 (d, J = 0.8 Hz, 1H), 2.43 (s, 3H).

^{13}C NMR (126 MHz, DMSO) δ: 165.48, 162.31, 160.12, 149.49 (d, J = 257.1 Hz), 137.56, 137.04 (d, J = 3.2 Hz), 136.22 (d, J = 7.8 Hz), 130.51, 128.38, 127.68, 126.38 (d, J = 7.9 Hz), 118.71 (d, J = 22.1 Hz), 115.45 (d, J = 3.3 Hz), 104.06, 23.81.

LC-MS (m/z) Calcd. for $C_{17}H_{13}FN_4O_2$ $[M+1]^+$: 325.10, Found: 324.9, Purity: 98.7 %.

5-((6-methyl-2-phenylpyrimidin-4-yl)amino)-2-nitrobenzoic acid (67)

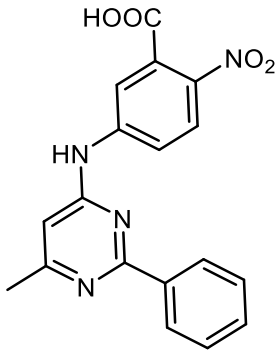

The title compound was synthesized from 4-chloro-6-methyl-2-phenylpyrimidine (125 mg, 0.61 mmol) and 5-amino-2-nitrobenzoic acid (111 mg, 0.61 mmol) as described in the general procedure above. Further purification was performed by recrystallization from ethanol/H_2O, yellow solid (87.6 mg, 41.0 %).

^{1}H NMR (500 MHz, DMSO-d_6) δ: 13.76 (s, 1H), 10.32 (s, 1H), 8.48 (d, J = 2.4 Hz, 1H), 8.42 – 8.38 (m, 2H), 8.12 (d, J = 9.0 Hz, 1H), 7.96 (dd, J = 2.4, 9.0 Hz, 1H), 7.56 – 7.49 (m, 3H), 6.70 (s, 1H), 2.46 (s, 3H).

^{13}C NMR (126 MHz, DMSO) δ: 166.87, 166.16, 162.40, 159.92, 145.21, 139.70, 137.38, 130.65, 128.47, 127.75, 125.84, 119.60, 118.26, 104.99, 23.86.

LC-MS (m/z) Calcd. for $C_{18}H_{14}N_4O_4$ $[M+1]^+$: 351.10, Found: 351.0, Purity: 98.8 %.

N-(3-chloro-4-nitrophenyl)-6-methyl-2-phenylpyrimidin-4-amine (68)

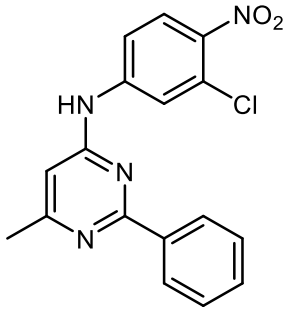

The title compound was synthesized from 4-chloro-6-methyl-2-phenylpyrimidine (114 mg, 0.56 mmol) and 3-chloro-4-nitroaniline(93 mg, 0.54 mmol) as described in the general procedure above. Pale yellow solid (75.0 mg, 41.1 %).

^{1}H NMR (500 MHz, DMSO-d_6) δ: 11.14 (s, 1H), 8.39 (d, J = 2.3 Hz, 1H), 8.36 – 8.28 (m, 2H), 8.22 (d, J = 9.0 Hz, 1H), 7.94 (dd, J = 2.3, 9.0 Hz, 1H), 7.64 – 7.55 (m, 3H), 6.90 (s, 1H), 2.53 (s, 3H).

^{13}C NMR (126 MHz, DMSO) δ: 163.29, 161.33, 160.27, 144.61, 140.48, 135.06, 131.63, 128.73, 128.12, 127.72, 126.96, 121.13, 118.25, 105.35, 22.24.

LC-MS (m/z) Calcd. for $C_{17}H_{13}ClN_4O_2$ $[M+1]^+$: 341.07, Found:341.2, Purity: 98.0 %.

N-(2,3-dihydrobenzo[*b*][1,4]dioxin-6-yl)-6-methyl-2-phenylpyrimidin-4-amine (69)

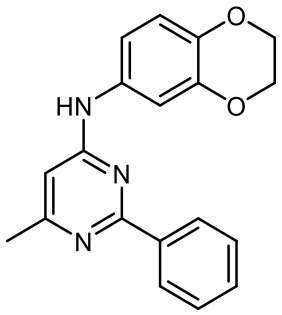

The title compound was synthesized from 4-chloro-6-methyl-2-phenylpyrimidine (102 mg, 0.50 mmol) and 2,3-dihydrobenzo[*b*][1,4]dioxin-6-amine (71 mg, 0.47 mmol) as described in the general procedure above. Beige solid (123.8 mg, 84.2 %).

^{1}H NMR (500 MHz, DMSO-d_6) δ: 9.65 (s, 1H), 8.34 – 8.26 (m, 2H), 7.56 – 7.48 (m, 3H), 7.38 (s, 1H), 7.09 (dd, J = 2.5, 8.7 Hz, 1H), 6.87 (d, J = 8.7 Hz, 1H), 6.55 (s, 1H), 4.30 – 4.20 (m, 4H), 2.39 (s, 3H).

^{13}C NMR (126 MHz, DMSO) δ: 161.96, 160.92, 143.26, 139.41, 133.19, 130.84, 128.57, 127.89, 117.09, 113.90, 109.62, 103.05, 64.38, 64.09, 23.02.

LC-MS (m/z) Calcd. for $C_{19}H_{17}N_3O_2$ $[M+1]^+$: 320.13, Found: 319.8, Purity: 98.8 %.

5-((6-methyl-2-phenylpyrimidin-4-yl)amino)isoindoline-1,3-dione (70)

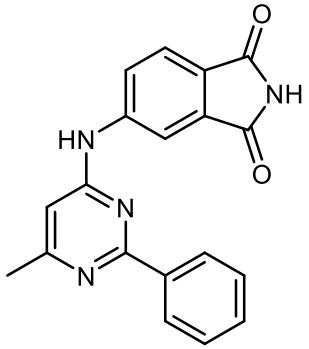

The title compound was synthesized from 4-chloro-6-methyl-2-phenylpyrimidine (100 mg, 0.49 mmol) and 5-aminoisoindoline-1,3-dione (75 mg, 0.47 mmol) as described in the general procedure above. Yellow solid (31.7 mg, 20.6 %).

^{1}H NMR (500 MHz, DMSO-d_6) δ: 11.17 (s, 1H), 10.58 (s, 1H), 8.46 (d, J = 1.9 Hz, 1H), 8.35 (dd, J = 1.9, 7.8 Hz, 2H), 8.06 (dd, J = 1.9, 8.3 Hz, 1H), 7.83 (d, J = 8.2 Hz, 1H), 7.61 – 7.51 (m, 3H), 6.78 (s, 1H), 2.48 (s, 3H).

^{13}C NMR (126 MHz, DMSO) δ: 169.20, 169.02, 161.98, 160.51, 145.45, 136.42, 134.42, 131.30, 128.76, 128.08, 125.47, 124.22, 123.86, 113.21, 104.98, 23.09.

LC-MS (m/z) Calcd. for $C_{19}H_{14}N_4O_2$ $[M+1]^+$: 331.11, Found: 331.1, Purity: 95.9 %.

N-(6-methyl-2-phenylpyrimidin-4-yl)quinolin-6-amine (71)

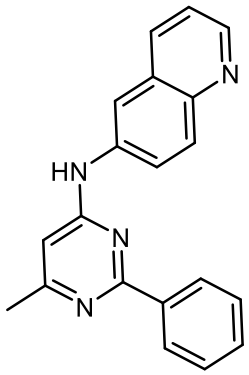

The title compound was synthesized from 4-chloro-6-methyl-2-phenylpyrimidine (55 mg, 0.27 mmol) and quinolin-6-amine (46 mg, 0.32 mmol) as described in the general

procedure above. Further purification was performed by recrystallization from ethyl acetate/n-hexane, yellow solid (13.5 mg, 16.2 %).

^{1}H NMR (500 MHz, DMSO-d_6) δ: 9.88 (s, 1H), 8.76 (dd, J = 1.7, 4.2 Hz, 1H), 8.56 (d, J = 2.4 Hz, 1H), 8.43 – 8.39 (m, 2H), 8.31 – 8.28 (m, 1H), 8.03 – 7.94 (m, 2H), 7.57 – 7.47 (m, 4H), 6.69 (d, J = 0.8 Hz, 1H), 2.43 (s, 3H).

^{13}C NMR (126 MHz, DMSO) δ: 165.15, 162.54, 160.62, 148.44, 144.24, 138.10, 137.89, 135.14, 130.32, 129.41, 128.52, 128.47, 127.68, 124.18, 121.74, 114.56, 103.89,23.85.

LC-MS (m/z) Calcd. for $C_{20}H_{16}N_4$ $[M+1]^+$: 313.14, Found: 313.2, Purity: 99.0 %.

N-(6-methyl-2-phenylpyrimidin-4-yl)quinoxalin-6-amine (72)

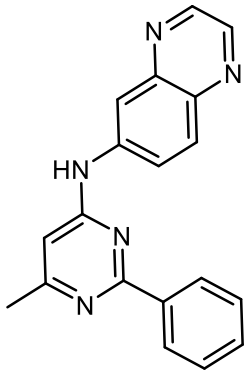

The title compound was synthesized from 4-chloro-6-methyl-2-phenylpyrimidine (120 mg, 0.58 mmol) and quinoxalin-6-amine (85 mg, 0.58 mmol) as described in the general procedure above. Further purification was performed by recrystallization from ethanol/H_2O, brown solid (38.2 mg, 20.9 %).

^{1}H NMR (500 MHz, DMSO-d_6) δ: 10.11 (s, 1H), 8.88 (dd, J = 2.1, 14.2 Hz, 2H), 8.78 (d, J = 1.8 Hz, 1H), 8.45 – 8.42 (m, 2H), 8.08 – 8.02 (m, 2H), 7.57 – 7.53 (m, 3H), 6.74 (d, J = 0.8 Hz, 1H), 2.46 (d, J = 0.6 Hz, 3H).

^{13}C NMR (126 MHz, DMSO) δ: 165.46, 162.59, 160.48, 145.84, 143.47, 143.20, 141.50, 138.63, 137.83, 130.51, 129.43, 128.50, 127.66, 124.48, 114.63, 104.60,23.88.

LC-MS (m/z) Calcd. for $C_{19}H_{15}N_5$ $[M+1]^+$: 314.13, Found: 314.0, Purity: 98.9 %.

8.2.4.1: Synthesis of 2-phenylpyrimidine-4,6-diol (73)

5.56 g (241.7 mmol) sodium was dissolved in 200 ml ethanol to afford sodium ethoxide solution. Subsequently, 12.18 g (66 mmol) benzamidine hydrochloride hydrate and 11.79 g (89 mmol) ethyl dimethyl malonate were added into sodium ethoxide solution respectively. The resulting mixture was heated to reflux overnight and cooled down to room temperature. After solvent was removed under reduced pressure, 50 ml water was added to the solid and the mixture was acidified with concentrated HCl to pH 5-6. The formed precipitate was vacuum filtered and washed with water 3 times. Finally, the obtained crude residue was recrystallized from DMF/H2O to give 2-phenylpyrimidine-4,6-diol as orange solid (5.8 g; 46.7 %).

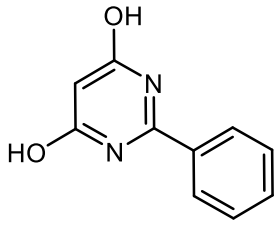

Molecular Weight: 188.19

^{1}H NMR (500 MHz, DMSO-d_6) δ: 11.80 (s, 2H), 8.11 – 8.07 (m, 2H), 7.60 – 7.56 (m, 1H), 7.54 – 7.50 (m, 2H), 5.35 (s, 1H).

^{13}C NMR APT (126 MHz, DMSO) δ: 131.81, 128.69, 127.87, 88.46.

8.2.4.2: Synthesis of 4,6-dichloro-2-phenylpyrimidine (74)

5.8 g (30.8 mmol) 2-phenylpyrimidine-4,6-diol was added into 20 ml $POCl_3$. The reaction was refluxed until the reaction was complete. Excess $POCl_3$ was removed by reduced pressure. The oily residue was transfer onto crushed ice portion by portion, while keeping the temperature of solution under 10 °C. Ethyl acetate was used to extract

products 3 times. The organic layer was washed by saturated $NaHCO_3$, saturated NaCl solution and dry over magnesium sulfate. After filtration, ethyl acetate was removed under reduced pressure. Final purification was performed by column chromatography with DCM/MeOH = 50:1 as eluent to yield white needle crystals (yield: 4.1 g; 59.4 %).

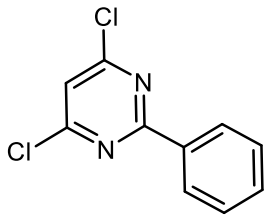

Molecular Weight: 225.07

^{1}H NMR (600 MHz, Chloroform-*d*) δ: 8.44 (d, *J* = 7.9 Hz, 2H), 7.56 – 7.48 (m, 3H), 7.28 (s, 1H).

^{13}C NMR (151 MHz, $CDCl_3$) δ: 165.91, 162.18, 135.02, 132.40, 129.02, 128.88, 118.91.

8.2.4.3 Synthesis of 4-((6-chloro-2-phenylpyrimidin-4-yl)amino)benzonitrile (75)

3.04 g (13.5 mmol) 4,6-dichloro-2-phenylpyrimidine was added into 30 ml isopropanol and this mixture was refluxed until all 4,6-dichloro-2-phenylpyrimidine was dissolved. 1.57 g (13.3 mmol) 4-cyanoaniline was dissolved in 30 ml isopropanol and this solution was added into refluxed 4,6-dichloro-2-phenylpyrimidine solution drop by drop. If reaction did not initiate, 0.1 equivalent of conc. HCl was added as catalyst. The precipitate was filtered off and washed with saturated sodium bicarbonate solution 3 times followed by distilled water 3 times. Further purification was performed by column chromatography with ethyl acetate/petroleum ether (40-60 °C) = 1:2 as eluent, yellow solid (3.6 g, 88.2 %).

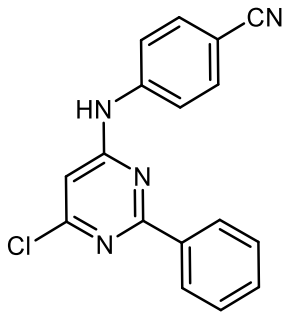

Molecular Weight: 306.75

^{1}H NMR (500 MHz, DMSO-d_6) δ: 10.34 (s, 1H), 8.32 – 8.29 (m, 2H), 7.97 – 7.94 (m, 2H), 7.87 – 7.84 (m, 2H), 7.58 – 7.53 (m, 3H), 6.85 (s, 1H).

^{13}C NMR (126 MHz, DMSO) δ: 163.70, 160.98, 158.82, 143.56, 136.07, 133.31, 131.43, 128.72, 127.92, 119.67, 119.10, 104.52, 104.15.

LC-MS (m/z) Calcd. for $C_{17}H_{11}ClN_4$ $[M+1]^+$: 307.07, Found: 307.2, Purity: 97.9 %.

8.2.4.3 Synthesis of novel pyrimdine derivatives.

Method A: A mixture of 1 equivalent 4-((6-chloro-2-phenylpyrimidin-4-yl)amino)benzonitrile, 10-20 equivalent of amine in 0.5 ml isopropanol was heated to 120 °C in microwave for 30 mins. Further purification for certain compounds was performed by column chromatography with ethyl acetate/petroleum ether (40-60 °C) = 1:2 as eluent.

Method B: To a three necked round-bottom flask were added 112 mg 4-((6-chloro-2-phenylpyrimidin-4-yl)amino)benzonitrile (0.37 mmol), 50 mg phenylboronic acid (0.41 mmol) and dry 8 ml Dioxane/2M K_2CO_3 = 3:1. The mixture was degassed by vacuum/Argon cycle three times. Catalyst 10 mg Pd(t-$Bu_3P)_2$ (0.02 mmol) was added and the mixture was degassed twice more. The mixture was heated to 85 °C for 7 h until TLC confirmed the completion of the reaction. It was cooled to ambient temperature, then the slurry was extracted with saturated $NaHCO_3$/ethyl acetate 3 times. The

collected ethyl acetate solution was dried over magnesium sulfate and concentrated under reduced pressure. Further purification was performed by recrystallization from ethyl acetate/n-Hexane.

Method C: A mixture of 1 equivalent 4-((6-chloro-2-phenylpyrimidin-4-yl)amino)benzonitrile, 10-15 equivalent of substituted aniline in 3 ml isopropanol and 0.1 equivalent conc. HCl was heated to 110 °C in microwave for 30 mins. The precipitate was filtered off and washed with saturated sodium bicarbonate solution 3 times followed by distilled water 3 times. Further purification was performed by column chromatography with ethyl acetate/petroleum ether (40-60 °C) = 1:2 as eluent.

4-((6-(methylamino)-2-phenylpyrimidin-4-yl)amino)benzonitrile (76)

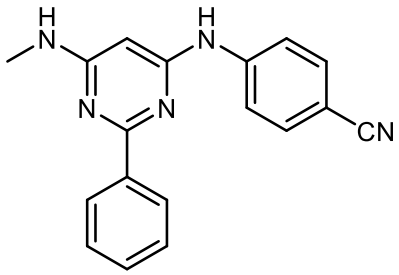

The title compound was synthesized from 4-((6-chloro-2-phenylpyrimidin-4-yl)amino)benzonitrile (136 mg, 0.44 mmol), methylamine hydrochloride (306 mg, 4.53 mmol) and N, N-diisopropylethylamine (0.8 ml, 4.48 mmol)as described in the general procedure of method A. Yellow solid (20.7 mg, 15.5 %).

^{1}H NMR (500 MHz, DMSO-d_6) δ: 9.57 (s, 1H), 8.32 (dd, J = 3.1, 6.6 Hz, 2H), 7.91 (d, J = 8.6 Hz, 2H), 7.75 – 7.68 (m, 2H), 7.51 – 7.40 (m, 3H), 7.07 (s, 1H), 5.80 (s, 1H), 2.87 (s, 3H).

^{13}C NMR (126 MHz, DMSO) δ: 163.78, 162.18, 159.71, 145.64, 138.29, 133.06, 130.03, 128.19, 127.55, 119.59, 118.26, 101.58, 27.35.

LC-MS (m/z) Calcd. for $C_{18}H_{15}N_5$ $[M+1]^+$: 302.13, Found:302.0, Purity: 98.3 %.

4-((6-(isopropylamino)-2-phenylpyrimidin-4-yl)amino)benzonitrile (77)

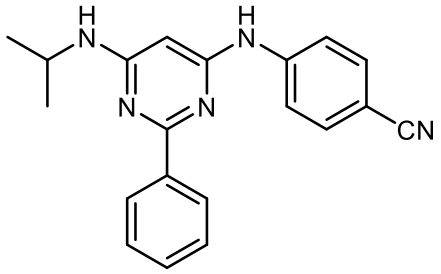

The title compound was synthesized from 4-((6-chloro-2-phenylpyrimidin-4-yl)amino)benzonitrile (141 mg, 0.46 mmol) and isopropylamine (880 mg, 14.89 mmol) as described in the general procedure of method A. Yellow solid (100.3 mg, 66.1 %).

^{1}H NMR (500 MHz, DMSO-d_6) δ: 9.54 (s, 1H), 8.32 – 8.29 (m, 2H), 7.89 (d, J = 8.7 Hz, 2H), 7.74 – 7.71 (m, 2H), 7.50 – 7.46 (m, 3H), 6.99 (d, J = 7.4 Hz, 1H), 5.81 (s, 1H), 1.21 (d, J = 6.5 Hz, 6H).

^{13}C NMR (126 MHz, DMSO) δ: 162.49, 162.25, 145.73, 138.42, 133.07, 130.02, 128.22, 127.53, 119.64, 118.25, 101.50, 59.71, 41.74, 22.50, 14.06.

LC-MS (m/z) Calcd. for $C_{20}H_{19}N_5$ $[M+1]^+$: 330.16, Found: 330.1, Purity: 99.0 %.

4-((2-phenyl-6-(propylamino)pyrimidin-4-yl)amino)benzonitrile (78)

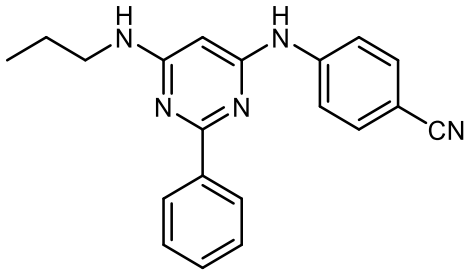

The title compound was synthesized from 4-((6-chloro-2-phenylpyrimidin-4-yl)amino)benzonitrile (168 mg, 0.55 mmol) and 1-propylamine (308 mg, 5.22 mmol) as described in the general procedure of method A. White solid (126.4 mg, 69.9 %).

^{1}H NMR (500 MHz, DMSO-d_6) δ: 9.54 (s, 1H), 8.33 – 8.28 (m, 2H), 7.90 (d, J = 8.9 Hz, 2H), 7.75 – 7.70 (m, 2H), 7.51 – 7.45 (m, 3H), 7.14 (s, 1H), 5.83 (s, 1H), 1.61 (h, J = 7.4 Hz, 2H), 0.95 (t, J = 7.4 Hz, 3H).

^{13}C NMR (126 MHz, DMSO) δ: 163.25, 162.20, 145.68, 138.36, 133.05, 130.00, 128.19, 127.52, 119.59, 118.24, 101.52, 42.20, 22.15, 11.52.

LC-MS (m/z) Calcd. for $C_{20}H_{19}N_5$ $[M+1]^+$: 330.16, Found:330.1, Purity: 99.3 %.

4-((6-(butylamino)-2-phenylpyrimidin-4-yl)amino)benzonitrile (79)

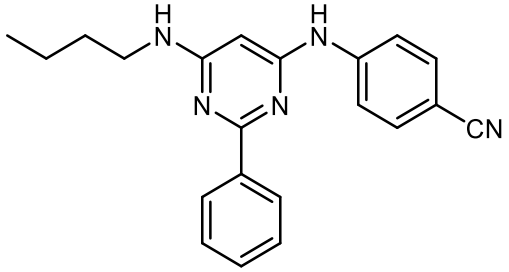

The title compound was synthesized from 4-((6-chloro-2-phenylpyrimidin-4-yl)amino)benzonitrile (125 mg, 0.41 mmol) and 1-butylamine (390 mg, 5.33 mmol) as described in the general procedure of method A. Brown solid (66.5 mg, 47.4 %).

^{1}H NMR (500 MHz, DMSO-d_6) δ: 9.55 (s, 1H), 8.32 – 8.29 (m, 2H), 7.90 (d, J = 8.4 Hz, 2H), 7.75 – 7.71 (m, 2H), 7.51 – 7.46 (m, 3H), 7.14 (s, 1H), 5.82 (s, 1H), 1.60 – 1.54 (m, 2H), 1.39 (q, J = 7.4 Hz, 2H), 0.93 (t, J = 7.4 Hz, 3H).

^{13}C NMR (126 MHz, DMSO) δ: 163.25, 162.22, 145.71, 138.39, 133.09, 130.05, 128.23, 127.54, 119.64, 118.27, 101.53, 19.68, 13.73.

LC-MS (m/z) Calcd. for $C_{21}H_{21}N_5$ $[M+1]^+$: 344.18, Found: 344.1, Purity: 98.9 %.

4-((2,6-diphenylpyrimidin-4-yl)amino)benzonitrile (80)

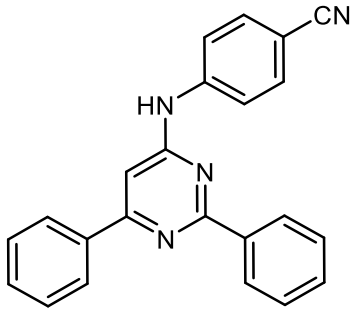

The title compound was synthesized as described in the general procedure of method B. Yellow solid (63.0 mg, 49.6 %).

^{1}H NMR (500 MHz, DMSO-d_6) δ: 10.26 (s, 1H), 8.51 – 8.48 (m, 2H), 8.21 – 8.18 (m, 2H), 8.07 – 8.04 (m, 2H), 7.87 – 7.84 (m, 2H), 7.62 – 7.55 (m, 6H), 7.29 (s, 1H).

^{13}C NMR (126 MHz, DMSO) δ: 163.02, 162.22, 161.01, 144.44, 137.68, 136.81, 133.31, 130.74, 130.63, 128.98, 128.61, 127.87, 126.61, 119.34, 119.16, 103.24, 101.47.

LC-MS (m/z) Calcd. for $C_{23}H_{16}N_4$ $[M+1]^+$: 349.14, Found: 349.0, Purity: 97.1 %.

4-((2-phenyl-6-(phenylamino)pyrimidin-4-yl)amino)benzonitrile (81)

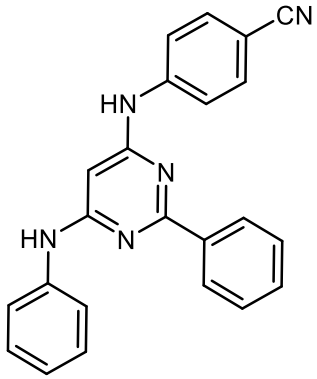

The title compound was synthesized from 4-((6-chloro-2-phenylpyrimidin-4-yl)amino)benzonitrile (127 mg, 0.41 mmol) and aniline (508 mg, 5.46 mmol) as described in the general procedure of method C. White solid (47.6 mg, 31.8 %).

^{1}H NMR (500 MHz, DMSO-d_6) δ: 9.77 (s, 1H), 9.37 (s, 1H), 8.36 – 8.32 (m, 2H), 7.95 – 7.91 (m, 2H), 7.79 – 7.75 (m, 2H), 7.69 – 7.64 (m, 2H), 7.56 – 7.50 (m, 3H), 7.41 – 7.35 (m, 2H), 7.04 (tt, J = 1.1, 7.3 Hz, 1H), 6.23 (s, 1H).

^{13}C NMR (126 MHz, DMSO) δ: 162.61, 161.09, 160.17, 145.25, 140.23, 138.03, 133.13, 130.37, 128.79, 128.42, 127.61, 122.09, 120.08, 119.49, 118.59, 102.11, 86.90. LC-MS (m/z) Calcd. for $C_{23}H_{17}N_5$ $[M+1]^+$: 364.15, Found: 364.0, Purity: 99.1 %.

4-((6-(benzylamino)-2-phenylpyrimidin-4-yl)amino)benzonitrile (82)

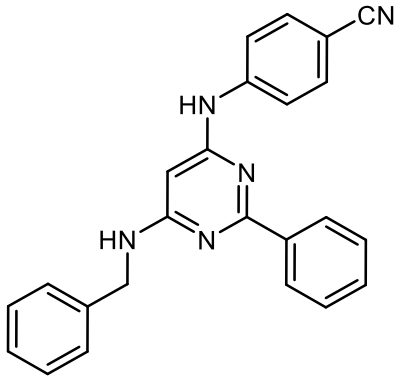

The title compound was synthesized from 4-((6-chloro-2-phenylpyrimidin-4-yl)amino)benzonitrile (76 mg, 0.25 mmol) and benzylamine (270 mg, 2.52 mmol) as described in the general procedure of method A. Brown solid (25.3 mg, 27.3 %).
^{1}H NMR (500 MHz, DMSO-d_6) δ: 9.58 (s, 1H), 8.30 (dd, J = 3.0, 6.7 Hz, 2H), 7.88 (d, J = 8.8 Hz, 2H), 7.75 – 7.70 (m, 3H), 7.48 (dd, J = 1.9, 5.0 Hz, 3H), 7.40 – 7.37 (m, 2H), 7.34 (t, J = 7.6 Hz, 2H), 7.24 (t, J = 7.3 Hz, 1H), 5.86 (s, 1H), 4.60 (s, 2H).
^{13}C NMR (126 MHz, DMSO) δ: 163.19, 162.25, 159.77, 145.58, 140.13, 138.23, 133.08, 130.12, 128.31, 128.25, 127.57, 127.17, 126.70, 119.60, 118.32, 101.65, 43.79. LC-MS (m/z) Calcd. for $C_{24}H_{19}N_5$ $[M+1]^+$: 378.16, Found: 378.3, Purity: 96.7 %.

4-((2-phenyl-6-((3-phenylpropyl)amino)pyrimidin-4-yl)amino)benzonitrile (83)

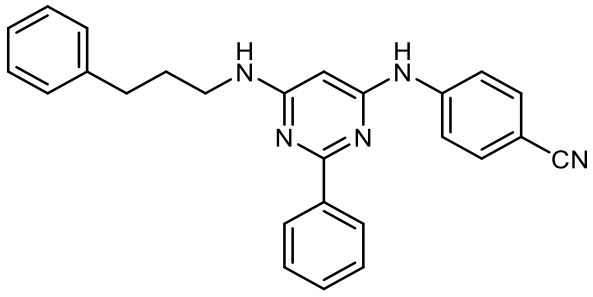

The title compound was synthesized from 4-((6-chloro-2-phenylpyrimidin-4-yl)amino)benzonitrile (86 mg, 0.28 mmol) and 3-phenylpropylamine (759 mg, 5.61 mmol) as described in the general procedure of method A. White solid (70.3 mg, 61.9 %).

^{1}H NMR (500 MHz, DMSO-d_6) δ: 9.54 (s, 1H), 8.30 – 8.25 (m, 2H), 7.90 (d, J = 8.6 Hz, 2H), 7.75 – 7.71 (m, 2H), 7.50 – 7.46 (m, 3H), 7.32 – 7.17 (m, 6H), 5.83 (s, 1H), 3.36 (d, J = 18.3 Hz, 0H), 2.69 (t, J = 7.6 Hz, 2H), 1.90 (p, J = 7.3 Hz, 2H).

^{13}C NMR (126 MHz, DMSO) δ: 163.21, 162.19, 159.55, 145.66, 141.72, 138.31, 133.05, 130.02, 128.28, 128.22, 128.18, 127.53, 125.67, 119.59, 118.27, 101.55, 32.62, 30.73.

LC-MS (m/z) Calcd. for $C_{26}H_{23}N_5$ $[M+1]^+$: 406.20, Found: 406.3, Purity: 98.0 %.

4-((2-phenyl-6-((4-phenylbutyl)amino)pyrimidin-4-yl)amino)benzonitrile (84)

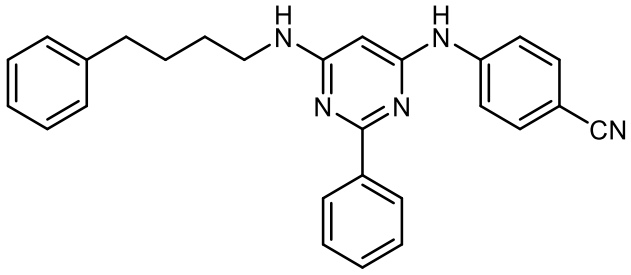

The title compound was synthesized from 4-((6-chloro-2-phenylpyrimidin-4-yl)amino)benzonitrile (130 mg, 0.42 mmol) and 4-phenylbutylamine (522 mg, 3.50 mmol) as described in the general procedure of method A. Pale brown solid (76.8 mg, 43.3 %).

^{1}H NMR (500 MHz, DMSO-d_6) δ: 9.55 (s, 1H), 8.32 – 8.28 (m, 2H), 7.89 (d, J = 8.4 Hz, 2H), 7.75 – 7.71 (m, 2H), 7.50 – 7.45 (m, 3H), 7.26 (t, J = 7.5 Hz, 2H), 7.20 (d, J = 6.8 Hz, 2H), 7.18 – 7.14 (m, 2H), 5.82 (s, 1H), 2.64 (t, J = 7.5 Hz, 2H), 1.71 – 1.64 (m, 2H), 1.64 – 1.57 (m, 2H).

^{13}C NMR (126 MHz, DMSO) δ: 163.23, 162.24, 145.70, 142.11, 138.38, 133.09, 130.05, 128.25, 128.22, 128.18, 127.56, 125.61, 119.64, 118.27, 101.53, 55.99, 34.84, 28.46, 18.52.

LC-MS (m/z) Calcd. for $C_{27}H_{25}N_5$ $[M+1]^+$: 420.21, Found: 420.3, Purity: 96.3 %.

4-((2-phenyl-6-((pyridin-2-ylmethyl)amino)pyrimidin-4-yl)amino)benzonitrile (85)

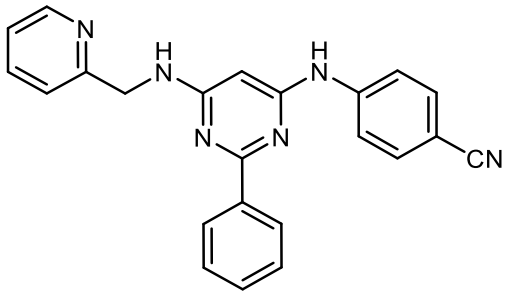

The title compound was synthesized from 4-((6-chloro-2-phenylpyrimidin-4-yl)amino)benzonitrile (95 mg, 0.31 mmol) and 2-picolylamine (585 mg, 5.39 mmol) as described in the general procedure of method A. Grey solid (22.0 mg, 18.8 %).

^{1}H NMR (500 MHz, DMSO-d_6) δ: 9.60 (s, 1H), 8.54 (d, J = 4.3 Hz, 1H), 8.26 (dd, J = 3.0, 6.6 Hz, 2H), 7.90 – 7.87 (m, 2H), 7.80 – 7.71 (m, 4H), 7.48 – 7.44 (m, 3H), 7.39 (d, J = 7.9 Hz, 1H), 7.26 (dd, J = 5.0, 7.3 Hz, 1H), 5.91 (s, 1H), 4.68 (s, 2H).

^{13}C NMR (126 MHz, DMSO) δ: 163.17, 162.23, 159.81, 159.25, 148.85, 145.54, 138.15, 136.67, 133.05, 130.10, 128.21, 127.54, 122.00, 121.01, 119.56, 118.33, 101.69, 45.93.

LC-MS (m/z) Calcd. for $C_{23}H_{18}N_6$ $[M+1]^+$: 379.16, Found: 379.3, Purity: 98.5 %.

4-((2-phenyl-6-((pyridin-3-ylmethyl)amino)pyrimidin-4-yl)amino)benzonitrile (86)

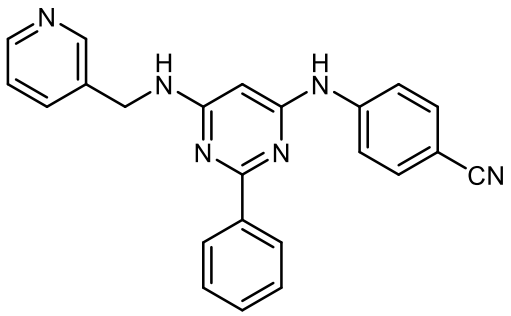

The title compound was synthesized from 4-((6-chloro-2-phenylpyrimidin-4-yl)amino)benzonitrile (86 mg, 0.28 mmol) and 3-picolylamine (687 mg, 6.35 mmol) as described in the general procedure of method A. White solid (80.3 mg, 75.8 %).

^{1}H NMR (500 MHz, DMSO-d_6) δ: 9.59 (s, 1H), 8.63 (s, 1H), 8.45 (d, J = 3.3 Hz, 1H), 8.32 – 8.27 (m, 2H), 7.90 – 7.87 (m, 2H), 7.79 – 7.71 (m, 4H), 7.50 – 7.46 (m, 3H), 7.36 (ddd, J = 0.9, 4.7, 7.9 Hz, 1H), 5.89 (s, 1H), 4.63 (s, 2H).

^{13}C NMR (126 MHz, DMSO) δ: 163.00, 162.28, 159.75, 148.82, 148.00, 145.51, 138.15, 134.99, 133.07, 130.15, 128.25, 127.56, 123.46, 119.56, 118.36, 101.73, 85.15, 41.45.

LC-MS (m/z) Calcd. for $C_{23}H_{18}N_6$ $[M+1]^+$: 379.16, Found: 379.3, Purity: 98.9 %.

4-((2-phenyl-6-((pyridin-4-ylmethyl)amino)pyrimidin-4-yl)amino)benzonitrile (87)

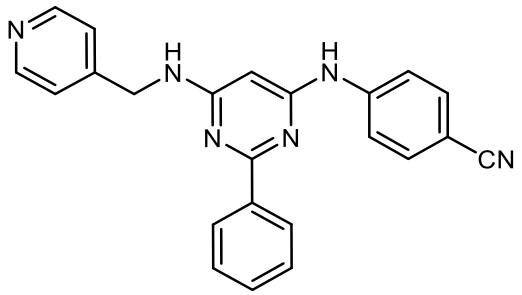

The title compound was synthesized from 4-((6-chloro-2-phenylpyrimidin-4-yl)amino)benzonitrile (86 mg, 0.28 mmol) and 4-picolylamine (861 mg, 7.96 mmol) as described in the general procedure of method A. White solid (74.2 mg, 69.5 %).

^{1}H NMR (500 MHz, DMSO-d_6) δ: 9.60 (s, 1H), 8.52 – 8.50 (m, 2H), 8.25 (dd, J = 3.0, 6.3 Hz, 2H), 7.90 – 7.87 (m, 2H), 7.80 (t, J = 6.1 Hz, 1H), 7.75 – 7.71 (m, 2H), 7.48 – 7.44 (m, 3H), 7.38 – 7.35 (m, 2H), 5.89 (s, 1H), 4.63 (s, 2H).

^{13}C NMR (126 MHz, DMSO) δ: 163.09, 162.28, 149.51, 145.48, 138.09, 133.07, 130.15, 128.23, 127.54, 122.09, 119.55, 118.37, 101.76, 42.98.

LC-MS (m/z) Calcd. for $C_{23}H_{18}N_6$ $[M+1]^+$: 379.16, Found: 379.3, Purity: 98.5 %.

4-((6-((2-hydroxyphenyl)amino)-2-phenylpyrimidin-4-yl)amino)benzonitrile (88)

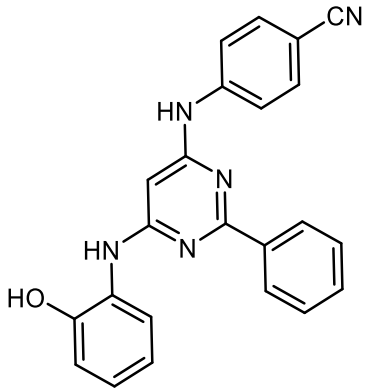

The title compound was synthesized from 4-((6-chloro-2-phenylpyrimidin-4-yl)amino)benzonitrile (102 mg, 0.33 mmol) and 2-hydroxyaniline (222 mg, 2.03 mmol) as described in the general procedure of method C. Yellow solid (48.8 mg, 38.6 %).

^{1}H NMR (500 MHz, DMSO-d_6) δ: 9.60 (s, 1H), 8.36 (dd, J = 3.0, 6.6 Hz, 2H), 7.91 – 7.87 (m, 2H), 7.78 – 7.71 (m, 3H), 7.52 – 7.47 (m, 3H), 7.36 (dd, J = 1.3, 5.0 Hz, 1H), 7.07 (dd, J = 1.3, 3.5 Hz, 1H), 6.97 (dd, J = 3.4, 5.1 Hz, 1H), 5.90 (s, 1H), 4.78 (s, 2H).

^{13}C NMR (126 MHz, DMSO) δ: 162.77, 162.20, 159.71, 145.54, 143.35, 138.16, 133.36, 133.06, 130.15, 128.24, 127.64, 126.54, 125.19, 124.88, 119.57, 118.35, 113.41, 101.70, 85.28.

LC-MS (m/z) Calcd. for $C_{23}H_{17}N_5O$ $[M+1]^+$: 380.14, Found: 380.1, Purity: 95.9 %.

4-((6-((3-hydroxyphenyl)amino)-2-phenylpyrimidin-4-yl)amino)benzonitrile (89)

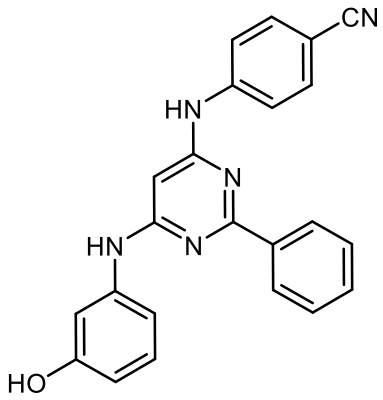

The title compound was synthesized from 4-((6-chloro-2-phenylpyrimidin-4-yl)amino)benzonitrile (106 mg, 0.34 mmol) and 3-hydroxyaniline (290 mg, 2.65 mmol) as described in the general procedure of method C. Grey solid (67.1 mg, 51.4 %).

^{1}H NMR (500 MHz, DMSO-d_6) δ: 9.76 (s, 1H), 9.38 (s, 1H), 9.24 (s, 1H), 8.37 – 8.33 (m, 2H), 7.94 – 7.91 (m, 2H), 7.78 – 7.75 (m, 2H), 7.56 – 7.50 (m, 3H), 7.16 – 7.12 (m, 2H), 7.06 (ddd, J = 1.0, 2.0, 8.1 Hz, 1H), 6.46 (ddd, J = 1.0, 2.4, 8.0 Hz, 1H), 6.23 (s, 1H).

^{13}C NMR (126 MHz, DMSO) δ: 162.63, 161.13, 160.13, 157.75, 145.29, 141.25, 138.04, 133.13, 130.35, 129.41, 128.39, 127.70, 119.51, 118.57, 110.97, 109.45, 107.26, 102.07, 86.91.

LC-MS (m/z) Calcd. for $C_{23}H_{17}N_5O$ $[M+1]^+$: 380.14, Found: 380.1, Purity: 99.0 %.

4-((6-((4-hydroxyphenyl)amino)-2-phenylpyrimidin-4-yl)amino)benzonitrile (90)

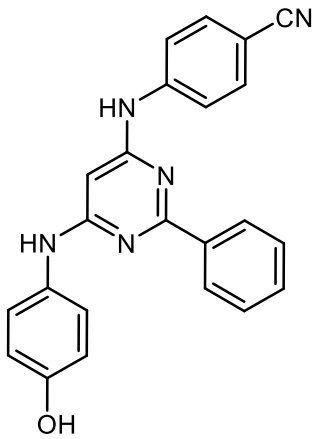

The title compound was synthesized from 4-((6-chloro-2-phenylpyrimidin-4-yl)amino)benzonitrile (101 mg, 0.33 mmol) and 4-hydroxyaniline (390 mg, 3.57 mmol) as described in the general procedure of method C. Grey solid (22.7 mg, 18.2 %).

^{1}H NMR (500 MHz, DMSO-d_6) δ: 9.66 (s, 1H), 9.22 (s, 1H), 8.98 (s, 1H), 8.34 – 8.30 (m, 2H), 7.93 – 7.90 (m, 2H), 7.76 – 7.73 (m, 2H), 7.54 – 7.48 (m, 3H), 7.33 (d, J = 8.3 Hz, 2H), 6.81 – 6.78 (m, 2H), 6.02 (s, 1H).

^{13}C NMR (126 MHz, DMSO) δ: 162.54, 161.87, 160.13, 153.51, 145.41, 138.14, 133.09, 131.11, 130.22, 128.33, 127.58, 123.52, 119.54, 118.41, 115.41, 101.86, 85.41.

LC-MS (m/z) Calcd. for $C_{23}H_{17}N_5O$ $[M+1]^+$: 380.14, Found: 380.1, Purity: 96.5 %.

4,4'-((2-phenylpyrimidine-4,6-diyl)bis(azanediyl))dibenzonitrile (91)

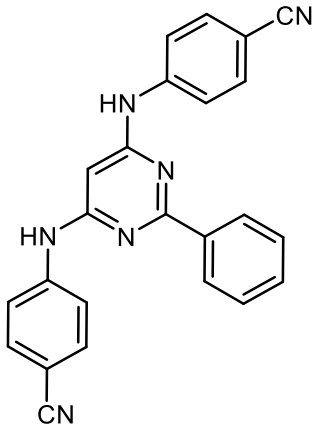

The title compound was the side product in synthesis of 4-((6-chloro-2-phenylpyrimidin-4-yl)amino)benzonitrile. Yellow solid.

^{1}H NMR (500 MHz, DMSO-d_6) δ: 9.92 (s, 2H), 8.34 (dd, J = 3.0, 6.7 Hz, 2H), 7.96 – 7.92 (m, 4H), 7.81 – 7.77 (m, 4H), 7.55 (dd, J = 2.0, 5.0 Hz, 3H), 6.32 (s, 1H).

^{13}C NMR (126 MHz, DMSO) δ: 162.71, 160.33, 144.92, 137.71, 133.18, 130.64, 128.57, 127.72, 119.42, 118.88, 102.57, 88.87.

LC-MS (m/z) Calcd. for $C_{24}H_{16}N_6$ $[M+1]^+$: 389.14, Found: 389.2, Purity: 98.2 %.

9 Appendix

9.1 List of Abbreviations

ABC transporter	ATP binding cassette transporter
ADP	adenosine diphosphate
ATP	adenosine-5´-triphosphate
APT	attached proton test
ALD	adrenoleukodystrophy
ALS	amyotrophic lateral sclerosis
AT	adenine-thymine
BBB	blood-brain barrier
BCRP	breast cancer resistance protein, ABCG2
Calcein AM	calcein acetoxymethylester
$CDCl_3$	Chloroform-*d*/deuterated chloroform
CFTR	cystic fibrosis transmembrane conductance regulator
CysLTR1	cysteinyl leukotriene receptor 1
d	doublet
DCM	dichloromethane
dd	doublet of doublets
ddd	doublet of doublets of doublets
DIPEA	N,N-Diisopropylethylamine
DMF	dimethylformamide
DMSO	dimethylsulfoxide
DNA	deoxyribonucleic acid
dt	doublet of triplets
EC_{50}	half-maximal effective concentration

EGFR	epidermal growth factor receptor
EL	extracellular loop
EM	electron microscopy
EM-SPA	electron microscopy-single-particle analysis
FACS	fluorescence-activated cell scanning
FTC	Fumitremorgin C
FTIR	Fourier-transform infrared spectroscopy
GlcNAc	N-Acetylglucosamine
GSH	glutathione
HCl	hydrochloric acid
HIV	human immunodeficiency virus
HTS	high throughput screening
IC_{50}	compound concentration leading to 50% inhibition
I_{max}	plateau value of maximal inhibition
LC-MS	Liquid chromatography–mass spectrometry
m	multiplet
MDR	multidrug resistance
MDR1	multidrug resistance protein 1
MeOH	methanol
MRP1	Multidrug Resistance related Protein 1
m/z	mass-to-charge ratio
n.a.	not active
NaOH	sodium hydroxide
n.d.	not determined
n.t.	not tested
NBD	nucleotide binding domain
NMR	nuclear magnetic resonance
NSCLC	non-small cell lung cancer

P-gp	permeability glycoprotein, ABCB1
ppm	parts per million
q	quartet
QSAR	quantitative structure-activity relationship
RT	room temperature
s	singlet
SD	standard deviation
SLC	solute carrier
SNP	single-nucleotide polymorphism
t	triplet
TBTU	2-(1H-Benzotriazole-1-yl)-1,1,3,3-tetramethylaminium tetrafluoroborate
t-BuOK	Potassium tert-butoxide
td	triplet of doublets
THF	Tetrahydrofuran
TKI	tyrosine kinase inhibitor
TLC	thin layer chromatography
TM	transmembrane
TMD	transmembrane domain

9.2 List of Tables

9.3 List of Figures

9.4 List of Schemes

9.5 IR spectra of quinazoline derivatives

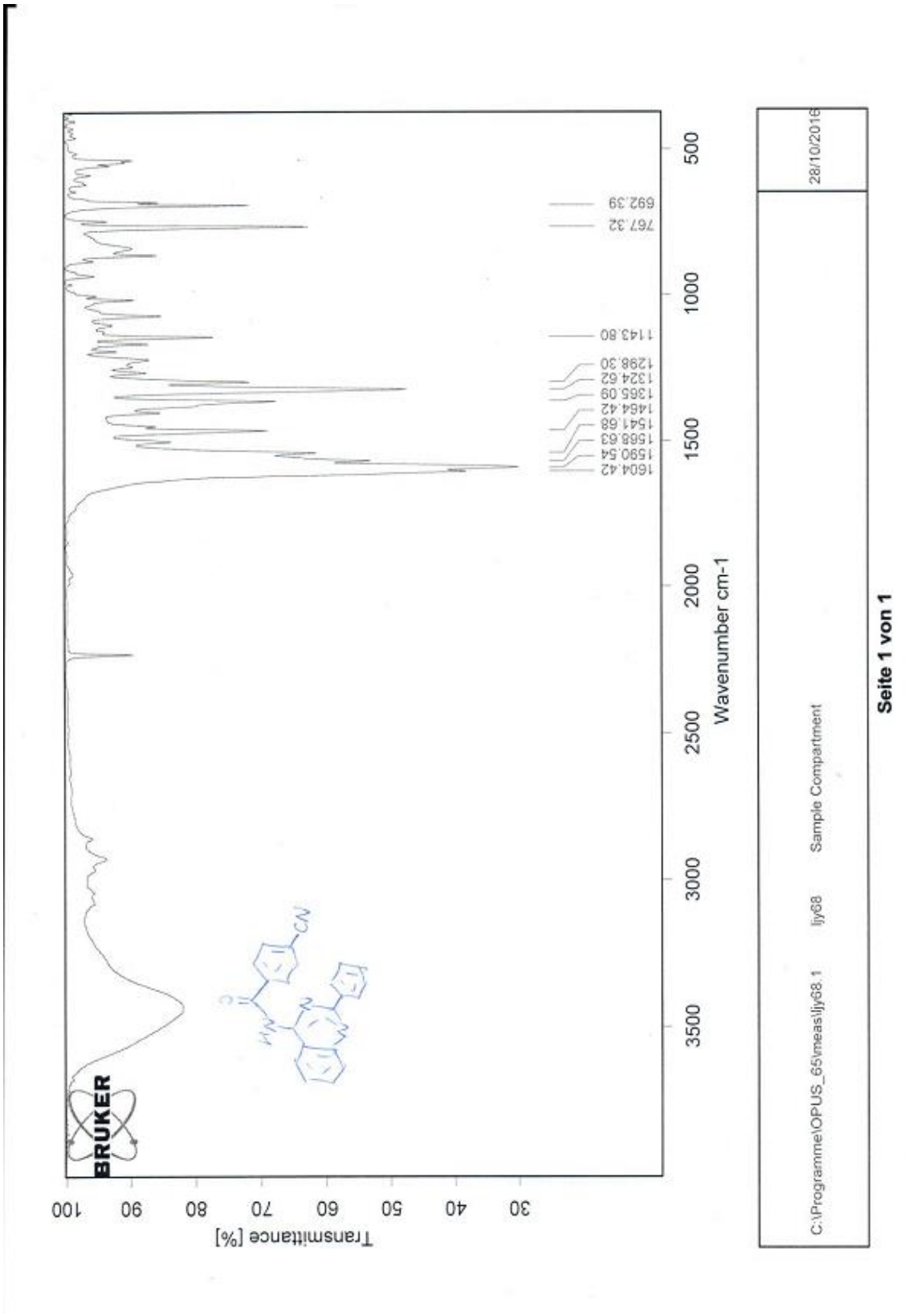

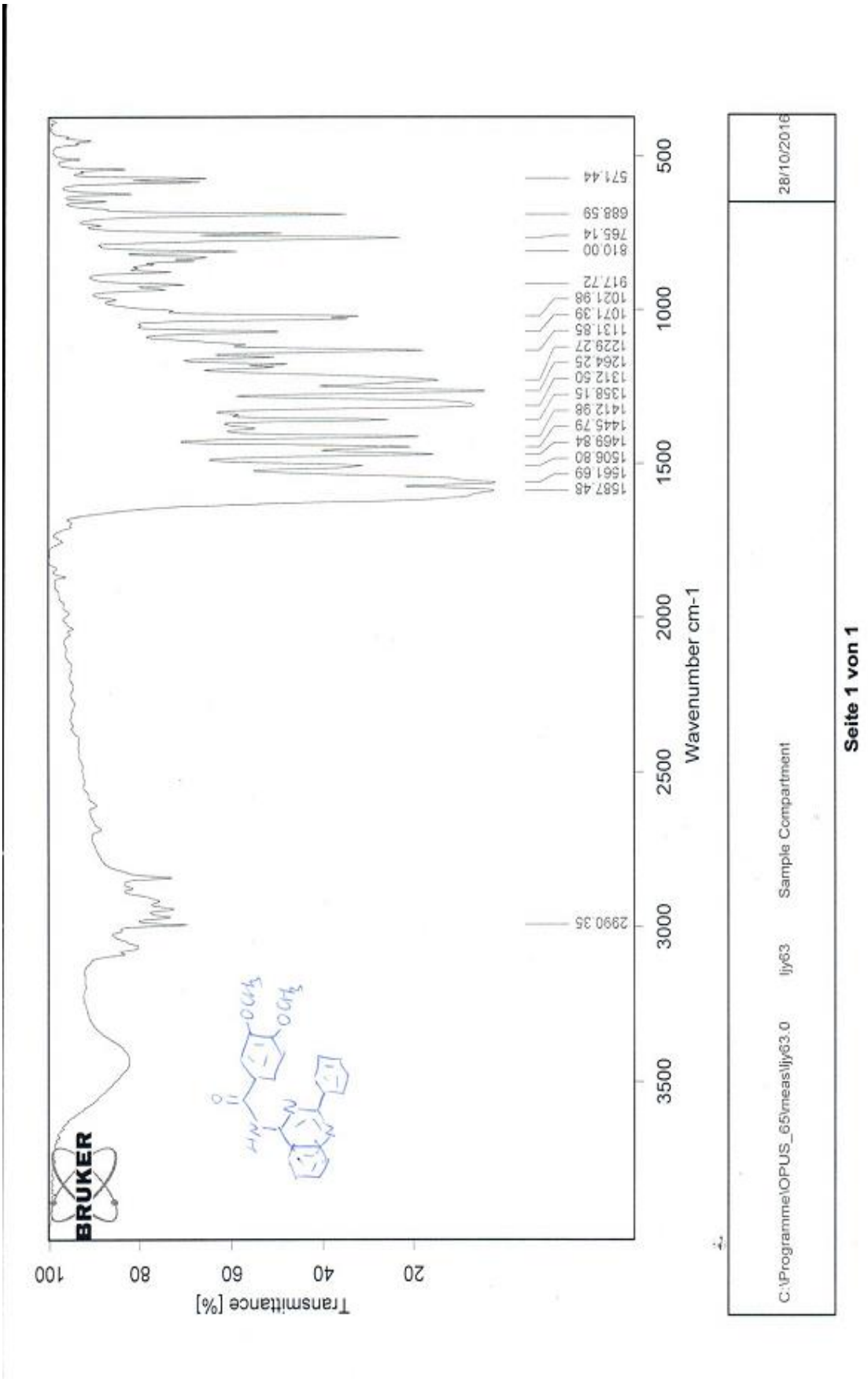
BRUKER
Transmittance [%]
100
80
60
40
20
Wavenumber cm-1
3500
3000
2500
2000
1500
1000
500
2990.35
1587.48
1561.69
1506.80
1469.84
1445.79
1412.98
1358.15
1312.50
1264.25
1229.27
1131.85
1071.39
1021.98
917.72
810.00
765.14
688.59
571.44
C:\Programme\OPUS_65\meas\ljy63.0
ljy63
Sample Compartment
28/10/2016
Seite 1 von 1

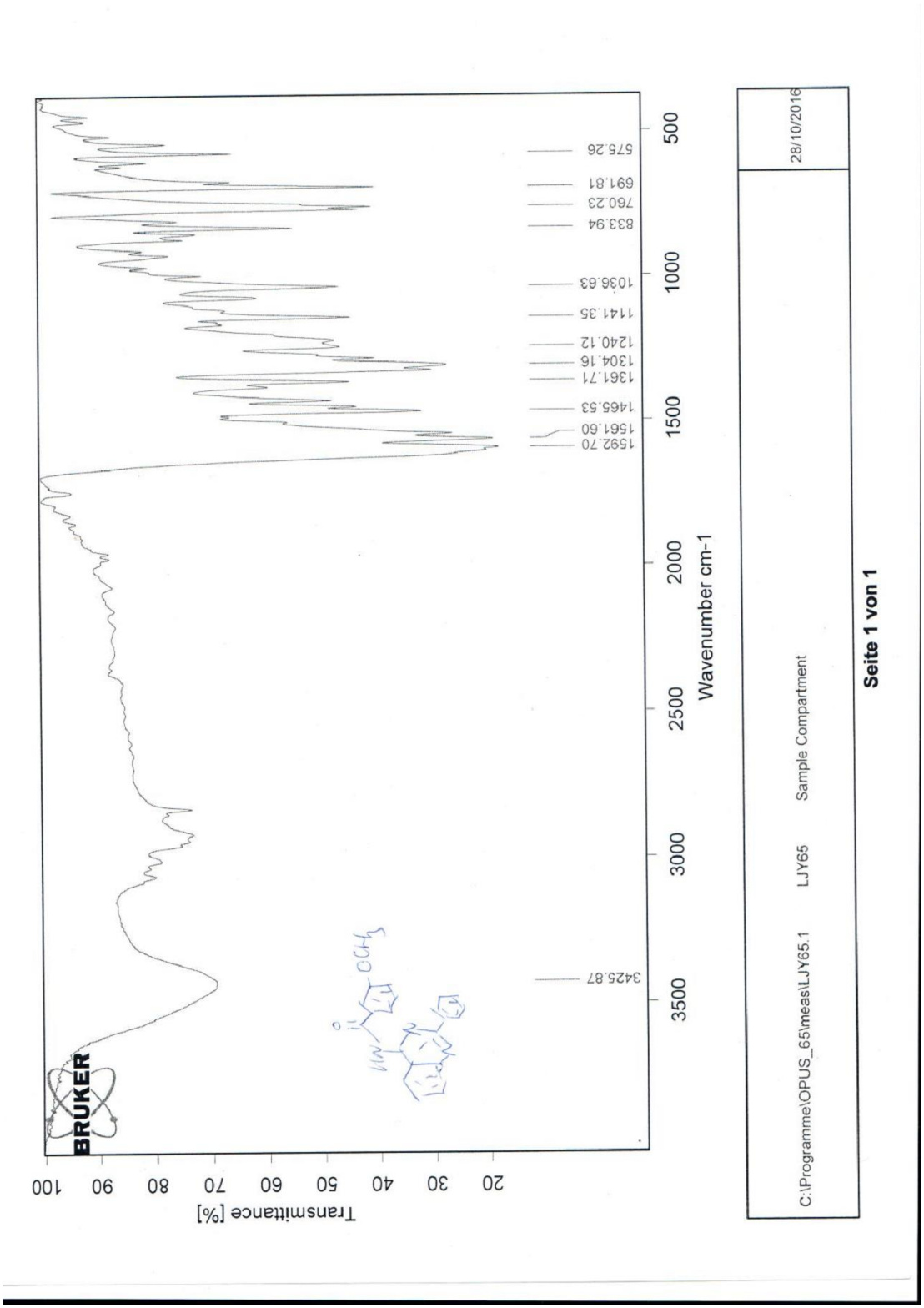
BRUKER
Transmittance [%]
100
90
80
70
60
50
40
30
20
3500
3000
2500
2000
1500
1000
500
Wavenumber cm-1
3425.87
1592.70
1561.60
1465.53
1361.71
1304.16
1240.12
1141.35
1036.63
833.94
760.23
691.81
575.26
C:\Programme\OPUS_65\meas\LJY65.1
LJY65
Sample Compartment
28/10/2016
Seite 1 von 1

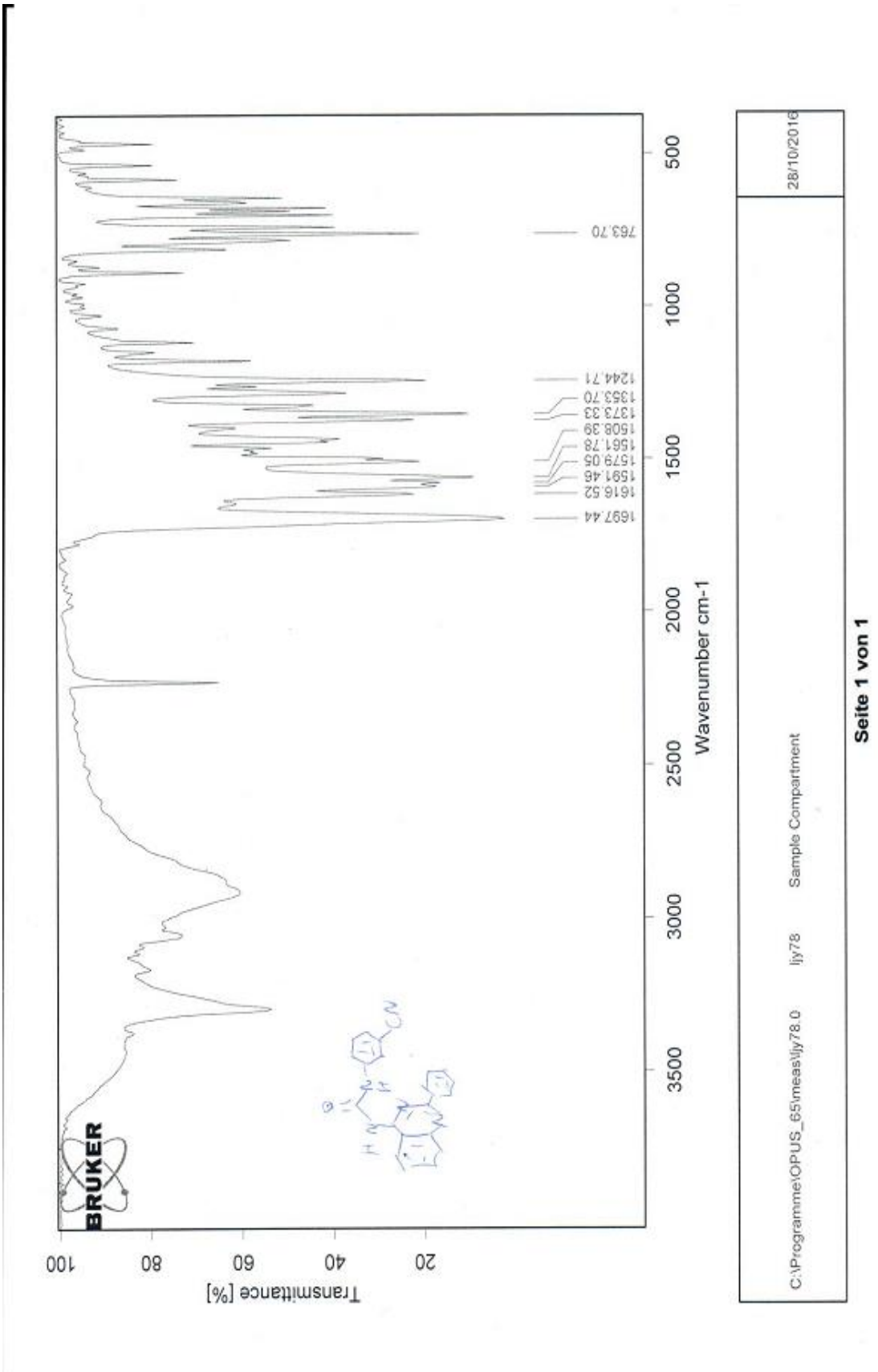
BRUKER
Transmittance [%]
100
80
60
40
20
3500
3000
2500
2000
1500
1000
500
Wavenumber cm-1
763.70
1244.71
1353.70
1373.33
1508.39
1561.78
1579.05
1591.46
1616.52
1697.44
C:\Programme\OPUS_65\meas\ljy78.0
ljy78
Sample Compartment
28/10/2016
Seite 1 von 1

10 Publications

Congress Poster

Jiyang Li, Katja Silbermann, Michael Wiese. Development of pyrimidine derivatives as potent ABCG2 inhibitors. EuroPPS, Valencia, 2017.

11 References

1. Fojo, A. T.; Ueda, K.; Slamon, D. J.; Poplack, D. G.; Gottesman, M. M.; Pastan, I., Expression of a multidrug-resistance gene in human tumors and tissues. *Proc. Natl. Acad. Sci. U. S. A.* **1987,** 265-269.
2. Gillet, J. P.; Gottesman, M. M., Mechanisms of multidrug resistance in cancer. *Methods Mol. Biol.* **2010,** 47-76.
3. Rees, D. C.; Johnson, E.; Lewinson, O., ABC transporters: the power to change. *Nat. Rev. Mol. Cell Biol.* **2009,** 218-227.
4. Choi, Y. H.; Yu, A. M., ABC transporters in multidrug resistance and pharmacokinetics, and strategies for drug development. *Curr. Pharm. Des.* **2014,** 793-807.
5. Rice, A. J.; Park, A.; Pinkett, H. W., Diversity in ABC transporters: type I, II and III importers. *Crit. Rev. Biochem. Mol. Biol.* **2014,** 426-437.
6. de Lange, E. C., Potential role of ABC transporters as a detoxification system at the blood-CSF barrier. *Adv. Drug Deliv. Rev.* **2004,** 1793-1809.
7. Holland, I. B.; Schmitt, L.; Young, J., Type 1 protein secretion in bacteria, the ABC-transporter dependent pathway (review). *Mol. Membr. Biol.* **2005,** 29-39.
8. Jones, P. M.; George, A. M., The ABC transporter structure and mechanism: perspectives on recent research. *Cell. Mol. Life Sci.* **2004,** 682-699.
9. ter Beek, J.; Guskov, A.; Slotboom, D. J., Structural diversity of ABC transporters. *J. Gen. Physiol.* **2014,** 419-435.
10. Jones, P. M.; George, A. M., Subunit interactions in ABC transporters: towards a functional architecture. *FEMS Microbiol. Lett.* **1999,** 187-202.
11. Manzano, J. I.; Garcia-Hernandez, R.; Castanys, S.; Gamarro, F., A new ABC half-transporter in Leishmania major is involved in resistance to antimony. *Antimicrob. Agents Chemother.* **2013,** 3719-3730.
12. Kerr, I. D.; Jones, P. M.; George, A. M., Multidrug efflux pumps: the structures of prokaryotic ATP-binding cassette transporter efflux pumps and implications for our understanding of eukaryotic P-glycoproteins and homologues. *FEBS J.* **2010,** 550-563.
13. Dean, M.; Rzhetsky, A.; Allikmets, R., The human ATP-binding cassette (ABC) transporter superfamily. *Genome Res.* **2001,** 1156-1166.
14. Vasiliou, V.; Vasiliou, K.; Nebert, D. W., Human ATP-binding cassette (ABC) transporter family. *Hum. Genomics* **2009,** 281-290.
15. Sarkadi, B.; Homolya, L.; Szakacs, G.; Varadi, A., Human multidrug resistance ABCB and ABCG transporters: participation in a chemoimmunity defense system. *Physiol. Rev.* **2006,** 1179-1236.
16. Chen, Z. S.; Tiwari, A. K., Multidrug resistance proteins (MRPs/ABCCs) in cancer chemotherapy and genetic diseases. *FEBS J.* **2011,** 3226-3245.
17. Hlavac, V.; Soucek, P., Role of family D ATP-binding cassette transporters (ABCD)

in cancer. *Biochem. Soc. Trans.* **2015,** 937-942.
18. Tian, Y.; Han, X.; Tian, D. L., The biological regulation of ABCE1. *IUBMB Life* **2012,** 795-800.
19. Kerr, I. D.; Haider, A. J.; Gelissen, I. C., The ABCG family of membrane-associated transporters: you don't have to be big to be mighty. *Br. J. Pharmacol.* **2011,** 1767-1779.
20. Theodoulou, F. L.; Kerr, I. D., ABC transporter research: going strong 40 years on. *Biochem. Soc. Trans.* **2015,** 1033-1040.
21. Gaudet, R.; Wiley, D. C., Structure of the ABC ATPase domain of human TAP1, the transporter associated with antigen processing. *EMBO J.* **2001,** 4964-4972.
22. Lewis, H. A.; Buchanan, S. G.; Burley, S. K.; Conners, K.; Dickey, M.; Dorwart, M.; Fowler, R.; Gao, X.; Guggino, W. B.; Hendrickson, W. A.; Hunt, J. F.; Kearins, M. C.; Lorimer, D.; Maloney, P. C.; Post, K. W.; Rajashankar, K. R.; Rutter, M. E.; Sauder, J. M.; Shriver, S.; Thibodeau, P. H.; Thomas, P. J.; Zhang, M.; Zhao, X.; Emtage, S., Structure of nucleotide-binding domain 1 of the cystic fibrosis transmembrane conductance regulator. *EMBO J.* **2004,** 282-293.
23. Ramaen, O.; Leulliot, N.; Sizun, C.; Ulryck, N.; Pamlard, O.; Lallemand, J. Y.; Tilbeurgh, H.; Jacquet, E., Structure of the human multidrug resistance protein 1 nucleotide binding domain 1 bound to Mg2+/ATP reveals a non-productive catalytic site. *J. Mol. Biol.* **2006,** 940-949.
24. Schmitt, L.; Benabdelhak, H.; Blight, M. A.; Holland, I. B.; Stubbs, M. T., Crystal structure of the nucleotide-binding domain of the ABC-transporter haemolysin B: identification of a variable region within ABC helical domains. *J. Mol. Biol.* **2003,** 333-342.
25. Higgins, C. F.; Linton, K. J., The ATP switch model for ABC transporters. *Nat. Struct. Mol. Biol.* **2004,** 918-926.
26. Ward, A.; Reyes, C. L.; Yu, J.; Roth, C. B.; Chang, G., Flexibility in the ABC transporter MsbA: Alternating access with a twist. *Proc. Natl. Acad. Sci. U. S. A.* **2007,** 19005-19010.
27. Dawson, R. J.; Locher, K. P., Structure of the multidrug ABC transporter Sav1866 from Staphylococcus aureus in complex with AMP-PNP. *FEBS Lett.* **2007,** 935-938.
28. Aller, S. G.; Yu, J.; Ward, A.; Weng, Y.; Chittaboina, S.; Zhuo, R.; Harrell, P. M.; Trinh, Y. T.; Zhang, Q.; Urbatsch, I. L.; Chang, G., Structure of P-glycoprotein reveals a molecular basis for poly-specific drug binding. *Science* **2009,** 1718-1722.
29. Li, J.; Jaimes, K. F.; Aller, S. G., Refined structures of mouse P-glycoprotein. *Protein Sci.* **2014,** 34-46.
30. Shintre, C. A.; Pike, A. C.; Li, Q.; Kim, J. I.; Barr, A. J.; Goubin, S.; Shrestha, L.; Yang, J.; Berridge, G.; Ross, J.; Stansfeld, P. J.; Sansom, M. S.; Edwards, A. M.; Bountra, C.; Marsden, B. D.; von Delft, F.; Bullock, A. N.; Gileadi, O.; Burgess-Brown, N. A.; Carpenter, E. P., Structures of ABCB10, a human ATP-binding cassette transporter in apo- and nucleotide-bound states. *Proc. Natl. Acad. Sci. U. S. A.* **2013,** 9710-9715.

31. Taylor, N. M. I.; Manolaridis, I.; Jackson, S. M.; Kowal, J.; Stahlberg, H.; Locher, K. P., Structure of the human multidrug transporter ABCG2. *Nature* **2017,** 504-509.
32. Kaback, H. R.; Smirnova, I.; Kasho, V.; Nie, Y.; Zhou, Y., The alternating access transport mechanism in LacY. *J. Membr. Biol.* **2011,** 85-93.
33. Wilkens, S., Structure and mechanism of ABC transporters. *F1000Prime Rep* **2015,** 14.
34. Locher, K. P., Mechanistic diversity in ATP-binding cassette (ABC) transporters. *Nat. Struct. Mol. Biol.* **2016,** 487-493.
35. Perez, C.; Gerber, S.; Boilevin, J.; Bucher, M.; Darbre, T.; Aebi, M.; Reymond, J. L.; Locher, K. P., Structure and mechanism of an active lipid-linked oligosaccharide flippase. *Nature* **2015,** 433-438.
36. George, A. M.; Jones, P. M., Perspectives on the structure-function of ABC transporters: the Switch and Constant Contact models. *Prog. Biophys. Mol. Biol.* **2012,** 95-107.
37. Juliano, R. L.; Ling, V., A surface glycoprotein modulating drug permeability in Chinese hamster ovary cell mutants. *Biochim. Biophys. Acta* **1976,** 152-162.
38. Callaghan, R., Providing a molecular mechanism for P-glycoprotein; why would I bother? *Biochem. Soc. Trans.* **2015,** 995-1002.
39. Cordon-Cardo, C.; O'Brien, J. P.; Boccia, J.; Casals, D.; Bertino, J. R.; Melamed, M. R., Expression of the multidrug resistance gene product (P-glycoprotein) in human normal and tumor tissues. *J. Histochem. Cytochem.* **1990,** 1277-1287.
40. Kwon, H.; Lionberger, R. A.; Yu, L. X., Impact of P-glycoprotein-mediated intestinal efflux kinetics on oral bioavailability of P-glycoprotein substrates. *Mol. Pharm.* **2004,** 455-465.
41. Tanigawara, Y., Role of P-glycoprotein in drug disposition. *Ther. Drug Monit.* **2000,** 137-140.
42. Ward, A. B.; Szewczyk, P.; Grimard, V.; Lee, C. W.; Martinez, L.; Doshi, R.; Caya, A.; Villaluz, M.; Pardon, E.; Cregger, C.; Swartz, D. J.; Falson, P. G.; Urbatsch, I. L.; Govaerts, C.; Steyaert, J.; Chang, G., Structures of P-glycoprotein reveal its conformational flexibility and an epitope on the nucleotide-binding domain. *Proc. Natl. Acad. Sci. U. S. A.* **2013,** 13386-13391.
43. Sauna, Z. E.; Kimchi-Sarfaty, C.; Ambudkar, S. V.; Gottesman, M. M., Silent polymorphisms speak: how they affect pharmacogenomics and the treatment of cancer. *Cancer Res.* **2007,** 9609-9612.
44. Kimchi-Sarfaty, C.; Oh, J. M.; Kim, I. W.; Sauna, Z. E.; Calcagno, A. M.; Ambudkar, S. V.; Gottesman, M. M., A "silent" polymorphism in the MDR1 gene changes substrate specificity. *Science* **2007,** 525-528.
45. Hodges, L. M.; Markova, S. M.; Chinn, L. W.; Gow, J. M.; Kroetz, D. L.; Klein, T. E.; Altman, R. B., Very important pharmacogene summary: ABCB1 (MDR1, P-glycoprotein). *Pharmacogenet. Genomics* **2011,** 152-161.
46. Loo, T. W.; Bartlett, M. C.; Clarke, D. M., Substrate-induced conformational changes in the transmembrane segments of human P-glycoprotein. Direct evidence for

the substrate-induced fit mechanism for drug binding. *J. Biol. Chem.* **2003,** 13603-13606.
47. Loo, T. W.; Bartlett, M. C.; Clarke, D. M., Simultaneous binding of two different drugs in the binding pocket of the human multidrug resistance P-glycoprotein. *J. Biol. Chem.* **2003,** 39706-39710.
48. Rosenberg, M. F.; Callaghan, R.; Ford, R. C.; Higgins, C. F., Structure of the multidrug resistance P-glycoprotein to 2.5 nm resolution determined by electron microscopy and image analysis. *J. Biol. Chem.* **1997,** 10685-10694.
49. Rosenberg, M. F.; Callaghan, R.; Modok, S.; Higgins, C. F.; Ford, R. C., Three-dimensional structure of P-glycoprotein: the transmembrane regions adopt an asymmetric configuration in the nucleotide-bound state. *J. Biol. Chem.* **2005,** 2857-2862.
50. Rosenberg, M. F.; Velarde, G.; Ford, R. C.; Martin, C.; Berridge, G.; Kerr, I. D.; Callaghan, R.; Schmidlin, A.; Wooding, C.; Linton, K. J.; Higgins, C. F., Repacking of the transmembrane domains of P-glycoprotein during the transport ATPase cycle. *EMBO J.* **2001,** 5615-5625.
51. Rosenberg, M. F.; Kamis, A. B.; Callaghan, R.; Higgins, C. F.; Ford, R. C., Three-dimensional structures of the mammalian multidrug resistance P-glycoprotein demonstrate major conformational changes in the transmembrane domains upon nucleotide binding. *J. Biol. Chem.* **2003,** 8294-8299.
52. Nicklisch, S. C.; Rees, S. D.; McGrath, A. P.; Gokirmak, T.; Bonito, L. T.; Vermeer, L. M.; Cregger, C.; Loewen, G.; Sandin, S.; Chang, G.; Hamdoun, A., Global marine pollutants inhibit P-glycoprotein: Environmental levels, inhibitory effects, and cocrystal structure. *Sci. Adv.* **2016,** e1600001.
53. Higgins, C. F.; Gottesman, M. M., Is the multidrug transporter a flippase? *Trends Biochem. Sci.* **1992,** 18-21.
54. Omote, H.; Al-Shawi, M. K., A novel electron paramagnetic resonance approach to determine the mechanism of drug transport by P-glycoprotein. *J. Biol. Chem.* **2002,** 45688-45694.
55. Romsicki, Y.; Sharom, F. J., Phospholipid flippase activity of the reconstituted P-glycoprotein multidrug transporter. *Biochemistry* **2001,** 6937-6947.
56. Hennessy, M.; Spiers, J. P., A primer on the mechanics of P-glycoprotein the multidrug transporter. *Pharmacol. Res.* **2007,** 1-15.
57. Sharom, F. J., Complex Interplay between the P-Glycoprotein Multidrug Efflux Pump and the Membrane: Its Role in Modulating Protein Function. *Front. Oncol.* **2014,** 41.
58. Sharom, F. J., The P-glycoprotein multidrug transporter. *Essays Biochem.* **2011,** 161-178.
59. Ueda, K.; Taguchi, Y.; Morishima, M., How does P-glycoprotein recognize its substrates? *Semin. Cancer Biol.* **1997,** 151-159.
60. Stouch, T. R.; Gudmundsson, O., Progress in understanding the structure–activity relationships of P-glycoprotein. *Adv. Drug Del. Rev.* **2002,** 315-328.

61. Dantzig, A. H.; de Alwis, D. P.; Burgess, M., Considerations in the design and development of transport inhibitors as adjuncts to drug therapy. *Adv. Drug Del. Rev.* **2003,** 133-150.
62. Thomas, H.; Coley, H. M., Overcoming multidrug resistance in cancer: an update on the clinical strategy of inhibiting p-glycoprotein. *Cancer Control* **2003,** 159-165.
63. Palmeira, A.; Sousa, E.; Vasconcelos, M. H.; Pinto, M. M., Three decades of P-gp inhibitors: skimming through several generations and scaffolds. *Curr. Med. Chem.* **2012,** 1946-2025.
64. Bachmakov, I.; Rekersbrink, S.; Hofmann, U.; Eichelbaum, M.; Fromm, M. F., Characterisation of (R/S)-propafenone and its metabolites as substrates and inhibitors of P-glycoprotein. *Naunyn Schmiedebergs Arch. Pharmacol.* **2005,** 195-201.
65. Zhang, Y.; Schuetz, J. D.; Elmquist, W. F.; Miller, D. W., Plasma membrane localization of multidrug resistance-associated protein homologs in brain capillary endothelial cells. *J. Pharmacol. Exp. Ther.* **2004,** 449-455.
66. Rosenberg, M. F.; Mao, Q.; Holzenburg, A.; Ford, R. C.; Deeley, R. G.; Cole, S. P., The structure of the multidrug resistance protein 1 (MRP1/ABCC1). crystallization and single-particle analysis. *J. Biol. Chem.* **2001,** 16076-16082.
67. Bakos, E.; Evers, R.; Calenda, G.; Tusnady, G. E.; Szakacs, G.; Varadi, A.; Sarkadi, B., Characterization of the amino-terminal regions in the human multidrug resistance protein (MRP1). *J. Cell Sci.* **2000,** 4451-4461.
68. Nooter, K.; Westerman, A. M.; Flens, M. J.; Zaman, G. J.; Scheper, R. J.; van Wingerden, K. E.; Burger, H.; Oostrum, R.; Boersma, T.; Sonneveld, P.; et al., Expression of the multidrug resistance-associated protein (MRP) gene in human cancers. *Clin. Cancer Res.* **1995,** 1301-1310.
69. Walsh, N.; Larkin, A.; Kennedy, S.; Connolly, L.; Ballot, J.; Ooi, W.; Gullo, G.; Crown, J.; Clynes, M.; O'Driscoll, L., Expression of multidrug resistance markers ABCB1 (MDR-1/P-gp) and ABCC1 (MRP-1) in renal cell carcinoma. *BMC Urol.* **2009,** 6.
70. Deeley, R. G.; Westlake, C.; Cole, S. P., Transmembrane transport of endo- and xenobiotics by mammalian ATP-binding cassette multidrug resistance proteins. *Physiol. Rev.* **2006,** 849-899.
71. Bakos, E.; Homolya, L., Portrait of multifaceted transporter, the multidrug resistance-associated protein 1 (MRP1/ABCC1). *Pflugers Arch.* **2007,** 621-641.
72. Cole, S. P.; Deeley, R. G., Transport of glutathione and glutathione conjugates by MRP1. *Trends Pharmacol. Sci.* **2006,** 438-446.
73. Keppler, D., Multidrug resistance proteins (MRPs, ABCCs): importance for pathophysiology and drug therapy. *Handb. Exp. Pharmacol.* **2011,** 299-323.
74. Gekeler, V.; Ise, W.; Sanders, K. H.; Ulrich, W. R.; Beck, J., The leukotriene LTD4 receptor antagonist MK571 specifically modulates MRP associated multidrug resistance. *Biochem. Biophys. Res. Commun.* **1995,** 345-352.
75. Nagayama, S.; Chen, Z. S.; Kitazono, M.; Takebayashi, Y.; Niwa, K.; Yamada, K.; Tani, A.; Haraguchi, M.; Sumizawa, T.; Furukawa, T.; Aikou, T.; Akiyama, S., Increased

sensitivity to vincristine of MDR cells by the leukotriene D4 receptor antagonist, ONO-1078. *Cancer Lett.* **1998,** 175-182.
76. Maeno, K.; Nakajima, A.; Conseil, G.; Rothnie, A.; Deeley, R. G.; Cole, S. P., Molecular basis for reduced estrone sulfate transport and altered modulator sensitivity of transmembrane helix (TM) 6 and TM17 mutants of multidrug resistance protein 1 (ABCC1). *Drug Metab. Dispos.* **2009,** 1411-1420.
77. Norman, B. H.; Lander, P. A.; Gruber, J. M.; Kroin, J. S.; Cohen, J. D.; Jungheim, L. N.; Starling, J. J.; Law, K. L.; Self, T. D.; Tabas, L. B.; Williams, D. C.; Paul, D. C.; Dantzig, A. H., Cyclohexyl-linked tricyclic isoxazoles are potent and selective modulators of the multidrug resistance protein (MRP1). *Bioorg. Med. Chem. Lett.* **2005,** 5526-5530.
78. Doyle, L. A.; Yang, W.; Abruzzo, L. V.; Krogmann, T.; Gao, Y.; Rishi, A. K.; Ross, D. D., A multidrug resistance transporter from human MCF-7 breast cancer cells. *Proc. Natl. Acad. Sci. U. S. A.* **1998,** 15665-15670.
79. Allikmets, R.; Schriml, L. M.; Hutchinson, A.; Romano-Spica, V.; Dean, M., A human placenta-specific ATP-binding cassette gene (ABCP) on chromosome 4q22 that is involved in multidrug resistance. *Cancer Res.* **1998,** 5337-5339.
80. Miyake, K.; Mickley, L.; Litman, T.; Zhan, Z.; Robey, R.; Cristensen, B.; Brangi, M.; Greenberger, L.; Dean, M.; Fojo, T.; Bates, S. E., Molecular cloning of cDNAs which are highly overexpressed in mitoxantrone-resistant cells: demonstration of homology to ABC transport genes. *Cancer Res.* **1999,** 8-13.
81. Maliepaard, M.; Scheffer, G. L.; Faneyte, I. F.; van Gastelen, M. A.; Pijnenborg, A. C.; Schinkel, A. H.; van De Vijver, M. J.; Scheper, R. J.; Schellens, J. H., Subcellular localization and distribution of the breast cancer resistance protein transporter in normal human tissues. *Cancer Res.* **2001,** 3458-3464.
82. Huls, M.; Brown, C. D.; Windass, A. S.; Sayer, R.; van den Heuvel, J. J.; Heemskerk, S.; Russel, F. G.; Masereeuw, R., The breast cancer resistance protein transporter ABCG2 is expressed in the human kidney proximal tubule apical membrane. *Kidney Int.* **2008,** 220-225.
83. Cooray, H. C.; Blackmore, C. G.; Maskell, L.; Barrand, M. A., Localisation of breast cancer resistance protein in microvessel endothelium of human brain. *Neuroreport* **2002,** 2059-2063.
84. Robillard, K. R.; Hoque, T.; Bendayan, R., Expression of ATP-binding cassette membrane transporters in rodent and human sertoli cells: relevance to the permeability of antiretroviral therapy at the blood-testis barrier. *J. Pharmacol. Exp. Ther.* **2012,** 96-108.
85. Asashima, T.; Hori, S.; Ohtsuki, S.; Tachikawa, M.; Watanabe, M.; Mukai, C.; Kitagaki, S.; Miyakoshi, N.; Terasaki, T., ATP-binding cassette transporter G2 mediates the efflux of phototoxins on the luminal membrane of retinal capillary endothelial cells. *Pharm. Res.* **2006,** 1235-1242.
86. Mao, Q.; Unadkat, J. D., Role of the Breast Cancer Resistance Protein (ABCG2) in Drug Transport-an update. *The AAPS Journal* **2015,** 65-82.

87. Mo, W.; Zhang, J. T., Human ABCG2: structure, function, and its role in multidrug resistance. *Int. J. Biochem. Mol. Biol.* **2012,** 1-27.
88. Jablonski, M. R.; Jacob, D. A.; Campos, C.; Miller, D. S.; Maragakis, N. J.; Pasinelli, P.; Trotti, D., Selective increase of two ABC drug efflux transporters at the blood-spinal cord barrier suggests induced pharmacoresistance in ALS. *Neurobiol. Dis.* **2012,** 194-200.
89. Wang, H.; Lee, E. W.; Cai, X.; Ni, Z.; Zhou, L.; Mao, Q., Membrane topology of the human breast cancer resistance protein (BCRP/ABCG2) determined by epitope insertion and immunofluorescence. *Biochemistry* **2008,** 13778-13787.
90. Ni, Z.; Mark, M. E.; Cai, X.; Mao, Q., Fluorescence resonance energy transfer (FRET) analysis demonstrates dimer/oligomer formation of the human breast cancer resistance protein (BCRP/ABCG2) in intact cells. *Int. J. Biochem. Mol. Biol.* **2010,** 1-11.
91. McDevitt, C. A.; Collins, R. F.; Conway, M.; Modok, S.; Storm, J.; Kerr, I. D.; Ford, R. C.; Callaghan, R., Purification and 3D structural analysis of oligomeric human multidrug transporter ABCG2. *Structure* **2006,** 1623-1632.
92. Rosenberg, M. F.; Bikadi, Z.; Chan, J.; Liu, X.; Ni, Z.; Cai, X.; Ford, R. C.; Mao, Q., The human breast cancer resistance protein (BCRP/ABCG2) shows conformational changes with mitoxantrone. *Structure* **2010,** 482-493.
93. Polgar, O.; Robey, R. W.; Morisaki, K.; Dean, M.; Michejda, C.; Sauna, Z. E.; Ambudkar, S. V.; Tarasova, N.; Bates, S. E., Mutational analysis of ABCG2: role of the GXXXG motif. *Biochemistry* **2004,** 9448-9456.
94. Macalou, S.; Robey, R. W.; Jabor Gozzi, G.; Shukla, S.; Grosjean, I.; Hegedus, T.; Ambudkar, S. V.; Bates, S. E.; Di Pietro, A., The linker region of breast cancer resistance protein ABCG2 is critical for coupling of ATP-dependent drug transport. *Cell. Mol. Life Sci.* **2016,** 1927-1937.
95. Henriksen, U.; Fog, J. U.; Litman, T.; Gether, U., Identification of intra- and intermolecular disulfide bridges in the multidrug resistance transporter ABCG2. *J. Biol. Chem.* **2005,** 36926-36934.
96. Nakagawa, H.; Wakabayashi-Nakao, K.; Tamura, A.; Toyoda, Y.; Koshiba, S.; Ishikawa, T., Disruption of N-linked glycosylation enhances ubiquitin-mediated proteasomal degradation of the human ATP-binding cassette transporter ABCG2. *FEBS J.* **2009,** 7237-7252.
97. Mao, Q.; Unadkat, J. D., Role of the breast cancer resistance protein (ABCG2) in drug transport. *The AAPS journal* **2005,** E118-E133.
98. Stacy, A. E.; Jansson, P. J.; Richardson, D. R., Molecular pharmacology of ABCG2 and its role in chemoresistance. *Mol. Pharmacol.* **2013,** 655-669.
99. Gupta, A.; Zhang, Y.; Unadkat, J. D.; Mao, Q., HIV protease inhibitors are inhibitors but not substrates of the human breast cancer resistance protein (BCRP/ABCG2). *J. Pharmacol. Exp. Ther.* **2004,** 334-341.
100. Zhang, Y.; Gupta, A.; Wang, H.; Zhou, L.; Vethanayagam, R. R.; Unadkat, J. D.; Mao, Q., BCRP transports dipyridamole and is inhibited by calcium channel

blockers. *Pharm. Res.* **2005,** 2023-2034.
101. Rabindran, S. K.; He, H.; Singh, M.; Brown, E.; Collins, K. I.; Annable, T.; Greenberger, L. M., Reversal of a novel multidrug resistance mechanism in human colon carcinoma cells by fumitremorgin C. *Cancer Res.* **1998,** 5850-5858.
102. van Loevezijn, A.; Allen, J. D.; Schinkel, A. H.; Koomen, G. J., Inhibition of BCRP-mediated drug efflux by fumitremorgin-type indolyl diketopiperazines. *Bioorg. Med. Chem. Lett.* **2001,** 29-32.
103. Köhler, S. C.; Wiese, M., HM30181 derivatives as novel potent and selective inhibitors of the breast cancer resistance protein (BCRP/ABCG2). *J. Med. Chem.* **2015,** 3910-3921.
104. Juvale, K.; Pape, V. F. S.; Wiese, M., Investigation of chalcones and benzochalcones as inhibitors of breast cancer resistance protein. *Biorg. Med. Chem.* **2012,** 346-355.
105. Winter, E.; Lecerf-Schmidt, F.; Gozzi, G.; Peres, B.; Lightbody, M.; Gauthier, C.; Ozvegy-Laczka, C.; Szakacs, G.; Sarkadi, B.; Creczynski-Pasa, T. B.; Boumendjel, A.; Di Pietro, A., Structure–Activity Relationships of Chromone Derivatives toward the Mechanism of Interaction with and Inhibition of Breast Cancer Resistance Protein ABCG2. *J. Med. Chem.* **2013,** 9849-9860.
106. Juvale, K.; Stefan, K.; Wiese, M., Synthesis and biological evaluation of flavones and benzoflavones as inhibitors of BCRP/ABCG2. *Eur. J. Med. Chem.* **2013,** 115-126.
107. Nakamura, Y.; Oka, M.; Soda, H.; Shiozawa, K.; Yoshikawa, M.; Itoh, A.; Ikegami, Y.; Tsurutani, J.; Nakatomi, K.; Kitazaki, T.; Doi, S.; Yoshida, H.; Kohno, S., Gefitinib ("Iressa", ZD1839), an epidermal growth factor receptor tyrosine kinase inhibitor, reverses breast cancer resistance protein/ABCG2-mediated drug resistance. *Cancer Res.* **2005,** 1541-1546.
108. Houghton, P. J.; Germain, G. S.; Harwood, F. C.; Schuetz, J. D.; Stewart, C. F.; Buchdunger, E.; Traxler, P., Imatinib mesylate is a potent inhibitor of the ABCG2 (BCRP) transporter and reverses resistance to topotecan and SN-38 in vitro. *Cancer Res.* **2004,** 2333-2337.
109. Dai, C. L.; Tiwari, A. K.; Wu, C. P.; Su, X. D.; Wang, S. R.; Liu, D. G.; Ashby, C. R., Jr.; Huang, Y.; Robey, R. W.; Liang, Y. J.; Chen, L. M.; Shi, C. J.; Ambudkar, S. V.; Chen, Z. S.; Fu, L. W., Lapatinib (Tykerb, GW572016) reverses multidrug resistance in cancer cells by inhibiting the activity of ATP-binding cassette subfamily B member 1 and G member 2. *Cancer Res.* **2008,** 7905-7914.
110. Mi, Y. J.; Liang, Y. J.; Huang, H. B.; Zhao, H. Y.; Wu, C. P.; Wang, F.; Tao, L. Y.; Zhang, C. Z.; Dai, C. L.; Tiwari, A. K.; Ma, X. X.; To, K. K.; Ambudkar, S. V.; Chen, Z. S.; Fu, L. W., Apatinib (YN968D1) reverses multidrug resistance by inhibiting the efflux function of multiple ATP-binding cassette transporters. *Cancer Res.* **2010,** 7981-7991.
111. Sodani, K.; Tiwari, A. K.; Singh, S.; Patel, A.; Xiao, Z. J.; Chen, J. J.; Sun, Y. L.; Talele, T. T.; Chen, Z. S., GW583340 and GW2974, human EGFR and HER-2

inhibitors, reverse ABCG2- and ABCB1-mediated drug resistance. *Biochem. Pharmacol.* **2012,** 1613-1622.
112.Minocha, M.; Khurana, V.; Qin, B.; Pal, D.; Mitra, A. K., Enhanced brain accumulation of pazopanib by modulating P-gp and Bcrp1 mediated efflux with canertinib or erlotinib. *Int. J. Pharm.* **2012,** 127-134.
113.Erlichman, C.; Boerner, S. A.; Hallgren, C. G.; Spieker, R.; Wang, X. Y.; James, C. D.; Scheffer, G. L.; Maliepaard, M.; Ross, D. D.; Bible, K. C.; Kaufmann, S. H., The HER tyrosine kinase inhibitor CI1033 enhances cytotoxicity of 7-ethyl-10-hydroxycamptothecin and topotecan by inhibiting breast cancer resistance protein-mediated drug efflux. *Cancer Res.* **2001,** 739-748.
114.Shukla, S.; Chen, Z. S.; Ambudkar, S. V., Tyrosine kinase inhibitors as modulators of ABC transporter-mediated drug resistance. *Drug Resist Updat.* **2012,** 70-80.
115.Shukla, S.; Patel, A.; Ambudkar, S. V., Mechanistic and Pharmacological Insights into Modulation of ABC Drug Transporters by Tyrosine Kinase Inhibitors. In *ABC Transporters - 40 Years on*, George, A. M., Ed. Springer International Publishing: Cham, 2016; pp 227-272.
116. George, A. M., ABC Transporters — 40 Years on. **2016,** 1-384.
117.Pick, A.; Wiese, M., Tyrosine Kinase Inhibitors Influence ABCG2 Expression in EGFR-Positive MDCK BCRP Cells via the PI3K/Akt Signaling Pathway. *ChemMedChem* **2012,** 650-662.
118.Juvale, K.; Gallus, J.; Wiese, M., Investigation of quinazolines as inhibitors of breast cancer resistance protein (ABCG2). *Bioorg. Med. Chem.* **2013,** 7858-7873.
119.Juvale, K.; Wiese, M., 4-Substituted-2-phenylquinazolines as inhibitors of BCRP. *Bioorg. Med. Chem. Lett.* **2012,** 6766-6769.
120. Spindler, A. Synthese und Untersuchung neuer ABCG2 Inhibitoren. 2017.(in German)
121. Krapf, M. K.; Gallus, J.; Wiese, M., 4-Anilino-2-pyridylquinazolines and -pyrimidines as Highly Potent and Nontoxic Inhibitors of Breast Cancer Resistance Protein (ABCG2). *J. Med. Chem.* **2017,** 4474-4495.
122. Krapf, M. K.; Wiese, M., Synthesis and Biological Evaluation of 4-Anilino-quinazolines and -quinolines as Inhibitors of Breast Cancer Resistance Protein (ABCG2). *J. Med. Chem.* **2016,** 5449-5461.
123. Krapf, M. K.; Gallus, J.; Wiese, M., Synthesis and biological investigation of 2,4-substituted quinazolines as highly potent inhibitors of breast cancer resistance protein (ABCG2). *Eur. J. Med. Chem.* **2017**.
124. Thomas, H., Nucleophilic Heteroaromatic Substitution. 11. Phthalazines. **1980,** 165-167.
125. Banks, C. K., Arylaminoheterocyclic Compounds. 1. Synthetic Method. *J. Am. Chem. Soc.* **1944,** 1127-1130.
126. Xathan, B.-. Nucleophilic Heteroaromatic Substitution. I. Pyridazines. **1964,** 1956-1959.
127. Saul G. Cohen, A. S. J. a. W. T., Nucleophilic Aromatic Substitution Reactions.

In *Progress in Physical Organic Chemistry* 1963; pp 31-74.
128. Valdameri, G.; Gauthier, C.; Terreux, R.; Kachadourian, R.; Day, B. J.; Winnischofer, S. M. B.; Rocha, M. E. M.; Frachet, V.; Ronot, X.; Di Pietro, A.; Boumendjel, A., Investigation of chalcones as selective inhibitors of the breast cancer resistance protein: critical role of methoxylation in both inhibition potency and cytotoxicity. *J. Med. Chem.* **2012,** 3193-3200.
129. Valdameri, G.; Genoux-Bastide, E.; Peres, B.; Gauthier, C.; Guitton, J.; Terreux, R.; Winnischofer, S. M. B.; Rocha, M. E. M.; Boumendjel, A.; Di Pietro, A., Substituted Chromones as Highly Potent Nontoxic Inhibitors, Specific for the Breast Cancer Resistance Protein. *J. Med. Chem.* **2012,** 966-970.
130. Boumendjel, A.; Nicolle, E.; Moraux, T.; Gerby, B.; Blanc, M.; Ronot, X.; Boutonnat, J., Piperazinobenzopyranones and phenalkylaminobenzopyranones: potent inhibitors of breast cancer resistance protein (ABCG2). *J. Med. Chem.* **2005,** 7275-7281.
131. Mao, Q.; Unadkat, J. D., Role of the breast cancer resistance protein (BCRP/ABCG2) in drug transport--an update. *AAPS J* **2015,** 65-82.
132. Honkanen, E.; Pippuri, A.; Kairisalo, P.; Nore, P.; Karppanen, H.; Paakkari, I., Synthesis and antihypertensive activity of some new quinazoline derivatives. *J. Med. Chem.* **1983,** 1433-1438.
133. Ugale, V. G.; Bari, S. B., Quinazolines: new horizons in anticonvulsant therapy. *Eur. J. Med. Chem.* **2014,** 447-501.
134. Guan, J.; Zhang, Q.; O'Neil, M.; Obaldia, N., 3rd; Ager, A.; Gerena, L.; Lin, A. J., Antimalarial activities of new pyrrolo[3,2-f]quinazoline-1,3-diamine derivatives. *Antimicrob. Agents Chemother.* **2005,** 4928-4933.
135. M, F. Z.; M, H. H., Synthesis and biological evaluation studies of novel quinazolinone derivatives as antibacterial and anti-inflammatory agents. *Saudi Pharm. J.* **2014,** 157-162.
136. Ogata, Y.; Kawasaki, A.; Nakagawa, K., Kinetics of the formation of acetoguanamines from dicyandiamide and acetonitriles. *Tetrahedron* **1966,** 157-165.
137. Ogata, Y.; Kawasaki, A.; Nakagawa, K., Kinetics of the formation of benzoguanamine from dicyandiamide and benzonitrile. *Tetrahedron* **1964,** 2755-2761.
138. Kawasaki, A.; Ogata, Y., Kinetics of the formation of melamine from dicyandiamide. *Tetrahedron* **1966,** 1267-1274.
139. Seijas, J. A.; Vázquez-Tato, M. P.; Montserrat Martínez, M., Microwave enhanced synthesis of 4-aminoquinazolines. *Tetrahedron Lett.* **2000,** 2215-2217.
140. Montalbetti, C. A. G. N.; Falque, V., Amide bond formation and peptide coupling. *Tetrahedron* **2005,** 10827-10852.
141. Valeur, E.; Bradley, M., Amide bond formation: beyond the myth of coupling reagents. *Chem. Soc. Rev.* **2009,** 606-631.
142. Chang, L. C. W.; Spanjersberg, R. F.; Von Frijtag Drabbe Künzel, J. K.; Mulder-Krieger, T.; Van Den Hout, G.; Beukers, M. W.; Brussee, J.; IJzerman, A. P., 2,4,6-Trisubstituted pyrimidines as a new class of selective adenosine A1 receptor antagonists. *J. Med. Chem.* **2004,** 6529-6540.

143. Madapa, S.; Tusi, Z.; Sridhar, D.; Kumar, A.; Siddiqi, M. I.; Srivastava, K.; Rizvi, A.; Tripathi, R.; Puri, S. K.; Shiva Keshava, G. B.; Shukla, P. K.; Batra, S., Search for new pharmacophores for antimalarial activity. Part I: synthesis and antimalarial activity of new 2-methyl-6-ureido-4-quinolinamides. *Bioorg. Med. Chem.* **2009,** 203-221.
144. Marek, J.; Pazdera, P., Reactivity Study on Morpholine-1-carbothioic Acid. **2002,** 2-9.
145. Pinner, A., Ueber die Einwirkung von Acetessigaether auf die Amidine. Pyrimidine. *Berichte der deutschen chemischen Gesellschaft* **1885,** 2845-2852.(in German)
146. Katritzky, A. R.; Yousaf, T. I., A C-13 nuclear magnetic resonance study of the pyrimidine synthesis by the reactions of 1,3-dicarbonyl compounds with amidines and ureas. *Can. J. Chem.* **1986,** 2087-2093.
147. Fandrick, D. R.; Reinhardt, D.; Desrosiers, J. N.; Sanyal, S.; Fandrick, K. R.; Ma, S.; Grinberg, N.; Lee, H.; Song, J. J.; Senanayake, C. H., General and rapid pyrimidine condensation by addressing the rate limiting aromatization. *Org. Lett.* **2014,** 2834-2837.
148. Olmstead, W. N.; Margolin, Z.; Bordwell, F. G., Acidities of Water and Simple Alcohols in Dimethyl Sulfoxide Solution. *J. Org. Chem.* **1980,** 3295-3299.
149. Bordwell, F. G.; Ji, G. Z., Effects of Structural Changes on Acidities and Homolytic Bond Dissociation Energies of the H-N Bonds in Amidines, Carboxamides, and Thiocarboxamides. *J. Am. Chem. Soc.* **1991,** 8398-8401.
150. Achmatowicz, M.; Thiel, O. R.; Wheeler, P.; Bernard, C.; Huang, J.; Larsen, R. D.; Faul, M. M., Practical synthesis of a p38 MAP kinase inhibitor. *The Journal of organic chemistry* **2009,** 795-809.
151. Thiel, O. R.; Achmatowicz, M.; Bernard, C.; Wheeler, P.; Savarin, C.; Correll, T. L.; Kasparian, A.; Allgeier, A.; Bartberger, M. D.; Tan, H.; Larsen, R. D., Development of a Practical Synthesis of a p38 MAP Kinase Inhibitor. *Organic Process Research & Development* **2009,** 230-241.